AFRL-SR-AR-TR-08-0153

REPORT DOCUMENTATION PAGE

1. REPORT DATE (DD-MM-YYYY)	2. REPORT TYPE	3. DATES COVERED (From - To)
02-12-2008	Final	3/1/04-8/31/07

4. TITLE AND SUBTITLE
Tracking with a swarm of GMTI Equipped UAV's

5a. CONTRACT NUMBER
FA9550-04-1-0141

5b. GRANT NUMBER

5c. PROGRAM ELEMENT NUMBER

6. AUTHOR(S)

Yaakov Bar-Shalom

5d. PROJECT NUMBER

5e. TASK NUMBER

5f. WORK UNIT NUMBER

7. PERFORMING ORGANIZATION NAME(S) AND ADDRESS(ES)

University of Connecticut, Unit 2157
Storrs, CT 06269-2157

8. PERFORMING ORGANIZATION REPORT NUMBER
ECE 070212

9. SPONSORING/MONITORING AGENCY NAME(S) AND ADDRESS(ES)
Office of Naval Research
Boston Regional Office
495 Summer Street, Room 627
Boston, MA 02210-2109

10. SPONSOR/MONITOR'S ACRONYM(S)

11. SPONSOR/MONITOR'S REPORT NUMBER(S)

12. DISTRIBUTION/AVAILABILITY STATEMENT
Unlimited

13. SUPPLEMENTARY NOTES

14. ABSTRACT

The problem considered in this report is the optimization of the information obtained by a group of UAVs carrying out surveillance -- - search and tracking — over a large region which includes a number of targets. The goal is to track detected targets as well as search for the undetected ones. The UAVs are assumed to be equipped with Ground Moving Target Indicator (GMTI) radars, which measure the locations of moving ground targets as well as their radial velocities (Doppler).

15. SUBJECT TERMS

16. SECURITY CLASSIFICATION OF: a. REPORT	b. ABSTRACT	c. THIS PAGE	17. LIMITATION OF ABSTRACT	18. NUMBER OF PAGES	19a. NAME OF RESPONSIBLE PERSON
U	U	U		1	Yaakov Bar-Shalom
					19b. TELEPHONE NUMBER (Include area code) 860-486-4823

Standard Form 298 (Rev. 8/98)

20101014472

DTIC Data

Purchase Request Number: FQ8671-0600467

BPN: F1ATA05256B467

Proposal Number: 04-NM-039

Research Title: TRACKING WITH A COOPERATIVELY CONTROLLED SWARM OF GMTI EQUIPPED UAVS

Type Submission:

Inst. Control Number: FA9550-04-1-0141P00003

Institution: UNIV OF CONNECTICUT

Primary Investigator: Professor Yaakov Bar-Shalom

Invention Ind: none

Project/Task: 2304T / B

Program Manager: Juan R. Vasquez

Objective:

To develop an autonomous UAV based surveillance of several ground targets distributed over a large area.

Approach:

To develop a cooperative control algorithm where the coupling of individual UAVs is not through their dynamics, but rather through their decision making algorithms that used target tracking metrics for their performance.

Progress:

Year: 2004 **Month:** 11
ANNUAL REPORT FOR: FA9550-04-1-0141

Status of Effort:

An algorithm for Optimal UAV placement for Suveillance was obtained and published in [273, 284].
The algorithm for optimal UAV placement for surveillance can improve their utilization [273, 284].

Year: 2005 **Month:** 09
Annual Report for FA9550-04-1-0141

Our current work deals with the development of practical advanced algorithms for the optimal cooperative placement of UAVs with GMTI (Doppler) radar for the purposes of surveillance and ground target tracking.

Year: 2006 **Month:** 10
Development of an autonomous UAV based surveillance of several ground targets distributed over a large area. Development of a cooperative control algorithm where the coupling of individual UAVs is not through their dynamics, but rather through their decision making algorithms that used target tracking metrics for their performance. An algorithm for Optimal UAV placement for surveillance was obtained and published. Current work deals with the development of practical advanced algorithms for placement of UAVs.

Year: 2008 **Month:** 02 **Final**
The problem considered in this paper is the optimization of the information obtained by a group of UAVs carrying out surveillance of several ground targets distributed over a large area. The UAVs are assumed to be equipped with Ground

Optimal Placement of GMTI UAVs for ground target tracking

Abhijit Sinha[a], Thia. Kirubarajan[a] and Yaakov Bar-Shalom[b]

[a]Electrical and Computer Engineering Dept.
McMaster University
Hamilton, ON L8S 4K1, Canada

[b]Electrical and Computer Engineering Dept.
University of Connecticut
Storrs, CT 06269, USA

Abstract—With the recent advent of moderate-cost unmanned (or uninhabited) aerial vehicles (UAV) and their success in surveillance, it is natural to proceed to consider the cooperative management of groups of UAVs. The problem considered in this paper is optimization of the information obtained by a group of UAVs carrying out surveillance of several ground targets distributed over a large area. The UAVs are assumed to be equipped with Ground Moving Target Indicator (GMTI) radars, which measure the locations of moving ground targets as well as their radial velocities. In this research entropic information, obtained from the information form of Riccati equation, is used as the criterion function. Sensor survival probability and target detection probability for each target-sensor pair are also included in the criterion function. The optimal sensor placement problem is solved via deterministic as well as randomized optimization. Simulation results on two different scenarios are presented for four different types of prior information.

TABLE OF CONTENTS

1. INTRODUCTION

Sensors like, for example, radars and MTI, are used to make observations of a moving target with the objective of estimating the state of the target. Multiple sensors, which give different perspectives of one or more targets at the same time or at different times, can be used to enhance estimation results. An important application of control theory is to manage multiple sensors such that the expected information obtained from them can be maximized. Management of multiple sensors involves gathering, exchanging and combining information. When the sensor platforms are mobile one has to decide the optimal placement of sensors. With the recent advent of affordable unmanned aerial vehicles (UAV) and their proven effectiveness in surveillance, it is natural to consider the cooperative management of groups of UAVs.

A number of UAV management algorithms can be found in the literature. In [3] a hierarchical approach, that uses modified Voronoi diagram to generate possible paths, to intercept a number of known targets using a number of UAVs, is presented. Similar approaches can be found in [7], [8]. A search algorithm for targets in a given area is proposed in [5], where a discrete time stochastic decision model is formulated as the path planning problem, which is then implemented with a dynamic programming algorithm [9]. However, the aim of [5] is only to detect (not to track) targets in the search region. In [4] a decentralized sensor management algorithm is presented. In this paper an entropic information measure is used as the objective function in a target cuing and target hand-off problem and a multi-platform bearing only tracking problem.

In this research we use an information theoretic approach similar to [4]. Here the GMTI radars measures radial velocity as well as position of the targets. Also, the survival probability of a sensor from hostile fire by the targets and detection probability of a target corresponding to a particular sensor are considered. Development of the criterion function is discussed in Section 2. In Section 3 different approaches, both randomized and deterministic, to find the maxima of the criterion function, are discussed and a mixed approach is developed. Simulation results are presented in Section 4.

2. CRITERION FUNCTION

The criterion function, obtained from the entropic information measure [4], is given by

$$J = \sum_j \log(|P_j(k|k)^{-1}|) \tag{1}$$

where $P_j(k|k)$ is the posterior covariance of the state vector corresponding to target j at time t_k and can be written in terms of the state prediction covariance $P_j(k|k-1)$ and new information $Y_j(k)$ as follows [1]

$$P_j(k|k)^{-1} = P_j(k|k-1)^{-1} + Y_j(k) \tag{2}$$

The matrix $Y_j(k)$ is the total new information about target j obtained by different sensors. The information obtained by a particular sensor s about target j is given by

$$Y(k,s,j) = H(k,s,j)'R(s,j)^{-1}H(k,s,j) \tag{3}$$

where $H(k,s,j)$ is the measurement matrix and $R(s,j)$ is the measurement covariance matrix corresponding to the sensor-target pair s-j. The new information also depends on target's detection probabilities corresponding to each sensor and the survival probability of the sensors. The new information obtained by sensor s about target j is reduced depending on this sensor's survivable probability. The modified information is given by

$$\hat{Y}(k,s,j) = \pi_S(s)Y(k,s,j) \tag{4}$$

Progress:

Year: 2008 **Month:** 02 **Final**

Moving Target Indicator (GMTI) radars, which measure the locations of moving ground targets as well as their radial velocities (Doppler). In this research the Fisher information, obtained from the information form of Riccati equation, is used in the objective function. Sensor survival probability and target detection probability for each target-sensor pair are also included in the objective function, where the detection probability is a function of both range and range rate. The optimal sensor placement problem is solved by a genetic algorithm based optimizer. Simulation results on two di?erent scenarios are presented for four di?erent types of prior information.

Keywords: Multisensor-multitarget tracking, sensor management, cooperative control, UAV placement, ground target tracking.

where $\pi_S(s)$ is the total survival probability of sensor s, which is equal to the product of survival probabilities of this sensor corresponding to each target.

$$\pi_S(s) = \prod_j \pi_S(s,j) \tag{5}$$

Let us assume that the target j is detected exactly by a set C of sensors. The probability of such an event is given by

$$\pi_D(C,j) = \prod_s \pi_D(s,j)^{I(C,s)}(1-\pi_D(s,j))^{1-I(C,s)} \tag{6}$$

where $I(C,s)$ is an indicator given by

$$I(C,s) = \begin{cases} 1 & \text{if } s \in C \\ 0 & \text{else} \end{cases} \tag{7}$$

Total information gain when a target j is detected exactly by a set C of sensors is given by

$$\hat{Y}(k,C,j) = \sum_{s\in C} \hat{Y}(k,s,j) \tag{8}$$

Hence considering all possible sets similar to C the updated information measure can be written as

$$\begin{aligned} P_j(k|k)^{-1} &= P_j(k|k-1)^{-1} + \sum_{\forall C} \pi_D(C,j)\hat{Y}(k,C,j) \quad (9) \\ &= P_j(k|k-1)^{-1} + \sum_{\forall C} \pi_D(C,j) \\ &\quad \cdot \sum_{s\in C} \pi_S(s) H(k,s,j)' R(s,j)^{-1} H(k,s,j) \quad (10) \end{aligned}$$

It can be shown that (10) reduces to

$$\begin{aligned} P_j(k|k)^{-1} &= P_j(k|k-1)^{-1} + \sum_s \pi_S(s)\pi_D(s,j) \\ &\quad \cdot H(k,s,j)' R(s,j)^{-1} H(k,s,j) \quad (11) \end{aligned}$$

Figure 1 shows a notional survival probability and detection probability vs. range between the target and the sensor. It is important to note that in a real life scenario the survival and detection probability depend on the terrain topography.

The state vector of target j is given by

$$\mathrm{v} = \begin{bmatrix} x^j & v_x^j & y^j & v_y^j \end{bmatrix} \tag{12}$$

where x and y are the position components in cartesian coordinate and v_x, v_y are the velocity components. The approximate measurement matrix, which comprises of x-y position and radial velocity $\dot{r}$, of target j corresponding to a sensor s, is given by

$$H(k,s,j) = \begin{bmatrix} 1 & 0 & 0 & 0 \\ 0 & 0 & 1 & 0 \\ 0 & \cos(\alpha(s,j)) & 0 & \sin(\alpha(s,j)) \end{bmatrix} \tag{13}$$

where $\alpha(s,j)$ is the azimuth angle of the target j measured by sensor s. The original position measurement are in form of range $r(s,j)$ and azimuth $\alpha(s,j)$ which are converted to x-y position using the standard conversion [1]. The measurement covariance matrix $R(s,j)$ is given by

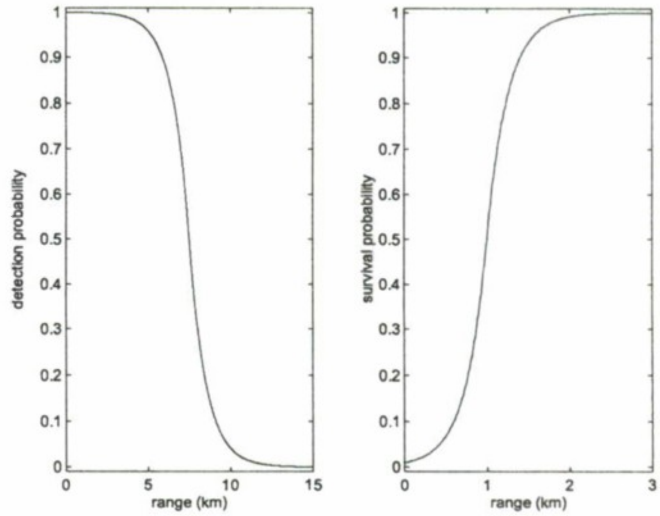

Figure 1. Detection probability and survival probability w.r.t. range

$$R(s,j) = \begin{bmatrix} R_{1,1} & R_{1,2} & 0 \\ R_{1,2} & R_{2,2} & 0 \\ 0 & 0 & \sigma_{\dot{r}}^2 \end{bmatrix} \tag{14}$$

where

$$\begin{aligned} R_{1,1} &= r(s,j)^2\sigma_\alpha^2 \sin(\alpha(s,j))^2 + \sigma_r^2\cos(\alpha(s,j))^2 \quad (15) \\ R_{2,2} &= r(s,j)^2\sigma_\alpha^2 \cos(\alpha(s,j))^2 + \sigma_r^2\sin(\alpha(s,j))^2 \quad (16) \\ R_{1,2} &= (\sigma_r^2 - r(s,j)^2\sigma_\alpha^2)\sin(\alpha(s,j))\cos(\alpha(s,j)) \quad (17) \end{aligned}$$

3. Search Techniques

In this work we have considered both gradient based search technique as well as randomized search technique to find the maxima of the criterion function.

Newton-Raphson Method—The Newton-Raphson method is a deterministic technique in which one step update is given by

$$\mathrm{s}_{\mathrm{new}} = \mathrm{s} - \beta\left(\nabla_{\mathrm{s}}^2 J\right)^{-1}\nabla_{\mathrm{s}} J \tag{18}$$

where s is a vector that denotes current x–y positions of the sensors, $\nabla_{\mathrm{s}} J$ denotes the gradient of the criterion function w.r.t. s and β is a factor that is decided by a line search technique. Thus, the Newton-Raphson method requires the first and second derivatives of the criterion function J w.r.t. x–y position of each radar. For each sensor-target pair s–t, the derivative of $Y_{s,t}(k)$ is first evaluated w.r.t. range $r(s,t)$ and azimuth $\alpha(s,t)$ and then converted to derivatives w.r.t. the x–y position of the sensor. Using these derivatives $\nabla_{\mathrm{s}} J$ and $\nabla_{\mathrm{s}}^2 J$ are obtained. A detailed discussion of the procedure can be found in Appendix. Although the Newton-Raphson method produces very fast convergence, it fails in the presence of local maxima, as is the case for the criterion function

J. However, it can be very useful to refine the results of other algorithms, which is discussed later in this section.

Genetic Algorithm—This is a randomized technique suitable for problems with multiple optimal points. To apply this algorithm in the current problem the positions of sensors are discretized to one meter resolution and converted to a bit string. A population size of 100 is used in this application. First generation is obtained randomly and next generations are obtained by crossover operation, which is applied separately on the x and y positions of each sensor. The parents are selected randomly depending on their fitness, which is a shifted version of the value of criterion function corresponding to the sensor positions indicated by the parent. Along with the crossover operation, the bits of the candidates in the next generation can also change due to mutation operation. In this application the mutation probability of each bit is 1/30. Elitism was used to preserve best parents in the next generation.

This algorithm eventually reaches the global maxima without being trapped by the local ones. However, rate of convergence of this algorithm slows down when it reaches close to the maxima. For fast convergence and to avoid the method being trapped by any local maxima we choose a combination of the search techniques discussed above. Initial search is performed randomly using the genetic algorithm and then the best result of this search is used as the initial point for the Newton-Raphson method.

4. RESULTS

In this section we present the results obtained on two target scenarios using the search technique discussed in Section 3 for the criterion function discussed in Section 2. Both of the target scenarios consist of two sets having three target each and one set having four targets. In the first type of scenario the target sets form a triangular shape (Figure 2) and in the second one the targets form a linear shape (Figure 6). In all scenarios the height of the sensors above the ground is considered to be 1 km and the ground is considered to be flat. The measurement noise standard deviations are $\sigma_r = 5\,\text{m}$, $\sigma_\theta = 1^\circ$ and $\sigma_{\dot r} = 1$ m/sec. To evaluate the criterion function a state prediction covariance matrix $P_j(k|k-1)$ is required for each target j. Steady state value of $P_j(k|k-1)$ can be used, which is obtained using the information filter form of Riccati equation given by

$$P_j(l+1|l)^{-1} = A_j(l) - A_j(l)\left(A_j(l) + Q(l)^{-1}\right)^{-1} A_j(l) \tag{19}$$

and

$$A_j(l) = \left(F(l)^{-1}\right)'\left(P_j(l|l-1)^{-1} + \sum_{s\in C_j(l)} H(l,s,j)' R(s,j)^{-1} H(l,s,j)\right) F(l)^{-1} \tag{20}$$

where $C_j(l)$ is the set of sensors that detects target j at time t_l and $F(l)$ is the transition matrix between time t_l to t_{l+1}, which depends on the revisit time $\Delta_l = t_{l+1} - t_l$, is given by

$$F_j(l) = \begin{bmatrix} 1 & \Delta_l & 0 & 0 \\ 0 & 1 & 0 & 0 \\ 0 & 0 & 1 & \Delta_l \\ 0 & 0 & 0 & 1 \end{bmatrix} \tag{21}$$

The process noise matrix $Q(l)$ is obtained following a discrete white noise acceleration model

$$Q(l) = \begin{bmatrix} \frac{1}{4}\Delta_l^4 & \frac{1}{2}\Delta_l^3 & 0 & 0 \\ \frac{1}{2}\Delta_l^3 & \Delta_l^2 & 0 & 0 \\ 0 & 0 & \frac{1}{4}\Delta_l^4 & \frac{1}{2}\Delta_l^3 \\ 0 & 0 & \frac{1}{2}\Delta_l^3 & \Delta_l^2 \end{bmatrix} \sigma_v^2 \tag{22}$$

where σ_v^2 is the variance of the white noise acceleration process. In our simulations $\sigma_v = 0.5\,\text{m/sec}$. One important property of information form of Riccati equation is that the information from different sensors can be written in the summation form as in (20).

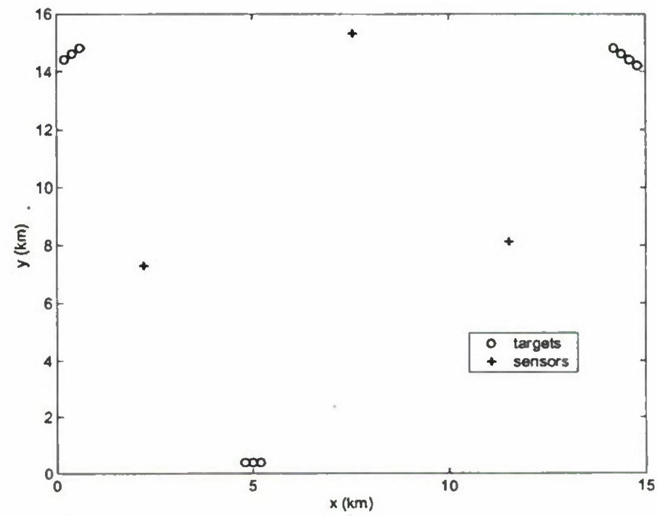

Figure 2. Scenario for the calculation of the steady state prediction covariance matrix

The steady state covariance matrix is obtained using the scenario shown in Figure 2. For simplicity it is assumed that the targets move in the same direction as the sensors and their relative position remains the same over time. The revisit time is assumed to be $\Delta_l = 10$ sec for all t_l. The resulting steady state prediction covariance matrices are different for different target. It is also observed that the correlations between x component of position or velocity and y component of position or velocity vary in a wide range and can have both positive and negative values. However, correlations between the position and velocity components of any particular direction (x or y) are very close to 1/3. The following steady state prediction covariance matrix, which shows an average behavior, was selected for each target

$$P_1 = \begin{bmatrix} 10^2 & \frac{1}{3}10 & 0 & 0 \\ \frac{1}{3}10 & 1 & 0 & 0 \\ 0 & 0 & 10^2 & \frac{1}{3}10 \\ 0 & 0 & \frac{1}{3}10 & 1 \end{bmatrix} \tag{23}$$

We can also observe the effect of a state prediction covariance matrix, which is far from the steady state, on optimal sensor positions. The following matrix is used for this purpose

$$P_2 = \begin{bmatrix} 100^2 & \frac{1}{3}500 & 0 & 0 \\ \frac{1}{3}500 & 5^2 & 0 & 0 \\ 0 & 0 & 100^2 & \frac{1}{3}500 \\ 0 & 0 & \frac{1}{3}500 & 5^2 \end{bmatrix} \tag{24}$$

The following two state prediction covariance matrices are used to obtain optimal sensor positions when variances are high in one direction (x or y) and low in another.

$$P_3 = \begin{bmatrix} 10^2 & \frac{1}{3}10 & 0 & 0 \\ \frac{1}{3}10 & 1^2 & 0 & 0 \\ 0 & 0 & 100^2 & \frac{1}{3}500 \\ 0 & 0 & \frac{1}{3}500 & 5^2 \end{bmatrix} \tag{25}$$

$$P_4 = \begin{bmatrix} 100^2 & \frac{1}{3}500 & 0 & 0 \\ \frac{1}{3}500 & 5^2 & 0 & 0 \\ 0 & 0 & 10^2 & \frac{1}{3}10 \\ 0 & 0 & \frac{1}{3}10 & 1^2 \end{bmatrix} \tag{26}$$

Figures 3–8 show the optimal sensor positions when the steady state prediction covariance matrix, which is shown in (23), is used in the criterion function. These figures show that for both scenarios the sensors concentrate near the largest group (particularly in Figures 3 and 4). Since in this case the predicted target state is highly accurate, some of the targets can be neglected while placing the sensors. Optimal target positions are presented in Figures 9–11 when state prediction covariance matrix, shown in (24), is used. This matrix represents much more noisy prediction than at steady state. Hence, none of the targets can be neglected in this case. Figures 12–14 show optimal sensor positions when predictions are relatively bad in y direction as presented in (25). The figures show that the sensors align along the y axis relative to the targets to get better position and velocity information in this direction. Opposite of this effect can be seen in 15–17, where due to relatively less predicted information along x the sensors align themselves along this direction.

5. Conclusions

In this paper an information theoretic approach for optimal GMTI sensor placement is presented. The sensors, that measure target's position along with its radial velocity, are mounted on UAVs that are tracking a number of ground targets. Target's detection probability and sensor's survival probability are considered while developing the criterion function. A combination of randomized and nonrandomized techniques is used to find the optimal sensor locations. Results are obtained for two scenarios each having 10 targets and for different number of sensors. Also, different state prediction covariances are used to observe their effect. The overall track estimation accuracy should increase significantly with this approach. The extension of this work to a dynamic scenario is under investigation.

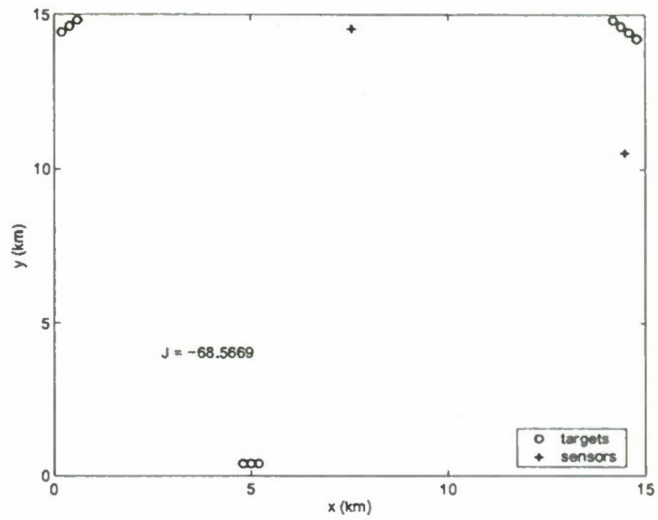

Figure 3. Optimal position of 2 sensors for target scenario 1 and steady state value of state prediction covariance

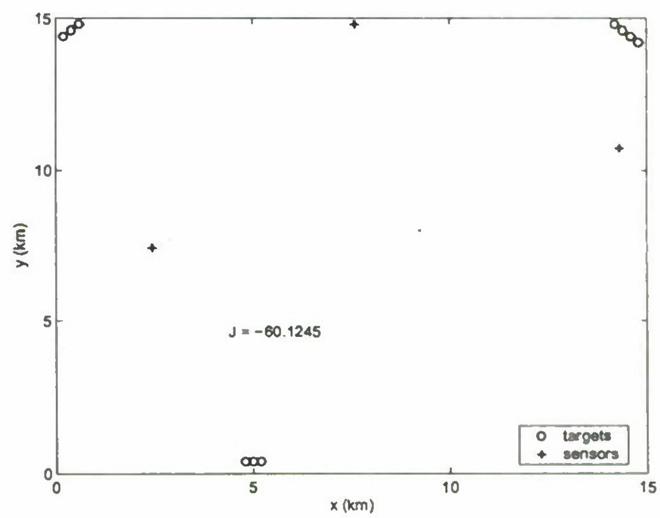

Figure 4. Optimal position of 3 sensors for target scenario 1 and steady state value of state prediction covariance

6. Appendix

In the following, the derivations required for the Newton Raphson method are presented. An approximation is made by assuming that the cross terms in the second derivative of the criterion function, related to two separate sensors, are all zero. This significantly reduces the computational requirements by allowing separate update for the sensors. For a sensor i one step update is given by

$$\mathbf{s}^i_{\text{new}} = \mathbf{s}^i - \beta \left(\nabla^2_{\mathbf{s}^i} J\right)^{-1} \nabla_{\mathbf{s}^i} J \tag{A.1}$$

where $\mathbf{s}^i$ is the current x–y position of the sensor

$$\mathbf{s}^i = \begin{bmatrix} x^i & y^i \end{bmatrix} \tag{A.2}$$

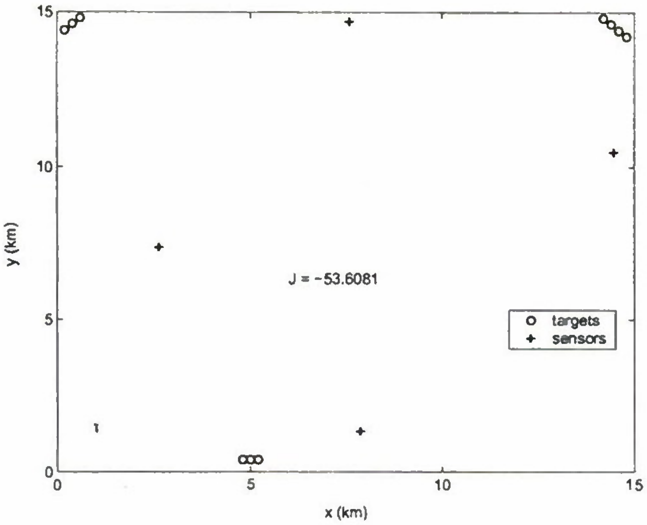

Figure 5. Optimal position of 4 sensors for target scenario 1 and steady state value of state prediction covariance

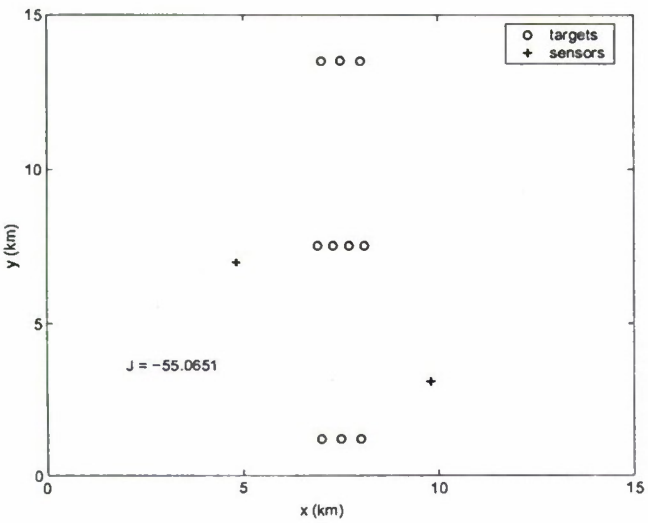

Figure 6. Optimal position of 2 sensors for target scenario 2 and steady state value of state prediction covariance

The criterion function is given by

$$J = \sum_t \log\left(\left|P_t(k|k-1)^{-1} + \sum_s \pi_S(s)\pi_D(s,t)Y(k,s,t)\right|\right) \tag{A.3}$$

Information of a target j obtained by a sensor i, assuming perfect detection and survival, is given by

$$\begin{aligned} Y(k,i,j) &= H(k,i,j)'R(i,j)^{-1}H(k,i,j) \\ &= \begin{bmatrix} Y_{11} & 0 & Y_{13} & 0 \\ 0 & Y_{22} & 0 & Y_{24} \\ Y_{13} & 0 & Y_{33} & 0 \\ 0 & Y_{24} & 0 & Y_{44} \end{bmatrix} \end{aligned} \tag{A.4}$$

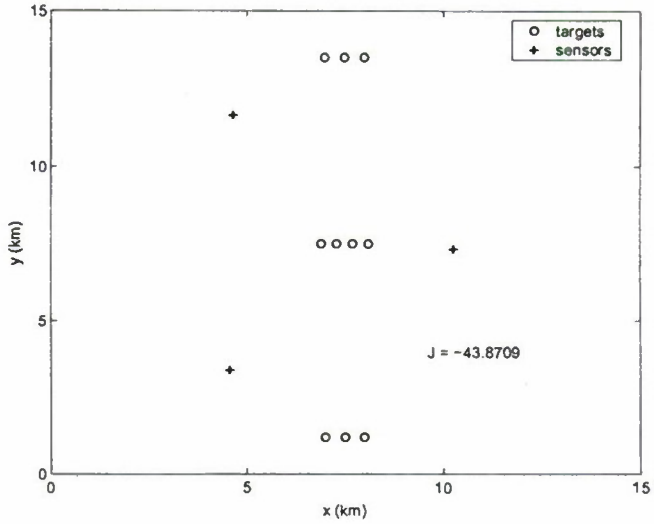

Figure 7. Optimal position of 3 sensors for target scenario 2 and steady state value of state prediction covariance

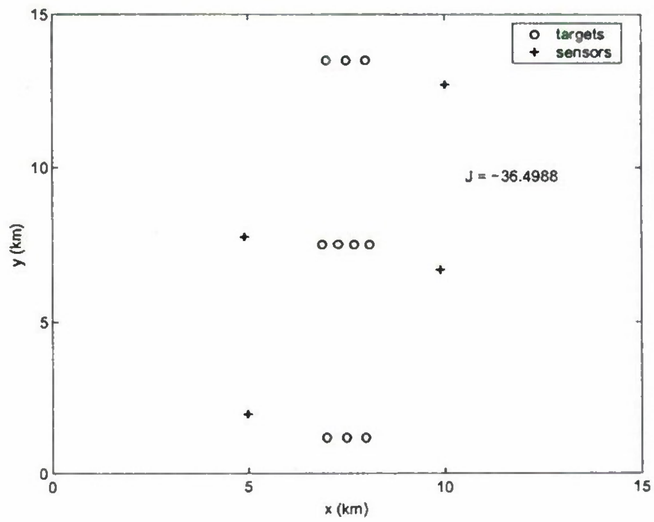

Figure 8. Optimal position of 4 sensors for target scenario 2 and steady state value of state prediction covariance

where the components of matrix $Y(k,i,j)$, obtained using (13) and (14), are given by

$$Y_{11} = \frac{r(i,j)^2\sigma_\alpha^2\cos(\alpha(i,j))^2 + \sigma_r^2\sin(\alpha(i,j))^2}{r(i,j)^2\sigma_\alpha^2\sigma_r^2} \tag{A.5}$$

$$Y_{22} = \frac{\cos(\alpha(i,j))^2}{\sigma_{\dot{r}}^2} \tag{A.6}$$

$$Y_{33} = \frac{r(i,j)^2\sigma_\alpha^2\sin(\alpha(i,j))^2 + \sigma_r^2\cos(\alpha(i,j))^2}{r(i,j)^2\sigma_\alpha^2\sigma_r^2} \tag{A.7}$$

$$Y_{13} = -\frac{(\sigma_r^2 - r(i,j)^2\sigma_\alpha^2)\sin(\alpha(i,j))\cos(\alpha(i,j))}{r(i,j)^2\sigma_\alpha^2\sigma_r^2} \tag{A.8}$$

$$Y_{44} = \frac{\sin(\alpha(i,j))^2}{\sigma_{\dot{r}}^2} \tag{A.9}$$

$$Y_{24} = \frac{\cos(\alpha(i,j))\sin(\alpha(i,j))}{\sigma_{\dot{r}}^2} \tag{A.10}$$

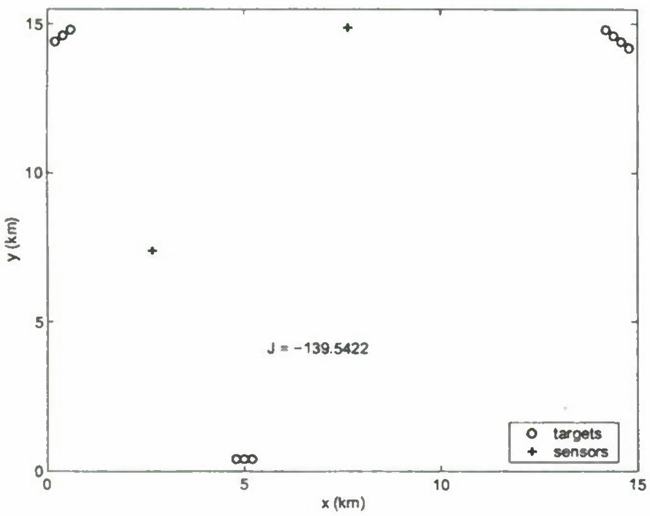

Figure 9. Optimal position of 2 sensors for target scenario 1 and high value of state prediction covariance

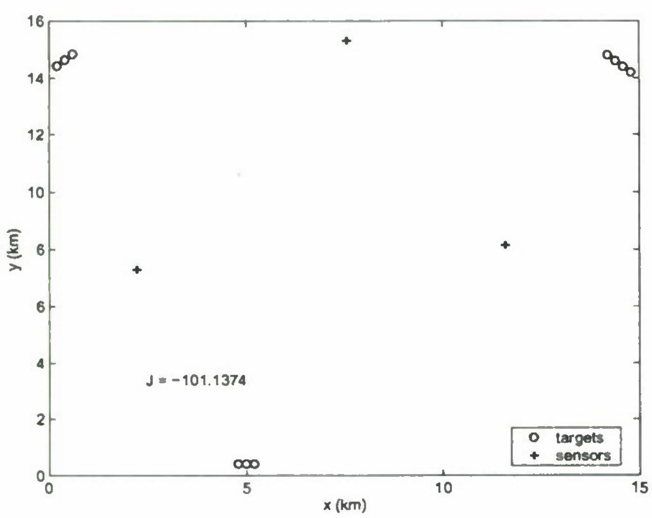

Figure 10. Optimal position of 3 sensors for target scenario 1 and high value of state prediction covariance

The derivatives of the criterion function w.r.t. the x–y position of sensor i are given by

$$\nabla_{s^i} J = \left[\begin{array}{cc} \frac{\partial J}{\partial x^i} & \frac{\partial J}{\partial y^i} \end{array} \right] \quad \text{(A.11)}$$

$$\nabla^2_{s^i} J = \left[\begin{array}{cc} \frac{\partial^2 J}{\partial {x^i}^2} & \frac{\partial^2 J}{\partial x^i \partial y^i} \\ \frac{\partial^2 J}{\partial x^i \partial y^i} & \frac{\partial^2 J}{\partial {y^i}^2} \end{array} \right] \quad \text{(A.12)}$$

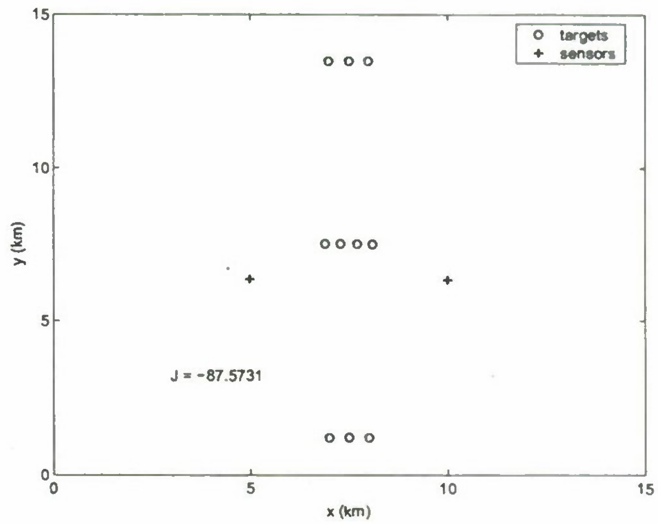

Figure 11. Optimal position of 2 sensors for target scenario 2 and high value of state prediction covariance

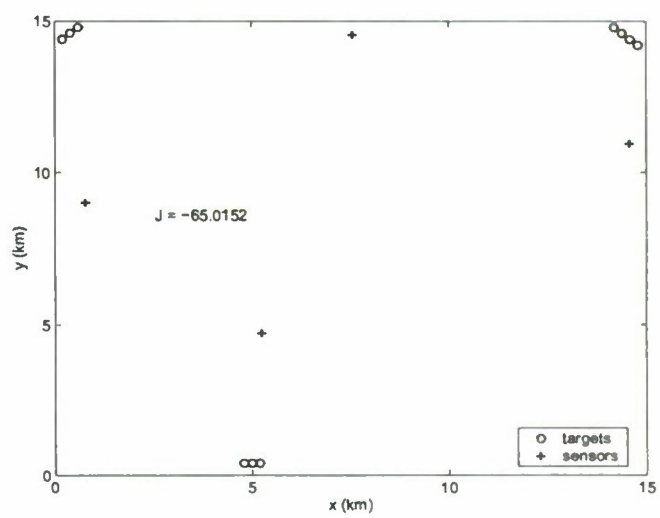

Figure 12. Optimal position of 4 sensors for target scenario 1 and a state prediction covariance that has low value along x-direction and high value along y-direction

The components can be expanded as

$$\frac{\partial J}{\partial x^i} = \sum_t |P_t(k|k)| \frac{\partial}{\partial x^i} |P_t(k|k)^{-1}| \quad \text{(A.13)}$$

$$\begin{aligned} \frac{\partial^2 J}{\partial {x^i}^2} &= \sum_t -|P_t(k|k)|^2 \left(\frac{\partial}{\partial x^i} |P_t(k|k)^{-1}| \right)^2 \\ &+ \sum_t |P_t(k|k)| \frac{\partial^2}{\partial {x^i}^2} |P_t(k|k)^{-1}| \end{aligned} \quad \text{(A.14)}$$

$$\begin{aligned} \frac{\partial^2 J}{\partial x^i \partial y^i} &= \sum_t -|P_t(k|k)|^2 \frac{\partial}{\partial x^i} |P_t(k|k)^{-1}| \frac{\partial}{\partial y^i} |P_t(k|k)^{-1}| \\ &+ \sum_t |P_t(k|k)| \frac{\partial^2}{\partial x^i \partial y^i} |P_t(k|k)^{-1}| \end{aligned} \quad \text{(A.15)}$$

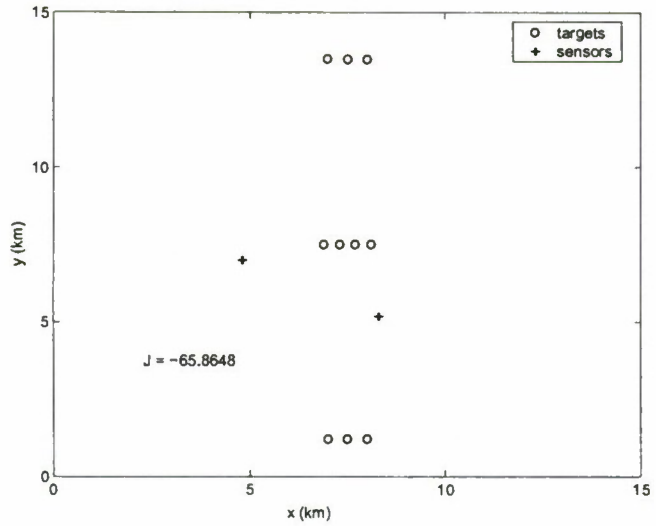

Figure 13. Optimal position of 2 sensors for target scenario 2 and a state prediction covariance that has low value along x-direction and high value along y-direction

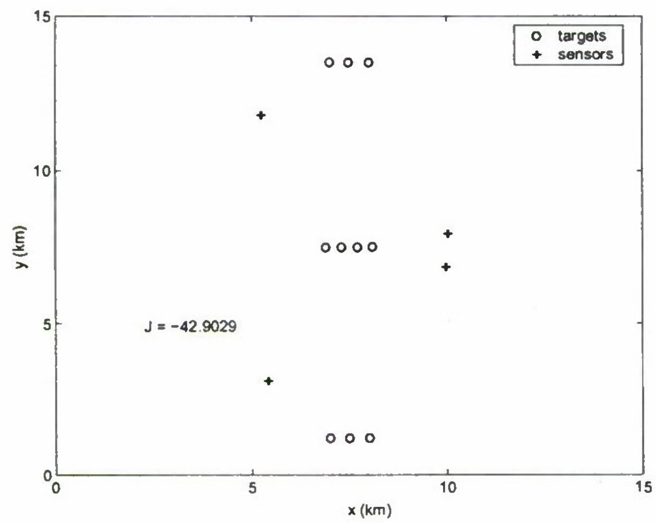

Figure 14. Optimal position of 4 sensors for target scenario 2 and a state prediction covariance that has low value along x-direction and high value along y-direction

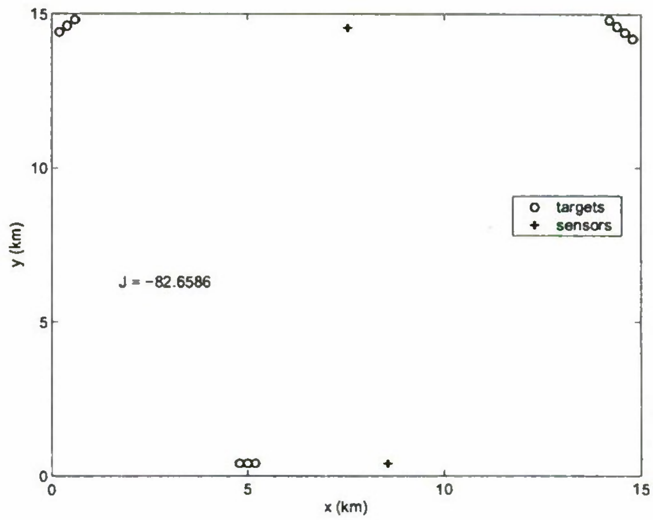

Figure 15. Optimal position of 2 sensors for target scenario 1 and a state prediction covariance that has high value along x-direction and low value along y-direction

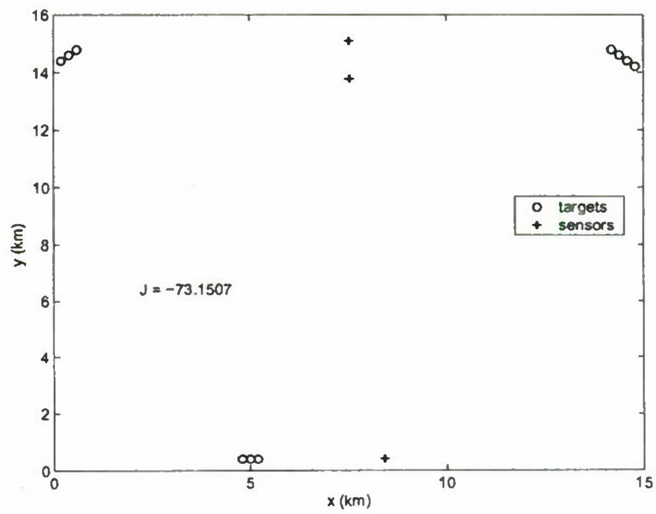

Figure 16. Optimal position of 3 sensors for target scenario 1 and a state prediction covariance that has high value along x-direction and low value along y-direction

where $P_t(k|k)$ is given by

$$P_t(k|k)^{-1} = P_t(k|k-1)^{-1} + \sum_s \pi_S(s)\pi_D(s,t)Y(k,s,t) \tag{A.16}$$

the terms $\frac{\partial J}{\partial y^i}$ and $\frac{\partial^2 J}{\partial y^{i2}}$ are similar to (A.13) and (A.14), respectively.

To obtain derivatives of the determinant of a matrix we need to compute derivatives of the matrix. First, these derivatives are obtained w.r.t. $r(i,j)$ and $\alpha(i,j)$, which are the polar coordinates of target j considering sensor i as the origin. Next, these derivatives are converted to derivatives w.r.t. x^i and y^i. It is important to note that the detection and survival probabilities are independent of azimuth angle α. We have

$$\begin{aligned}\frac{\partial P_j(k|k)^{-1}}{\partial r(i,j)} &= \pi_S(i)\pi_D(i,j)\frac{\partial Y(k,i,j)}{\partial r(i,j)} \\ &+\pi_S(i)\frac{\partial \pi_D(i,j)}{\partial r(i,j)}Y(k,i,j) \\ &+\pi_D(i,j)\frac{\partial \pi_S(j)}{\partial r(i,j)}Y(k,i,j)\end{aligned} \tag{A.17}$$

$$\frac{\partial P_j(k|k)^{-1}}{\partial \alpha(i,j)} = \pi_S(i)\pi_D(i,j)\frac{\partial Y(k,i,j)}{\partial \alpha(i,j)} \tag{A.18}$$

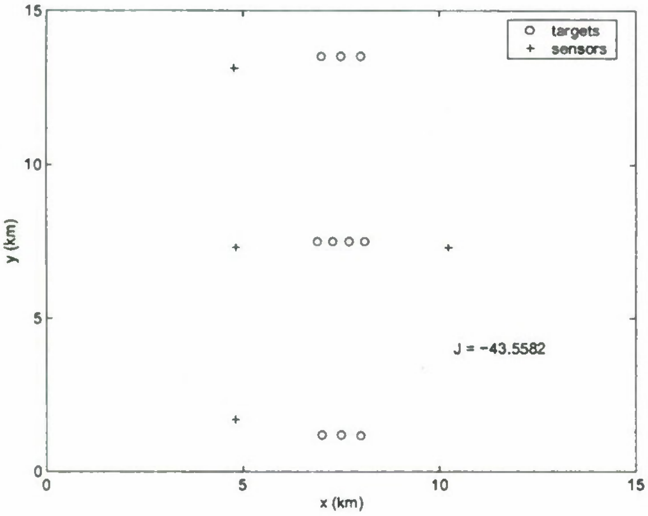

Figure 17. Optimal position of 4 sensors for target scenario 2 and a state prediction covariance that has high value along x-direction and low value along y-direction

$$\begin{aligned}
\frac{\partial^2 P_j(k|k)^{-1}}{\partial r(i,j)^2} &= \pi_S(i)\pi_D(i,j)\frac{\partial^2 Y(k,i,j)}{\partial r(i,j)^2} \\
&+\pi_S(i)\frac{\partial^2 \pi_D(i,j)}{\partial r(i,j)^2}Y(k,i,j) \\
&+\pi_D(i,j)\frac{\partial^2 \pi_S(j)}{\partial r(i,j)^2}Y(k,i,j) \\
&+2\pi_S(i)\frac{\partial \pi_D(i,j)}{\partial r(i,j)}\frac{\partial Y(k,i,j)}{\partial r(i,j)} \\
&+2\frac{\partial \pi_S(i)}{\partial r(i,j)}\frac{\partial \pi_D(i,j)}{\partial r(i,j)}Y(k,i,j) \\
&+2\pi_D(i,j)\frac{\partial \pi_S(j)}{\partial r(i,j)}\frac{\partial Y(k,i,j)}{\partial r(i,j)}
\end{aligned} \tag{A.19}$$

$$\frac{\partial^2 P_j(k|k)^{-1}}{\partial \alpha(i,j)^2} = \pi_S(i)\pi_D(i,j)\frac{\partial^2 Y(k,i,j)}{\partial \alpha(i,j)^2} \tag{A.20}$$

$$\begin{aligned}
\frac{\partial^2 P_j(k|k)^{-1}}{\partial r(i,j)\partial \alpha(i,j)} &= \pi_S(i)\pi_D(i,j)\frac{\partial^2 Y(k,i,j)}{\partial r(i,j)\partial \alpha(i,j)} \\
&+2\pi_S(i)\frac{\partial \pi_D(i,j)}{\partial r(i,j)}\frac{\partial Y(k,i,j)}{\partial \alpha(i,j)} \\
&+2\pi_D(i,j)\frac{\partial \pi_S(j)}{\partial r(i,j)}\frac{\partial Y(k,i,j)}{\partial \alpha(i,j)}
\end{aligned} \tag{A.21}$$

where

$$\frac{\partial Y(k,i,j)}{\partial r(i,j)} = \begin{bmatrix} -\frac{2\sin(\alpha(i,j))^2}{r(i,j)^3\sigma_\alpha^2} & 0 & \frac{\sin(2\alpha(i,j))}{r(i,j)^3\sigma_\alpha^2} & 0 \\ 0 & 0 & 0 & 0 \\ \frac{\sin(2\alpha(i,j))}{r(i,j)^3\sigma_\alpha^2} & 0 & -\frac{2\cos(\alpha(i,j))^2}{r(i,j)^3\sigma_\alpha^2} & 0 \\ 0 & 0 & 0 & 0 \end{bmatrix} \tag{A.22}$$

$$\frac{\partial^2 Y(k,i,j)}{\partial r(i,j)^2} = \begin{bmatrix} \frac{6\sin(\alpha(i,j))^2}{r(i,j)^4\sigma_\alpha^2} & 0 & -\frac{3\sin(2\alpha(i,j))}{r(i,j)^4\sigma_\alpha^2} & 0 \\ 0 & 0 & 0 & 0 \\ -\frac{3\sin(2\alpha(i,j))}{r(i,j)^4\sigma_\alpha^2} & 0 & \frac{6\cos(\alpha(i,j))^2}{r(i,j)^4\sigma_\alpha^2} & 0 \\ 0 & 0 & 0 & 0 \end{bmatrix} \tag{A.23}$$

$$\frac{\partial Y(k,i,j)}{\partial \alpha(i,j)} = A \tag{A.24}$$

$$\frac{\partial^2 Y(k,i,j)}{\partial \alpha(i,j)^2} = B \tag{A.25}$$

$$\frac{\partial^2 Y(k,i,j)}{\partial r(i,j)\partial \alpha(i,j)} = \begin{bmatrix} -\frac{2\sin(2\alpha(i,j))}{r(i,j)^3\sigma_\alpha^2} & 0 & \frac{2\cos(2\alpha(i,j))}{r(i,j)^3\sigma_\alpha^2} & 0 \\ 0 & 0 & 0 & 0 \\ \frac{2\cos(2\alpha(i,j))}{r(i,j)^3\sigma_\alpha^2} & 0 & -\frac{2\sin(2\alpha(i,j))}{r(i,j)^3\sigma_\alpha^2} & 0 \\ 0 & 0 & 0 & 0 \end{bmatrix} \tag{A.26}$$

The matrices A and B are symmetric and the nonzero components of these matrices are given by

$$A(1,1) = \frac{(\sigma_r^2 - r(i,j)^2\sigma_\alpha^2)\sin(2\alpha(i,j))}{r(i,j)^2\sigma_\alpha^2\sigma_r^2} \tag{A.27}$$

$$A(2,2) = -\frac{\sin(2\alpha(i,j))}{\sigma_{\dot{r}}^2} \tag{A.28}$$

$$A(3,3) = -\frac{(\sigma_r^2 - r(i,j)^2\sigma_\alpha^2)\sin(2\alpha(i,j))}{r(i,j)^2\sigma_\alpha^2\sigma_r^2} \tag{A.29}$$

$$A(1,3) = -\frac{(\sigma_r^2 - r(i,j)^2\sigma_\alpha^2)\cos(2\alpha(i,j))}{r(i,j)^2\sigma_\alpha^2\sigma_r^2} \tag{A.30}$$

$$A(4,4) = \frac{\sin(2\alpha(i,j))}{\sigma_{\dot{r}}^2} \tag{A.31}$$

$$A(2,4) = \frac{\cos(2\alpha(i,j))}{\sigma_{\dot{r}}^2} \tag{A.32}$$

$$B(1,1) = \frac{2\,(\sigma_r^2 - r(i,j)^2\sigma_\alpha^2)\cos(2\alpha(i,j))}{r(i,j)^2\sigma_\alpha^2\sigma_r^2} \tag{A.33}$$

$$B(2,2) = -\frac{2\cos(2\alpha(i,j))}{\sigma_{\dot{r}}^2} \tag{A.34}$$

$$B(3,3) = -\frac{2\,(\sigma_r^2 - r(i,j)^2\sigma_\alpha^2)\cos(2\alpha(i,j))}{r(i,j)^2\sigma_\alpha^2\sigma_r^2} \tag{A.35}$$

$$B(1,3) = \frac{2\,(\sigma_r^2 - r(i,j)^2\sigma_\alpha^2)\sin(2\alpha(i,j))}{r(i,j)^2\sigma_\alpha^2\sigma_r^2} \tag{A.36}$$

$$B(4,4) = \frac{2\cos(2\alpha(i,j))}{\sigma_{\dot{r}}^2} \tag{A.37}$$

$$B(2,4) = -\frac{2\sin(2\alpha(i,j))}{\sigma_{\dot{r}}^2} \tag{A.38}$$

The derivatives w.r.t. x-y can be obtained using the following conversions

$$\frac{\partial}{\partial x^i} = \frac{\partial r(i,j)}{\partial x^i}\frac{\partial}{\partial r(i,j)} + \frac{\partial \alpha(i,j)}{\partial x^i}\frac{\partial}{\partial \alpha(i,j)} \quad (A.39)$$

$$\frac{\partial}{\partial y^i} = \frac{\partial r(i,j)}{\partial y^i}\frac{\partial}{\partial r(i,j)} + \frac{\partial \alpha(i,j)}{\partial y^i}\frac{\partial}{\partial \alpha(i,j)} \quad (A.40)$$

$$\begin{aligned}\frac{\partial^2}{\partial {x^i}^2} = {} & \frac{\partial^2 r(i,j)}{\partial {x^i}^2}\frac{\partial}{\partial r(i,j)} + \left(\frac{\partial r(i,j)}{\partial x^i}\right)^2 \frac{\partial^2}{\partial r(i,j)^2} \\ & +2\frac{\partial r(i,j)}{\partial x^i}\frac{\partial \alpha(i,j)}{\partial x^i}\frac{\partial^2}{\partial r(i,j)\partial \alpha(i,j)} \\ & +\frac{\partial^2 \alpha(i,j)}{\partial {x^i}^2}\frac{\partial}{\partial \alpha(i,j)} + \left(\frac{\partial \alpha(i,j)}{\partial x^i}\right)^2 \frac{\partial^2}{\partial \alpha(i,j)^2}\end{aligned} \quad (A.41)$$

$$\begin{aligned}\frac{\partial^2}{\partial {y^i}^2} = {} & \frac{\partial^2 r(i,j)}{\partial {y^i}^2}\frac{\partial}{\partial r(i,j)} + \left(\frac{\partial r(i,j)}{\partial y^i}\right)^2 \frac{\partial^2}{\partial r(i,j)^2} \\ & +2\frac{\partial r(i,j)}{\partial y^i}\frac{\partial \alpha(i,j)}{\partial y^i}\frac{\partial^2}{\partial r(i,j)\partial \alpha(i,j)} \\ & +\frac{\partial^2 \alpha(i,j)}{\partial y^2}\frac{\partial}{\partial \alpha(i,j)} + \left(\frac{\partial \alpha(i,j)}{\partial y^i}\right)^2 \frac{\partial^2}{\partial \alpha(i,j)^2}\end{aligned} \quad (A.42)$$

$$\begin{aligned}\frac{\partial^2}{\partial x^i \partial y^i} = {} & \frac{\partial^2 r(i,j)}{\partial x^i \partial y^i}\frac{\partial}{\partial r(i,j)} + \frac{\partial r(i,j)}{\partial x^i}\frac{\partial r(i,j)}{\partial y^i}\frac{\partial^2}{\partial r(i,j)^2} \\ & +\frac{\partial r(i,j)}{\partial x^i}\frac{\partial \alpha(i,j)}{\partial y^i}\frac{\partial^2}{\partial r(i,j)\partial \alpha(i,j)} \\ & +\frac{\partial^2 \alpha(i,j)}{\partial x^i \partial y^i}\frac{\partial}{\partial \alpha(i,j)} \\ & +\frac{\partial \alpha(i,j)}{\partial x^i}\frac{\partial r(i,j)}{\partial y^i}\frac{\partial^2}{\partial r(i,j)\partial \alpha(i,j)} \\ & +\frac{\partial \alpha(i,j)}{\partial x^i}\frac{\partial \alpha(i,j)}{\partial y^i}\frac{\partial^2}{\partial \alpha(i,j)^2}\end{aligned} \quad (A.43)$$

The partial derivatives of $r(i,j)$-$\alpha(i,j)$ w.r.t. x^i-y^i are given by

$$\frac{\partial r(i,j)}{\partial x^i} = -\cos(\alpha(i,j)) \quad (A.44)$$

$$\frac{\partial r(i,j)}{\partial y^i} = -\sin(\alpha(i,j)) \quad (A.45)$$

$$\frac{\partial \alpha(i,j)}{\partial x^i} = \frac{\sin(\alpha(i,j))}{r(i,j)} \quad (A.46)$$

$$\frac{\partial \alpha(i,j)}{\partial y^i} = -\frac{\cos(\alpha(i,j))}{r(i,j)} \quad (A.47)$$

$$\frac{\partial^2 r(i,j)}{\partial {x^i}^2} = \frac{\sin(\alpha(i,j))^2}{r(i,j)} \quad (A.48)$$

$$\frac{\partial^2 r(i,j)}{\partial {y^i}^2} = \frac{\cos(\alpha(i,j))^2}{r(i,j)} \quad (A.49)$$

$$\frac{\partial^2 r(i,j)}{\partial x^i \partial y^i} = -\frac{\sin(2\alpha(i,j))}{2r(i,j)} \quad (A.50)$$

$$\frac{\partial^2 \alpha(i,j)}{\partial {x^i}^2} = \frac{\sin(2\alpha(i,j))}{r(i,j)^2} \quad (A.51)$$

$$\frac{\partial^2 \alpha(i,j)}{\partial {y^i}^2} = -\frac{\sin(2\alpha(i,j))}{r(i,j)^2} \quad (A.52)$$

$$\frac{\partial^2 \alpha(i,j)}{\partial x^i \partial y^i} = -\frac{\cos(2\alpha(i,j))}{r(i,j)^2} \quad (A.53)$$

The derivatives of $\pi_S(i,j)$ and $\pi_D(i,j)$ are depends on the choice of these functions.

REFERENCES

[1] Bar-Shalom, Y., Li, X. R. and Kirubarajan, T., *Estimation with Applications to Tracking and Navigation.* New York: Wiley, 2001.

[2] Bar-Shalom, Y. and Li, X. R., *Multitarget-Multisensor Tracking: Principles and Techniques*, YBS Publishing, 1995.

[3] Beard, R. W., McLain, T. W., Goodrich, M. A. and Anderson, E. P., Coordinated Target Assignment and Intercept for Unmanned Air Vehicles, *IEEE Trans on Robotics and Automation*, Vol. 18, No. 6, pp. 911-922, Dec. 2002.

[4] Durrant-Whyte, H. and Grocholsky, B., Management and Control in Decentralised Networks, *Proc. of International Conference on Information Fusion*, pp. 560-565, Cairns, Queensland, Australia, July 2003.

[5] Flint, M., Polycarpou, M. and Fernandez-Gaucherand., E., Cooperative Control for Multiple Autonomous UAV's Searching for Targets, Proc. of IEEE Conference on Decision and Control, pp. 2823-2828, Las Vegas, Nevada, Dec. 2002.

[6] Kirubarajan, T., Bar-Shalom, Y., Pattipati, K.R., and Kadar, 1, Ground Target Tracking with Variable Structure IMM Estimator. *IEEE Trans. on on Aerospace and Electrical Systems*, Vol. 36, No. 1, pp. 26-46, Jan. 2000.

[7] Li, S. M. et al., Automonous Hierachical Control of Multiple Unmanned Combat Vehicles, Proc. of American Control Conference, pp. 274-279, Anchorage, AK, May 2002.

[8] McLain, T. W., Chandler, P. R. and Pachter, M., A Decomposition Strategy for Optimal Coordination of Unmanned Air Vehicles, *Proc. of American Control Conference*, pp. 369-373, Chicago, IL, June 2000.

[9] Patek, S. D., Logan, D. A. and Castanon, D. A., Approximate Dynamic Programming for the Solution of Multiplatform Path Planning Problems, *Proc. of IEEE conference on Systems, Man, and Cybernetics*, Vol. 1, pp. 1061-1066, Oct. 1999.

Optimal Cooperative Placement of UAVs for Ground Target Tracking with Doppler Radar*

A. Sinha[a], T. Kirubarajan[a] and Y. Bar-Shalom[b]

[a]Electrical and Computer Engineering Dept. McMaster University Hamilton, ON L8S 4K1, Canada

[b]Electrical and Computer Engineering Dept. University of Connecticut Storrs, CT 06269, USA

ABSTRACT

With the recent advent of moderate-cost unmanned (or uninhabited) aerial vehicles (UAV) and their success in surveillance, it is natural to consider the cooperative management of groups of UAVs. The problem considered in this paper is the optimization of the information obtained by a group of UAVs carrying out surveillance of several ground targets distributed over a large area. The UAVs are assumed to be equipped with Ground Moving Target Indicator (GMTI) radars, which measure the locations of moving ground targets as well as their radial velocities (Doppler). In this research the Fisher information, obtained from the information form of Riccati equation, is used in the objective function. Sensor survival probability and target detection probability for each target-sensor pair are also included in the objective function, where the detection probability is a function of both range and range rate. The optimal sensor placement problem is solved by a genetic algorithm based optimizer. Simulation results on two different scenarios are presented for four different types of prior information.

Keywords: Multisensor-multitarget tracking, sensor management, cooperative control, UAV placement, ground target tracking.

1. INTRODUCTION

GMTI radars are used to make observations of moving targets with the objective of estimating the target states. Multiple sensors, which give different perspectives of one or more targets at the same time or at different times, can be used to enhance the estimation results. An important application of control theory is to manage multiple sensors such that the expected information obtained from them is maximized. Management of multiple sensors involves gathering, exchanging and combining information. When the sensor platforms are mobile, one has to decide the optimal placement of sensors. With the recent advent of affordable unmanned aerial vehicles (UAV) and their proven effectiveness in surveillance, it is natural to consider the cooperative management of groups of UAVs.

A number of UAV management algorithms can be found in the literature. In [3] a hierarchical approach, which uses modified Voronoi diagram to generate possible paths and to intercept a number of known targets using a number of UAVs, is presented. Similar approaches can be found in [7, 8]. A search algorithm for targets in a given area is proposed in [5], where a discrete time stochastic decision model is formulated as the path planning problem, which is then implemented with a dynamic programming algorithm [9]. However, the aim of [5] is only to detect (not to track) the targets in the search region. In [4] a decentralized sensor management algorithm is presented based on the change in entropy. In this paper the Fisher information measure is used in the objective function in a target cuing and target hand-off problem and a multi-platform bearing only tracking problem.

In a recent work [10] we have used a Fisher information based approach somewhat similar to [4]. Here the GMTI radars measure radial velocity as well as position of the targets. Also, the survival probability of a sensor from hostile fire by the targets and detection probability of a target corresponding to a particular sensor are considered. In [10] the detection probability of a target by a radar is assumed to be dependent only on the range. However, for GMTI radar the detection probability is a function of both range and range rate. In this paper the corresponding modification is done and it is found that target heading, which can change the range rate in an otherwise constant target-sensor geometry, influences the optimal sensor position. Development of the objective function is discussed in Section 2. In Section 3 a genetic algorithm to find the maximum of the objective function is discussed. Simulation results are presented in Section 4.

*Proc. of SPIE Conf. on Signal Processing, Sensor Fusion, and Target Recognition (#5429-10), Orlando, FL, April 2004.

2. OBJECTIVE FUNCTION

The objective function, based on the Fisher information measure is the product of uncertainty volumes [10]

$$J = \sum_j \log |P_j(k|k)^{-1}| \tag{1}$$

where $P_j(k|k)$ is the posterior covariance matrix of the state vector corresponding to target j at time t_k and can be written in terms of the state prediction covariance $P_j(k|k-1)$ and new information $Y_j(k)$ as follows [1]

$$P_j(k|k)^{-1} = P_j(k|k-1)^{-1} + Y_j(k) \tag{2}$$

The matrix $Y_j(k)$ is the total new information about target j obtained by the different sensors. The information obtained by a particular sensor s about target j is given by

$$Y(k,s,j) = H(k,s,j)'R(k,s,j)^{-1}H(k,s,j) \tag{3}$$

where $H(k,s,j)$ is the measurement matrix and $R(k,s,j)$ is the measurement covariance matrix corresponding to the sensor-target pair s,j. The new information also depends on the target's detection probabilities corresponding to each sensor and the survival probability of the sensors. The new information obtained by sensor s about target j is reduced depending on this sensor's survival probability. The modified information is given by

$$\hat{Y}(k,s,j) = \pi_S(s)Y(k,s,j) \tag{4}$$

where $\pi_S(s)$ is the total survival probability of sensor s, which is equal to the product of survival probabilities of this sensor in view of each target, i.e.,

$$\pi_S(s) = \prod_j \pi_S(s,j) \tag{5}$$

Let us further assume that target j is detected exactly by a set C of sensors. The probability of such an event is given by

$$\pi_D(C,j) = \prod_s \pi_D(s,j)^{I(C,s)}(1-\pi_D(s,j))^{1-I(C,s)} \tag{6}$$

where $\pi_D(s,j)$ is the detection probability of target j by sensor s and $I(C,s)$ is an indicator function given by

$$I(C,s) = \begin{cases} 1 & \text{if } s \in C \\ 0 & \text{else} \end{cases} \tag{7}$$

The total information gain when target j is detected exactly by a set C of sensors is given by

$$\hat{Y}(k,C,j) = \sum_{s\in C} \hat{Y}(k,s,j) \tag{8}$$

Hence, considering all possible sets, similar to C, the updated information matrix can be written as

$$\begin{aligned} P_j(k|k)^{-1} &= P_j(k|k-1)^{-1} + \sum_{\forall C} \pi_D(C,j)\hat{Y}(k,C,j) & (9) \\ &= P_j(k|k-1)^{-1} + \sum_{\forall C} \pi_D(C,j) \sum_{s\in C} \pi_S(s)H(k,s,j)'R(k,s,j)^{-1}H(k,s,j) & (10) \end{aligned}$$

It can be shown that (10) reduces to

$$P_j(k|k)^{-1} = P_j(k|k-1)^{-1} + \sum_s \pi_S(s)\pi_D(s,j)H(k,s,j)'R(k,s,j)^{-1}H(k,s,j) \tag{11}$$

The state vector of target j is taken as

$$\mathbf{x} = [\ x^j \quad v_x^j \quad y^j \quad v_y^j\ ] \tag{12}$$

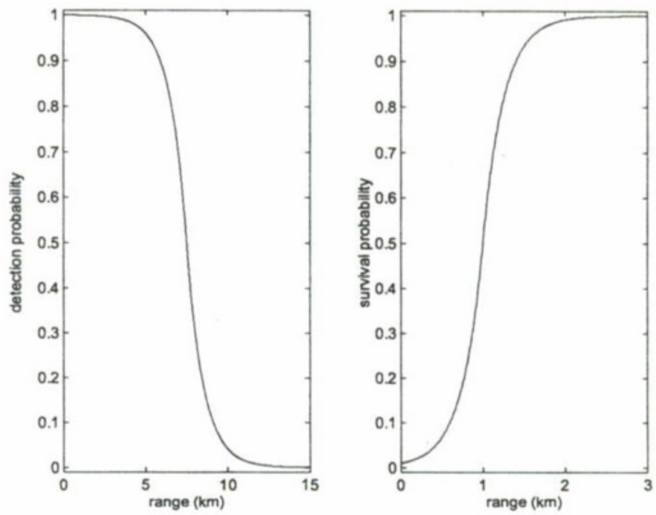

Figure 1: Detection probability and survival probability w.r.t. range.

where x and y are the position components in Cartesian coordinate and v_x, v_y are the velocity components. The approximate measurement matrix, which comprises x-y position and radial velocity $\dot{r}$, of target j corresponding to sensor s, is given by

$$H(k,s,j) = \begin{bmatrix} 1 & 0 & 0 & 0 \\ 0 & 0 & 1 & 0 \\ 0 & \cos\alpha(k,s,j) & 0 & \sin\alpha(k,s,j) \end{bmatrix} \tag{13}$$

where $\alpha(k,s,j)$ is the azimuth angle of the target j measured by sensor s at time t_k. The original position measurements are in the form of range $r(k,s,j)$ and azimuth $\alpha(k,s,j)$ which are converted to x,y position using the standard conversion [1]. The measurement covariance matrix $R(k,s,j)$ is given by

$$R(k,s,j) = \begin{bmatrix} R_{1,1} & R_{1,2} & 0 \\ R_{1,2} & R_{2,2} & 0 \\ 0 & 0 & \sigma_{\dot{r}}^2 \end{bmatrix} \tag{14}$$

where (skipping the arguments)

$$R_{1,1} = r^2\sigma_\alpha^2 \sin\alpha^2 + \sigma_r^2 \cos\alpha^2 \tag{15}$$
$$R_{2,2} = r^2\sigma_\alpha^2 \cos\alpha^2 + \sigma_r^2 \sin\alpha^2 \tag{16}$$
$$R_{1,2} = (\sigma_r^2 - r^2\sigma_\alpha^2)\sin\alpha\cos\alpha \tag{17}$$

The detection probability of target j by sensor s can be approximated as

$$\pi_D(s,j) = \pi_D^1(s,j)\pi_D^2(s,j) \tag{18}$$

where $\pi_D^1(s,j)$ is the detection probability as a function of the range and $\pi_D^2(s,j)$ is the detection probability as a function of the range rate. The nature of the first term is shown in Figure 1 and the derivation of the second term is discussed in the following.

For a GMTI radar if, the magnitude of the measured value of the range rate for a target falls below a threshold $\dot{r}_{\min}$ then the target will not be detected. Hence, $\pi_D^2(s,j)$ is given by

$$\pi_D^2(s,j) = 1 - P\{-\dot{r}_{\min} < \dot{r}(k,s,j) < \dot{r}_{\min} \mid \dot{r}(k,s,j|k-1), \sigma_{\dot{r}}(k,s,j|k-1)^2\} \tag{19}$$

where $\dot{r}(k,s,j)$ is the measured range rate and $\dot{r}(k,s,j|k-1)$ is the predicted range rate given by

$$\dot{r}(k,s,j|k-1) = v_x^j(k|k-1)\cos\alpha(k,s,j|k-1) + v_y^j(k|k-1)\sin\alpha(k,s,j,|k-1) \tag{20}$$

here $v_x^j(k|k-1)$, $v_y^j(k|k-1)$ are the components of predicted velocity and $\alpha(k,s,j,|k-1)$ is the predicted azimuth angle for target j.

The variance term $\sigma_{\dot{r}}(k,s,j|k-1)^2$ in (19) is the range rate measurement prediction variance which is the third diagonal term of the innovation covariance matrix

$$S(k,s,j) = H(k,s,j)P_j(k|k-1)H(k,s,j)' + R(k,s,j) \tag{21}$$

where in $H(k,s,j)$ the measured azimuth angle $\alpha(k,s,j)$ is replaced by the predicted azimuth angle $\alpha(k,s,j|k-1)$.

Hence $\pi_D^2(s,j)$ in (19) is evaluated by integrating a Gaussian density with mean $\dot{r}(k,s,j|k-1)$ and variance $\sigma_{\dot{r}}(k,s,j|k-1)^2$ in the interval $-\dot{r}_{\text{min}}$ to $\dot{r}_{\text{min}}$ and subtracting the result from unity.

Figure 1 shows a notional survival probability and detection probability vs. range between the target and the sensor. It is important to note that in a real life scenario the survival and detection probability depend on the terrain topography.

3. SEARCH TECHNIQUES

In this work we have used a genetic algorithm to find the global maximum of the objective function. This is a randomized technique suitable for problems with multiple maxima. To apply this algorithm in the current problem, the positions of sensors are discretized to 1 meter resolution and converted to a bit string. A population size of 100 is used in this application. First generation is obtained randomly and next generations are obtained by a crossover operation, which is applied separately on the x and y positions of each sensor. The parents are selected randomly depending on their fitness, which is the value of the objective function corresponding to the sensor positions indicated by the parent. Along with the crossover operation, the bits of the candidates in the next generation can also change due to mutation operation. In this application the mutation probability of each bit is 1/30. Elitism was used to preserve best parents in the next generation. Although its rate of convergence slows down close to the maxima, this algorithm eventually reaches the global maximum without being trapped by the local ones.

4. RESULTS

In this section we present the results obtained on two scenarios using the search technique discussed in Section 3 for the objective function discussed in Section 2. Both scenarios consist of two sets having three targets each and one set having four targets. In the first scenario the target sets form a triangular shape (Figure 2) and in the second one the targets form a linear shape (Figure 6). Three types of target velocities are considered, the components of velocity are $[0, -10]$ m/s, $[10, 0]$ m/s and $[5\sqrt{2}, -5\sqrt{2}]$ m/s and will be referred as type 1, type 2 and type 3, respectively. In all scenarios the height of the sensors above the ground is considered to be 1 km and the ground is considered to be flat. The measurement noise standard deviations are $\sigma_r = 5\,\text{m}$, $\sigma_\theta = 1^\circ$ and $\sigma_{\dot{r}} = 1\,\text{m/s}$. The minimum detectable range rate $\dot{r}_{\text{min}}$ is taken to be $2\,\text{m/s}$ for this simulation. To evaluate the objective function a state prediction covariance matrix $P_j(k|k-1)$ is required for each target j. The steady state value of $P_j(k|k-1)$ can be used, which is obtained using the information filter form of Riccati equation given by

$$P_j(l+1|l)^{-1} = A_j(l) - A_j(l)\left(A_j(l) + Q(l)^{-1}\right)^{-1} A_j(l) \tag{22}$$

and

$$\begin{aligned} A_j(l) \quad = \quad & \left(F(l)^{-1}\right)' (P_j(l|l-1)^{-1} \\ & + \sum_{s \in C_j(l)} H(l,s,j)'R(s,j)^{-1}H(l,s,j))F(l)^{-1} \end{aligned} \tag{23}$$

where $C_j(l)$ is the set of sensors that detects target j at time t_l and $F(l)$ is the transition matrix between time t_l to t_{l+1}, which depends on the revisit time $\Delta_l = t_{l+1} - t_l$, is given by

$$F_j(l) = \begin{bmatrix} 1 & \Delta_l & 0 & 0 \\ 0 & 1 & 0 & 0 \\ 0 & 0 & 1 & \Delta_l \\ 0 & 0 & 0 & 1 \end{bmatrix} \tag{24}$$

The process noise matrix $Q(l)$ is obtained following a discrete white noise acceleration model

$$Q(l) = \begin{bmatrix} \frac{1}{4}\Delta_l^4 & \frac{1}{2}\Delta_l^3 & 0 & 0 \\ \frac{1}{2}\Delta_l^3 & \Delta_l^2 & 0 & 0 \\ 0 & 0 & \frac{1}{4}\Delta_l^4 & \frac{1}{2}\Delta_l^3 \\ 0 & 0 & \frac{1}{2}\Delta_l^3 & \Delta_l^2 \end{bmatrix} \sigma_v^2 \tag{25}$$

where σ_v^2 is the variance of the white noise acceleration process. In our simulations $\sigma_v = 0.5\,\mathrm{m/s^2}$. One important property of the information form of Riccati equation is that the information from different sensors, if they are independent, can be written in the summation form as in (23).

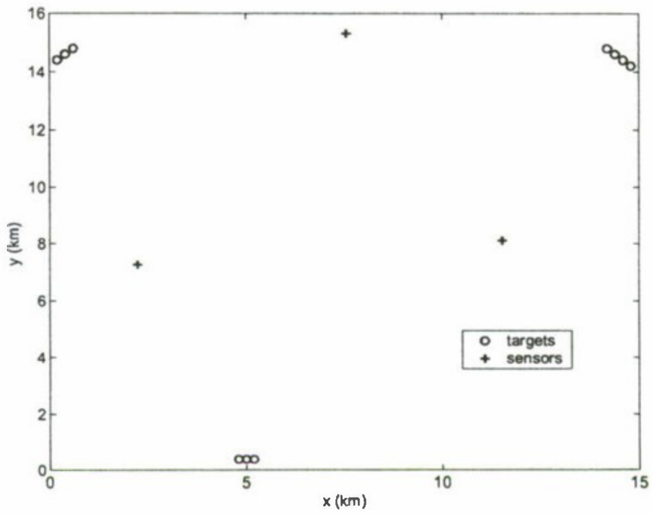

Figure 2: Scenario for the calculation of the steady state prediction covariance matrix.

The steady state covariance matrix is obtained using the scenario shown in Figure 2. For simplicity it is assumed that the targets move in the same direction as the sensors and their relative position remains the same over time. The revisit interval is assumed to be $\Delta_l = 10\,\mathrm{sec}$ for all t_l. The resulting steady state prediction covariance matrices are different for the different targets. It is also observed that the correlations between the x component of position or velocity and the y component of position or velocity vary and can have both positive and negative values. However, correlations between the position and velocity components of any particular direction (x or y) are very close to $1/3$. The following steady state prediction covariance matrix, which shows an average behavior, was selected for each target

$$P_1 = \begin{bmatrix} 10^2 & \frac{10}{3} & 0 & 0 \\ \frac{10}{3} & 1 & 0 & 0 \\ 0 & 0 & 10^2 & \frac{10}{3} \\ 0 & 0 & \frac{10}{3} & 1 \end{bmatrix} \tag{26}$$

We also evaluate the effect of a state prediction covariance matrix, that is far from the steady state, on the optimal sensor positions. The following matrix is used for this purpose

$$P_2 = \begin{bmatrix} 100^2 & \frac{500}{3} & 0 & 0 \\ \frac{500}{3} & 5^2 & 0 & 0 \\ 0 & 0 & 100^2 & \frac{500}{3} \\ 0 & 0 & \frac{500}{3} & 5^2 \end{bmatrix} \tag{27}$$

Figures 3–5 show the optimal positions of three sensors for the first target scenario and a low predicted covariance P_1 in (26). It can be seen that the optimal sensor positions depend on the headings of the targets. Also, the closest two sensors form a close to right angle triangle formation at each target so that they obtain complimentary information

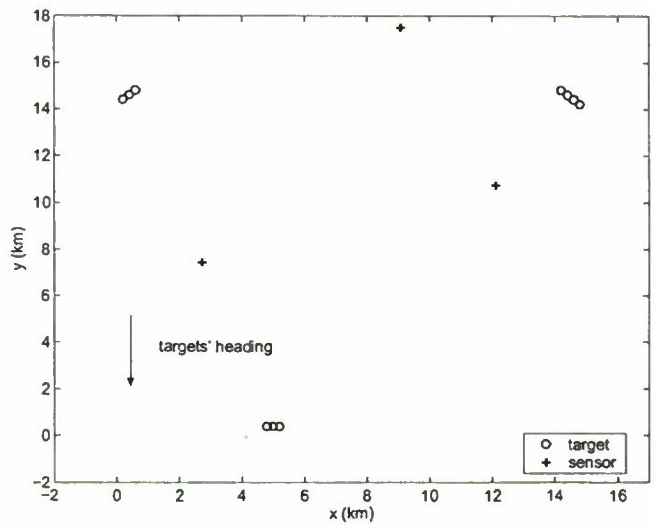

Figure 3: Optimal position of three sensors for target scenario 1 with a low state prediction covariance and velocity type 1.

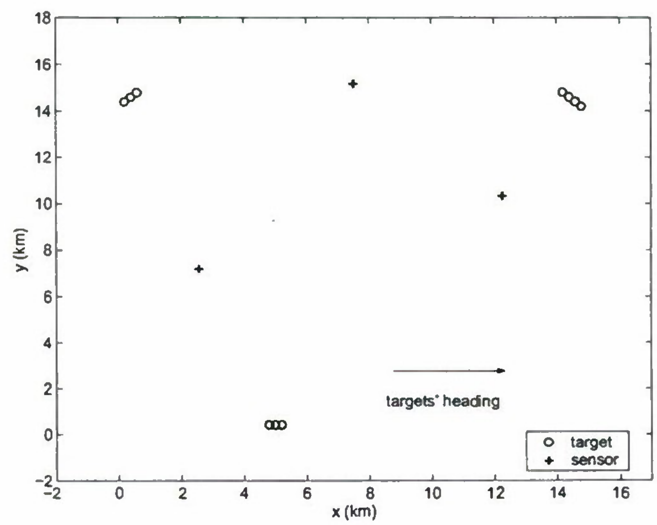

Figure 4: Optimal position of three sensors for target scenario 1 with a low state prediction covariance and velocity type 2.

about the target. There is also a tendency for the sensors to concentrate on the group of four targets as this increases the obtainable information.

Figures 6–8 show the similar nature of the optimal positions of three sensors for the second target scenario. However, in each of these cases, due to symmetry, a mirror image of sensors w.r.t. the targets along the x axis produces another set of optimal sensor positions. In Figure 8 the sensors abandon the three targets at the bottom and get the information about the rest of the targets.

Figure 9 shows optimal positions of three sensors with targets from the second scenario and each of them having velocity type 3. The difference from Figure 8 is that in this case the targets have a high prediction covariance P_2 as shown in (27). Because of this high prediction uncertainty the sensors are placed more uniformly from the targets compared to those in Figure 8.

Finally, Figures 10 and 11 show the optimal positions of two sensors for the targets of scenario 1 moving along the negative y direction. A low prediction covariance matrix P_1 is used for the first figure, while a high prediction

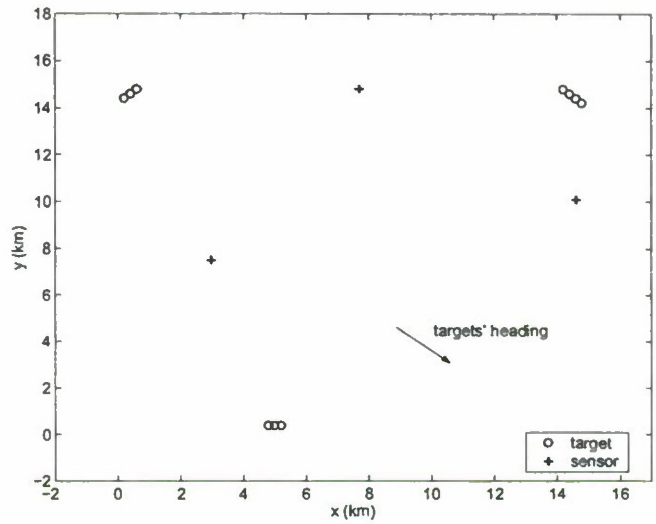

Figure 5: Optimal position of three sensors for target scenario 1 with a low state prediction covariance and velocity type 3.

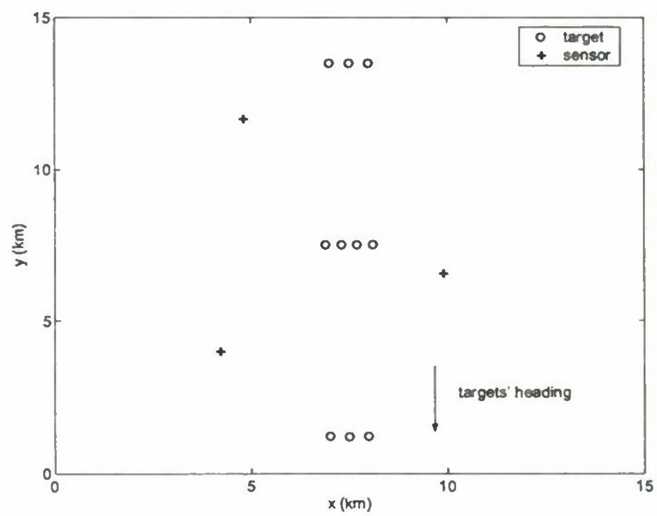

Figure 6: Optimal position of three sensors for target scenario 2 with a low state prediction covariance and velocity type 1.

covariance matrix P_2 is used in the second case. Similar to the previous observations, the sensors in the second case place themselves more uniformly w.r.t. the targets.

5. CONCLUSIONS

In this paper a Fisher information based approach for optimal GMTI sensor placement is presented. The sensors, which measure targets' position along with its radial velocity, are on UAVs that are tracking a number of ground targets. The target detection probability and sensor survival probability are considered while developing the objective function. The target detection probability depends on the target range as well as range rate. A genetic algorithm based search techniques is used to find the optimal sensor locations. Results are obtained for two scenarios each having 10 targets and for different number of sensors. Also, different state prediction covariances and velocity directions are used to observe their effect. The overall track estimation accuracy should increase significantly with this approach. The extension of this work to a dynamic scenario is under investigation.

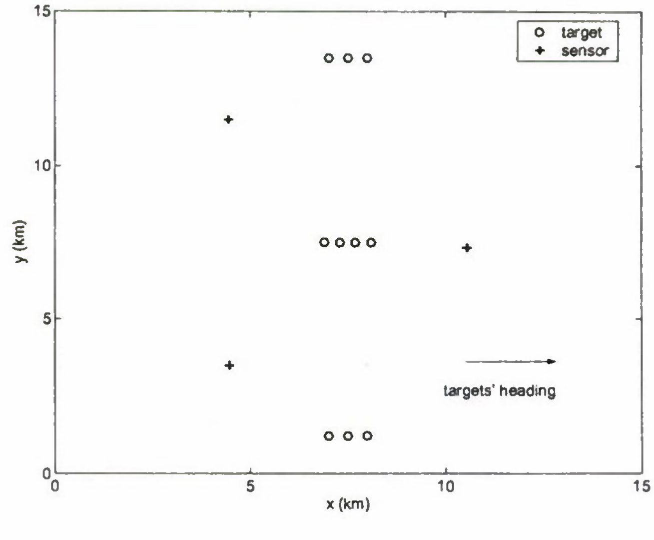

Figure 7: Optimal position of three sensors for target scenario 2 with a low state prediction covariance and velocity type 2.

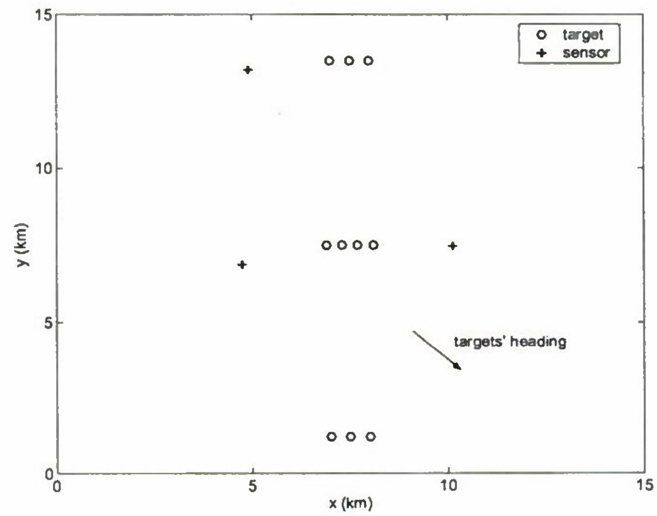

Figure 8: Optimal position of three sensors for target scenario 2 with a low state prediction covariance and velocity type 3.

References

[1] Bar-Shalom, Y., Li, X. R. and Kirubarajan, T., *Estimation with Applications to Tracking and Navigation.* New York: Wiley, 2001.

[2] Bar-Shalom, Y. and Li, X. R., *Multitarget-Multisensor Tracking: Principles and Techniques*, YBS Publishing, 1995.

[3] Beard, R. W., McLain, T. W., Goodrich, M. A. and Anderson, E. P., "Coordinated Target Assignment and Intercept for Unmanned Air Vehicles," *IEEE Trans on Robotics and Automation*, Vol. 18, No. 6, pp. 911-922, Dec. 2002.

[4] Durrant-Whyte, H. and Grocholsky, B., "Management and Control in Decentralised Networks," *Proc. of International Conference on Information Fusion*, pp. 560-565, Cairns, Queensland, Australia, July 2003.

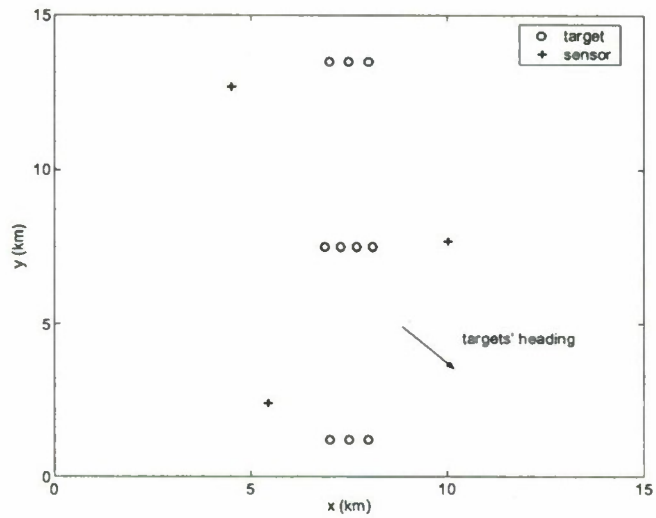

Figure 9: Optimal position of three sensors for target scenario 2 with a high state prediction covariance and velocity type 3.

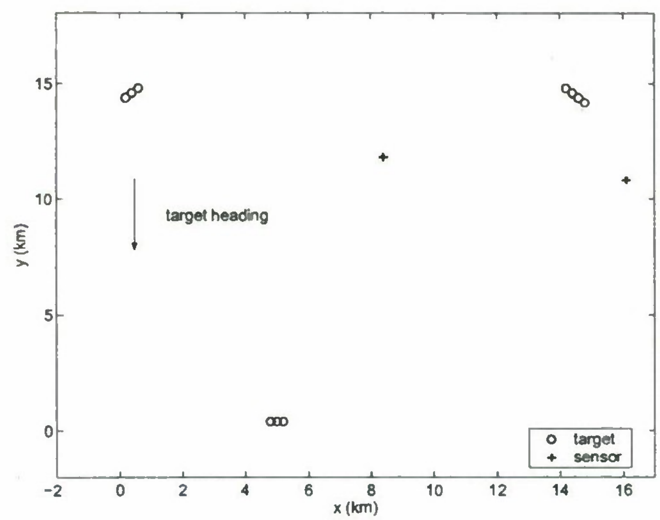

Figure 10: Optimal position of two sensors for target scenario 1 with a low state prediction covariance and velocity type 1.

[5] Flint, M., Polycarpou, M. and Fernandez-Gaucherand., E., "Cooperative Control for Multiple Autonomous UAV's Searching for Targets," Proc. of IEEE Conference on Decision and Control, pp. 2823-2828, Las Vegas, Nevada, Dec. 2002.

[6] Kirubarajan, T., Bar-Shalom, Y., Pattipati, K.R., and Kadar, I, "Ground Target Tracking with Variable Structure IMM Estimator," *IEEE Trans. on on Aerospace and Electrical Systems*, Vol. 36, No. 1, pp. 26-46, Jan. 2000.

[7] Li, S. M. et al., "Automonous Hierachical Control of Multiple Unmanned Combat Vehicles," Proc. of American Control Conference, pp. 274-279, Anchorage, AK, May 2002.

[8] McLain, T. W., Chandler, P. R. and Pachter, M., "A Decomposition Strategy for Optimal Coordination of Unmanned Air Vehicles," *Proc. of American Control Conference*, pp. 369-373, Chicago, IL, June 2000.

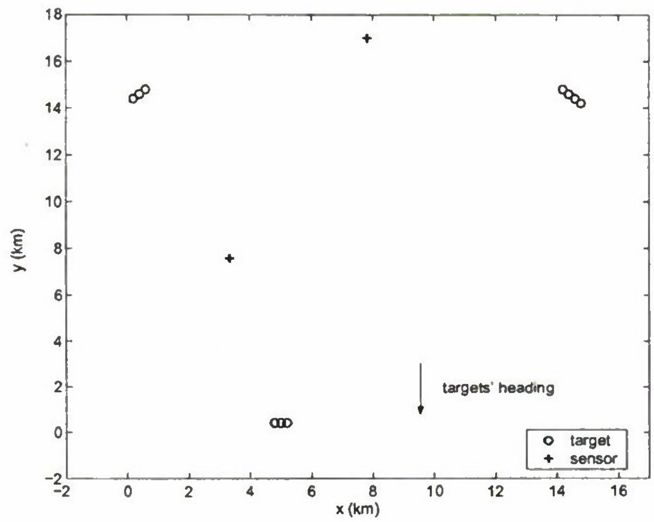

Figure 11: Optimal position of two sensors for target scenario 1 with a high state prediction covariance and velocity type 1.

[9] Patek, S. D., Logan, D. A. and Castanon, D. A., "Approximate Dynamic Programming for the Solution of Multiplatform Path Planning Problems," *Proc. of IEEE conference on Systems, Man, and Cybernetics*, Vol. 1, pp. 1061-1066, Oct. 1999.

[10] Sinha, A., Kirubarajan, T. and Bar-Shalom, Y., "Optimal Cooperative Placement of GMTI UAVs for Ground Target Tracking," *Proc. of IEEE Aerospace Conference*, Big Sky, MT, March 2004.

Autonomous Ground Target Tracking by Multiple Cooperative UAVs

Abhijit Sinha[a], Thiagalingam Kirubarajan[a] and Yaakov Bar-Shalom[b]

[a]Electrical and Computer Engineering Dept.
McMaster University
Hamilton, ON L8S 4K1, Canada

[b]Electrical and Computer Engineering Dept.
University of Connecticut
Storrs, CT 06269, USA

Abstract—With the recent advent of moderate-cost unmanned (or uninhabited) aerial vehicles (UAV) and their success in surveillance, it is natural to consider the cooperative management of groups of UAVs. The problem considered in this paper is the optimization of the information obtained by a group of UAVs carrying out surveillance of several ground targets distributed over a large area. The UAVs are assumed to be equipped with Ground Moving Target Indicator (GMTI) radars, which measure the locations of moving ground targets as well as their radial velocities (Doppler). In this paper, a cooperative control algorithm is proposed, according to which each UAV decides its path independently based on an information theoretic criterion function. The criterion function also incorporates target detection probability and survival probability for sensors corresponding to hostile fire by targets as well as collision with other UAVs. The control algorithm requires limited communication and modest computation.

TABLE OF CONTENTS

1. INTRODUCTION

An important application of control theory is to manage multiple sensors such that the expected information obtained from them is maximized. Management of multiple sensors involves gathering, exchanging and fusing information. With the recent advent of affordable unmanned aerial vehicles (UAV) and their proven effectiveness in surveillance, it is natural to consider the cooperative management of groups of UAVs.

A number of UAV management algorithms can be found in the literature. In [3] a hierarchical approach, which uses a modified Voronoi diagram to generate possible paths and to intercept a number of known targets using a number of UAVs in the presence of dynamic threats, is presented. Similar approaches can be found in [8], [9]. A search algorithm for targets in a given area is proposed in [6], where a discrete time stochastic decision model is formulated as the path planning problem, which is then implemented with a dynamic programming algorithm [11]. However, the aim of [6] is only to detect (not to track) the targets in the search region. In [5] a decentralized sensor management algorithm is presented based on maximizing information gain. In this paper, a online bargaining arrangement between the sensors was used to decide assignment of known targets in two different sensor management problems. The first one addresses a target cueing and hand-off problem related to static sensors and dynamic targets, while the second problem is to generate a coordinated sensor-platform trajectory to obtain information about static features (targets). Another algorithm, presented in [10], uses a coordination framework of virtual bodies and artificial potentials for cooperative control of mobile sensor networks. This algorithm focuses on "gradient climbing missions in which the mobile sensor network seeks out local maxima or minima in the environmental field".

In this paper, a cooperative control algorithm is developed for a number of UAVs, equipped with GMTI sensors, tracking multiple ground targets. An information theoretic criterion, somewhat similar to [5], is used to select the future path of an UAV such that the total information, obtainable by the sensors in the UAVs as a group, corresponding to the detected targets, is maximized. The algorithm proposed in this paper, unlike the one in [5], assumes no prior information about the number of targets or their positions. The criterion function used in this paper, which was partly presented in [12], takes into account the detection probabilities of targets, which are based on both range and range rate, and survival probabilities of the sensors due to hostile fire from targets and possible collision with other UAVs, in computing the information for a particular target-sensor geometry. The simulation results show that the algorithm enables a group of UAVs to gather information in a cooperative manner in the region of interest. The algorithm can incorporate initial information if available; however, it can also work without any initial knowledge. This adaptive algorithm can account for new targets as they appear. The computational complexity and communication requirements of this algorithm are modest enough for the realtime applications related to small UAVs with limited computing power. Finally, because of its distributed approach the algorithm is robust and hence, it does not fail in the eventuality of the loss of some UAVs or communication failure.

Proc. IEEE Aerosp. Conf., Big Sky, MT, March 2005

The paper is organized as follows. Development of the objective function is discussed in Section 2. In Section 3 the cooperative control algorithm is described in detail. Simulation results are presented in Section 4 and Section 5 presents the concluding remarks.

2. OBJECTIVE FUNCTION

The objective function, based on the Fisher information measure is the product of uncertainty volumes [12]

$$J = \sum_j \log |P_j(k|k)^{-1}| \tag{1}$$

where $P_j(k|k)$ is the posterior covariance matrix of the state vector corresponding to target j at time t_k and can be written in terms of the state prediction covariance $P_j(k|k-1)$ and the new information $Y_j(k,s)$ obtainable by the sensors (UAVs) as follows [1]

$$P_j(k|k)^{-1} = P_j(k|k-1)^{-1} + \sum_s \pi_S(s)\pi_D(s,j)Y_j(k,s) \tag{2}$$

where $\pi_D(s,j)$ is the detection probability of target j by UAV s. This probability can be expressed as

$$\pi_D(s,j) = \pi_D^1(s,j)\pi_D^2(s,j) \tag{3}$$

where $\pi_D^1(s,j)$ is the detection probability as a function of the range and $\pi_D^2(s,j)$ is the detection probability factor as a function of the range rate. The nature of the first term is discussed in Section 4. The second term is the probability that the range rate measured by the GMTI sensor is higher than the "minimum detectable velocity" (MDV) and the corresponding computation is available in [12]. The term $\pi_S(s)$ in (2) is the total survival probability of UAV s, which is equal to the product of target-fire survival probability $\pi_S^1(s)$ and collision survival probability $\pi_S^2(s)$ of this UAV, i.e.,

$$\pi_S(s) = \pi_S^1(s)\pi_S^2(s) \tag{4}$$

where $\pi_S^1(s)$, in turn, is the product of target-fire survival probabilities of UAV s in view of each target, i.e.,

$$\pi_S^1(s) = \prod_j \pi_S^1(s,j) \tag{5}$$

and $\pi_S^2(s)$ is the product of collision survival probabilities corresponding to all other UAVs

$$\pi_S^2(s) = \prod_{i,i\neq s} \pi_S^2(s,i) \tag{6}$$

The information $Y_j(k,s)$ obtained by a particular UAV s about target j is given by

$$Y_j(k,s) = H(k,s,j)'R(k,s,j)^{-1}H(k,s,j) \tag{7}$$

where $H(k,s,j)$ is the measurement matrix and $R(k,s,j)$ is the measurement noise covariance matrix corresponding to the sensor-target pair s,j.

In this work, the UAVs are assumed to be equipped with GMTI sensors and the state vector of target j is taken as

$$\mathbf{x} = \begin{bmatrix} x^j & v_x^j & y^j & v_y^j \end{bmatrix} \tag{8}$$

where x and y are the position components in Cartesian coordinate and v_x, v_y are the velocity components. The measurement vector comprises x-y position and radial velocity $\dot{r}$. The measurement matrix, of target j corresponding to sensor s, is given by

$$H(k,s,j) = \begin{bmatrix} 1 & 0 & 0 & 0 \\ 0 & 0 & 1 & 0 \\ 0 & \cos\alpha(k,s,j) & 0 & \sin\alpha(k,s,j) \end{bmatrix} \tag{9}$$

where $\alpha(k,s,j)$ is the azimuth angle of the target j measured by sensor s at time t_k. The original position measurements are in the form of range $r(k,s,j)$ and azimuth $\alpha(k,s,j)$ in the presence of noise, which are converted to x,y position using the standard conversion [1]. The original position measurements in range, azimuth angle and range rate contains independent additive Gaussian noise and the corresponding noise variances are given by σ_r^2, σ_α^2 and $\sigma_{\dot{r}}^2$, respectively. After conversion, the measurement covariance matrix $R(k,s,j)$ is given by

$$R(k,s,j) = \begin{bmatrix} R_{1,1} & R_{1,2} & 0 \\ R_{1,2} & R_{2,2} & 0 \\ 0 & 0 & \sigma_{\dot{r}}^2 \end{bmatrix} \tag{10}$$

where (skipping the arguments)

$$R_{1,1} = r^2\sigma_\alpha^2 \sin\alpha^2 + \sigma_r^2\cos\alpha^2 \tag{11}$$

$$R_{2,2} = r^2\sigma_\alpha^2 \cos\alpha^2 + \sigma_r^2\sin\alpha^2 \tag{12}$$

$$R_{1,2} = (\sigma_r^2 - r^2\sigma_\alpha^2)\sin\alpha\cos\alpha \tag{13}$$

As shown in [13] one can use in (9) the observed azimuth.

3. ALGORITHM

In this section, the algorithm followed by each UAV, which results in cooperative control of the UAVs as a group, is discussed in detail. Each UAV performs the tasks shown in Figure 1 asynchronously w.r.t. the other UAVs. Each UAV scans its environment using a GMTI sensor at an interval of T. The detections, along with this UAV's current position and velocity, are then transmitted to the other UAVs. There is a π_c probability that another UAV will receive this transmission. Each UAV maintains its own set of target tracks, which are updated when a new set of detections is either obtained by this UAV or received from another UAV.

After scanning for measurements, transmitting them and updating the target tracks, each UAV determines its path for the next interval T. For a coordinated operation this decision depends on the corresponding UAV's knowledge about the current locations of the other UAVs and the current state of the target tracks maintained by it. The criterion function J in (1)

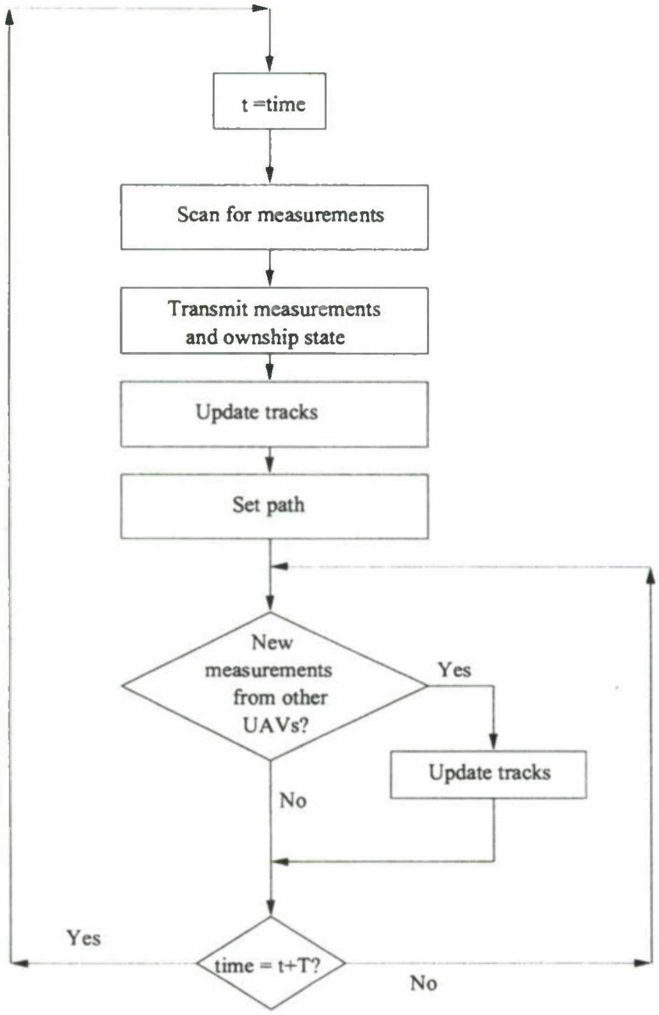

Figure 1. Flow chart of the tasks of each UAV.

is maximized to obtain the paths of the UAVs. The knowledge of the state of another UAV is updated when information is received from that UAV. In case of a failure in communication, the path decided for the particular UAV in the last iteration is assumed to be its actual path. If no information is received from a particular UAV for a number of times, the corresponding UAV is considered to be lost.

After setting its course for next interval T each UAV then waits for any transmission from the other UAVs as shown in Figure 1. If a new set of detections is received from another UAV, then the target tracks, maintained by this UAV, are updated. After T seconds the UAV once again scans its environment with its GMTI sensor and so on.

4. Results

In this section, we present the simulation results obtained for a scenario which has 10 targets moving in three groups as shown in Figure 4. The first group has 4 targets and the other two have 3 targets each. The separation between the targets in each group is 70 m. The target groups move in different directions.

The number of UAVs considered for different cases is from 2 to 4 and each of them starts at y position of -12 km while keeping a distance of 1 km from the closest ones along the x direction. Initially, the UAVs move at a rate of 30 m/s along the $+y$ direction. The UAVs start with no knowledge about the targets and continue in the $+y$ direction until target tracks are formed. Once target measurements are obtained and tracks are formed, each UAV decides its path by maximizing J in (1) based on its knowledge of the positions of the other UAVs and target tracks maintained by the corresponding UAV. Each UAV repetitively performs a set of operations as discussed in Section 3. For this simulation, T is 5 s, which means each UAV performs the set of tasks shown in Figure 1 within that time. Also, the success probability of a communication between two UAVs, which is denoted by π_c in Section 3, is 0.9. In this simulation one point track initialization [13] is applied and track maintenance is performed by a two stage procedure: measurement to track association, which is performed by the auction algorithm [4], and track update using a Kalman filter. A white noise acceleration model is assumed for the targets with process noise standard deviation (s.d.) being 1 m/s^2. The measurement noise s.d. are $\sigma_r = 5$ m, $\sigma_\theta = 10^{-3}$ rad and $\sigma_{\dot{r}} = 1$ m/s. The probability of false alarm in this simulation is 10^{-6} (in a resolution cell of size 20 m $\times$ 4 mrad $\times$ 4 m/s).

Commonly for the tracking algorithms presented in the literature, a track is deleted if it is not associated with measurements for more than a predetermined number of updates. However, this rule is not based on the observability criterion and may result in deletion of tracks because they are unobservable by the sensors used. To avoid this, in this work, a quantity π_{track} is updated each time a set of detections is received, as follows

$$\pi_{\text{track}}(k+1) = \begin{cases} \pi_{\text{track}}(k)(1-\pi_D) & \text{if not associated} \\ 1 & \text{otherwise} \end{cases} \tag{14}$$

where π_D is the probability of detection of the particular track. If π_{track} falls below a predetermined fraction, 10^{-3} in this simulation, the track is deleted from the track list.

In this simulation, the altitude of the UAVs above the ground is considered to be 1 km and the ground is considered to be flat. The UAVs fly at a constant speed of 30 m/s and can perform coordinated turns with angular turn rate upto 3°/s. To set its path for the next period, each UAV decides its angular turn rate by maximizing J in (1). Since J also includes the angular turn rates of the other UAVs, these quantities are also determined in a joint maximization procedure. Matlab function 'fmincon' is used to perform this constrained optimization. The angular turn rates of the other UAVs are not transmitted as each UAV performs this operation independently.

Figure 2 shows the survival probabilities and detection proba-

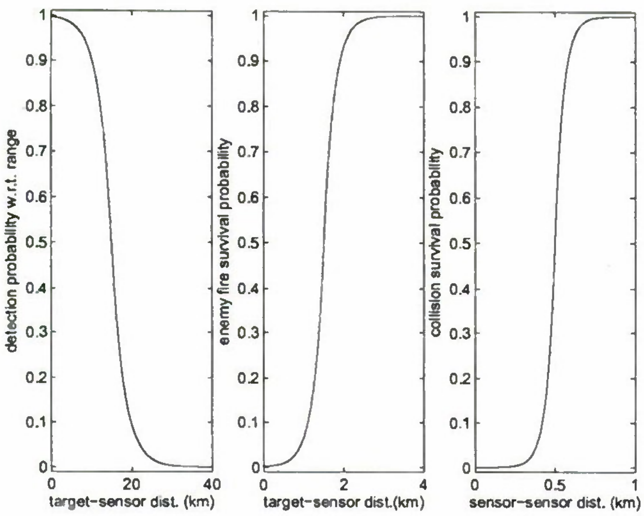

Figure 2. Detection and survival probabilities assumed in this simulation.

bility as a function of range, as used in this simulation. It can be seen that the survival probabilities increase as the target-sensor distance and sensor-sensor distance increase. However, the detection probability w.r.t. range increases as the distance between target-sensor decreases. It is important to note that in a real life scenario the survival and detection probabilities depend on the terrain topography and the algorithm proposed in this work is applicable for any assumption on these probabilities. The detection probability factor as a function of the range rate of a target w.r.t. a sensor is a step function being 1 if the target range rate magnitude is more that 2 m/s and 0 otherwise.

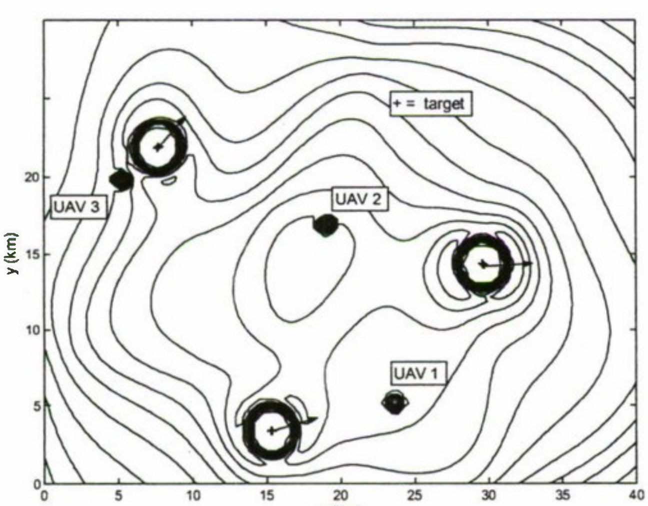

Figure 3. Contour plot of criterion function w.r.t. different position of a fourth UAV.

Figure 3 shows the contour plot of the criterion function for different positions of the fourth UAV in a scenario that has 3 UAVs tracking 10 targets. The criterion function drops near the targets or the sensors forming a barrier. The reason of this behavior is the very low survival probability of the fourth UAV close to the targets or other sensors. Farther from the targets, there are local minima in the direction of target motion. The global minimum is near the center of the plot between 3 targets groups.

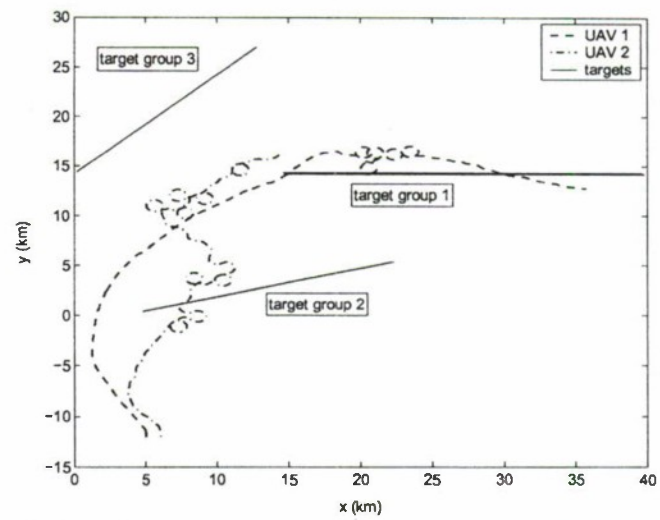

Figure 4. A typical set of paths for 2 UAVs when tracking 10 targets.

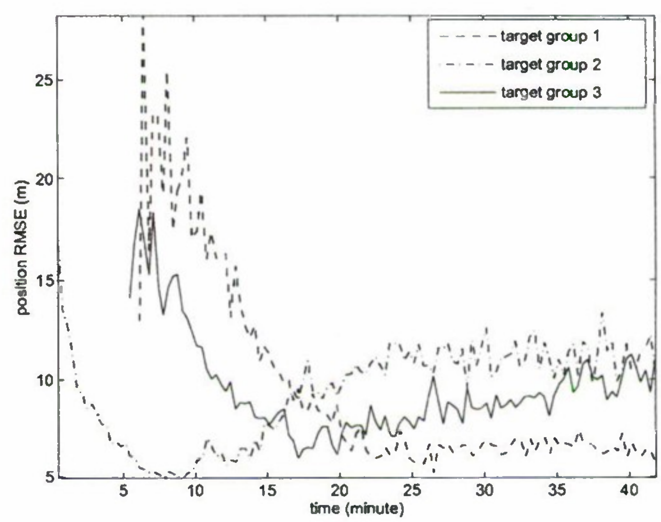

Figure 5. 20 run position RMSE for tracks maintained separately by 2 UAVs.

Figure 4 shows a typical set of paths of UAVs when only two of them are present. It can be seen that UAV 1 tracks target group 1 and UAV 2 tracks target groups 2 and 3[1]. The particular attention to group 1 can be explained by the fact that

[1]None of the UAVs are assigned to a particular target group. However, they can move to a particular target group if that maximizes the total information and in doing so the other groups go out of its detectable range.

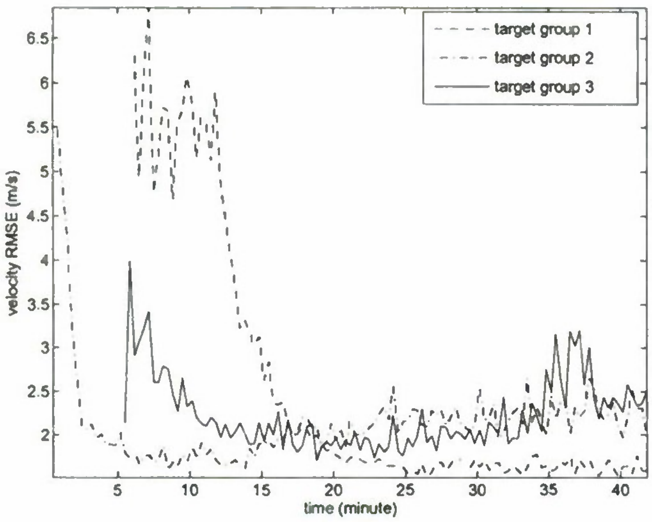

Figure 6. 20 run velocity RMSE for tracks maintained separately by 2 UAVs.

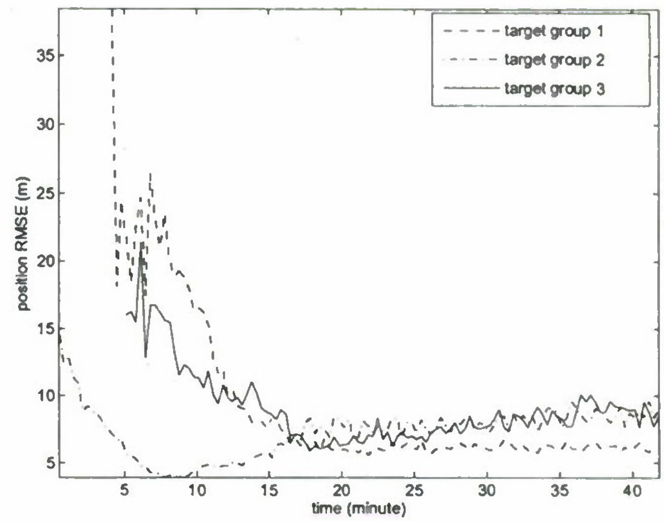

Figure 8. 20 run position RMSE for tracks maintained separately by 3 UAVs.

this group has 4 targets, one more than the other groups. Figures 5 and 6 show a 20 run position and velocity RMSE of the tracks maintained separately by the two UAVs. Since the UAVs start close to target Group 2, these targets are detected first and the RMSEs of the corresponding tracks decrease as the UAVs start moving in their direction. However, once other targets are detected, the UAVs start moving towards them and the RMSEs of the tracks corresponding to target group 2 increase and that for the other groups decrease. At the end of the simulations, the tracks corresponding to target group 1 have minimum position and velocity RMSE.

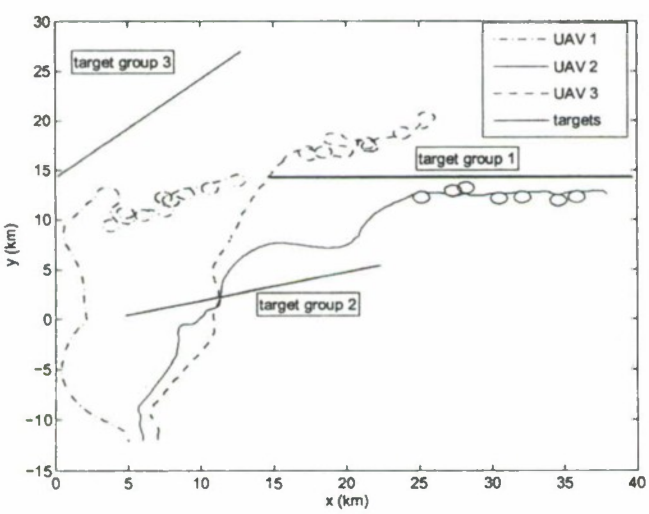

Figure 7. A typical set of paths for 3 UAVs when tracking 10 targets.

Figure 7 shows a typical set of paths of 3 UAVs when tracking the ten targets of the target scenario. In this case, UAV 2 tracks target group 1 and UAV 1 tracks target groups 2 and 3,

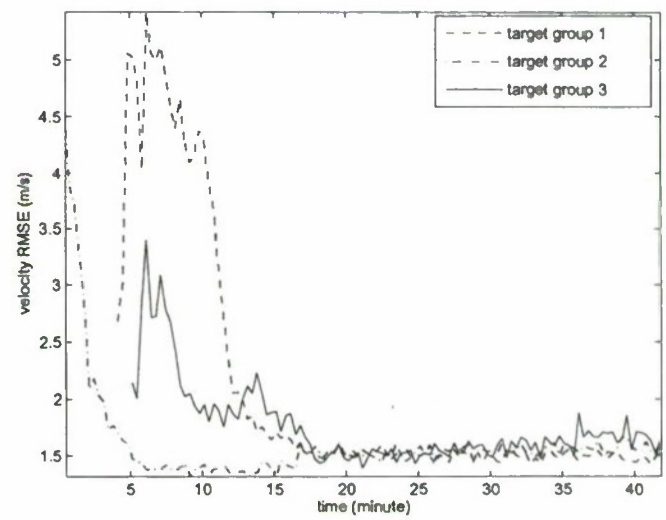

Figure 9. 20 run velocity RMSE for tracks maintained separately by 3 UAVs.

while UAV 3 pays attention to all three target groups. Figures 8 and 9 show a 20 run track position and velocity RMSE when the targets are tracked by 3 UAVs. Once again, target group 2 is detected first and the corresponding tracks have lower position and velocity RMSE in the first part of each simulation. However, once the other targets are detected, the UAVs start moving towards them. Finally, the tracks from target group 1 have the highest position accuracy and all tracks have velocity error of the similar magnitude. The overall RMSE of these tracks are considerably smaller than those of the tracks formed by two UAVs.

Figure 10 shows a typical set of paths of 4 UAVs when tracking the ten targets of the scenario. In this case, UAV 1, 2 and 4

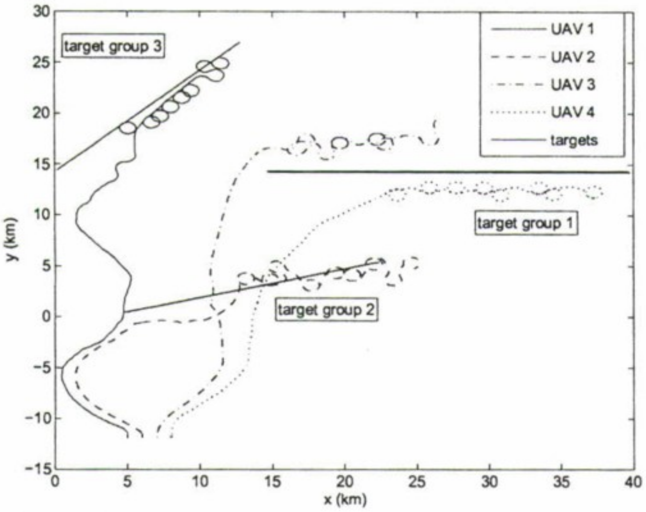

Figure 10. A typical set of paths for 4 UAVs when tracking 10 targets.

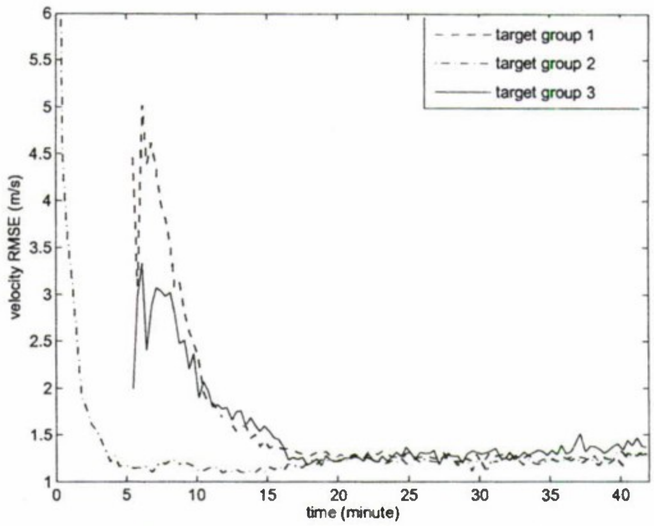

Figure 12. 20 run velocity RMSE for tracks maintained separately by 4 UAVs.

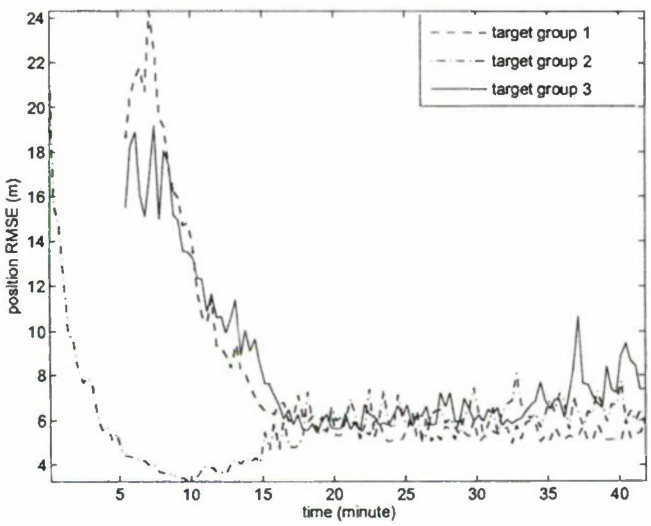

Figure 11. 20 run position RMSE for tracks maintained separately by 4 UAVs.

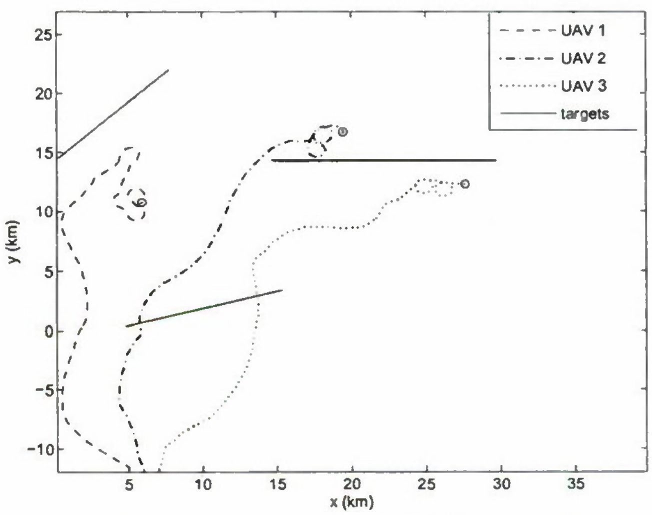

Figure 13. A typical set of paths for 3 UAVs before UAV 3 is lost when tracking 10 targets.

tracks one group each and UAV 3 stays in between and looks over all groups. Figures 11 and 12 show a 20 run position and velocity RMSE of the tracks corresponding to the ten targets. In this case, both of the RMSEs are even smaller. These figures show that at the final stage of the runs target set 3 gets less attention from the UAVs as they concentrate their efforts on the tracks corresponding to the other two target groups which are close to each other.

Figure 13 shows the path of the targets and 3 UAVs for the first 25 minutes of a typical simulation. In this case, UAV 1 is tracking target groups 2 and 3, UAV 2 is tracking all target groups and UAV 3 is tracking target group 1. UAV 3 is lost at 25 minutes and Figure 14, which is the continuation of Figure 13, shows the path of the remaining UAVs and targets after UAV 3 is lost. The end of the UAV paths in Figure 13 and the beginning of the paths in Figure 14 are marked by small circles. From Figure 14 it can be seen that in the absence of UAV 3, UAV 2 moves towards target group 1 and it simultaneously tracks target group 2, while UAV 1 keeps tracking target groups 2 and 3. Figures 15 and 16 show the position and velocity RMSE of the tracks maintained separately by the UAVs. It can be seen that the position and velocity RMSE increase after UAV 3 is lost.

Figure 17 shows a typical path of 3 UAVs when the target-fire survival probabilities of the UAVs are not considered in the criterion function. In this simulation, the minimum distance

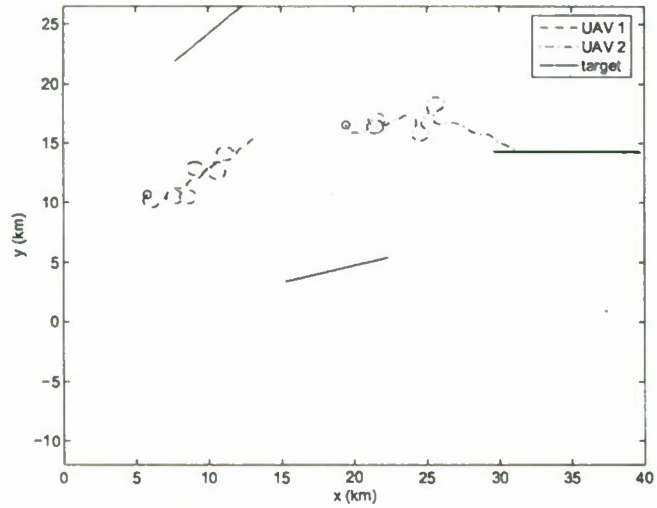

Figure 14. A typical set of paths for 2 UAVs when tracking 10 targets after an UAV is lost. (time 0–25 min)

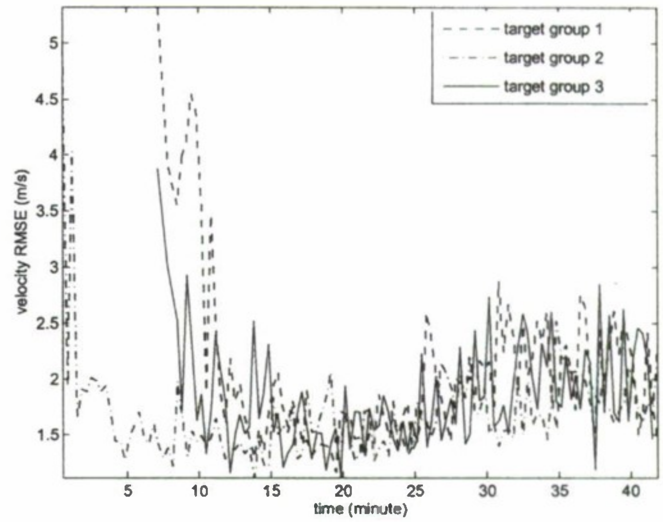

Figure 16. Velocity RMSEs for targets when tracked by 3 UAVs and one of the UAVs is lost.

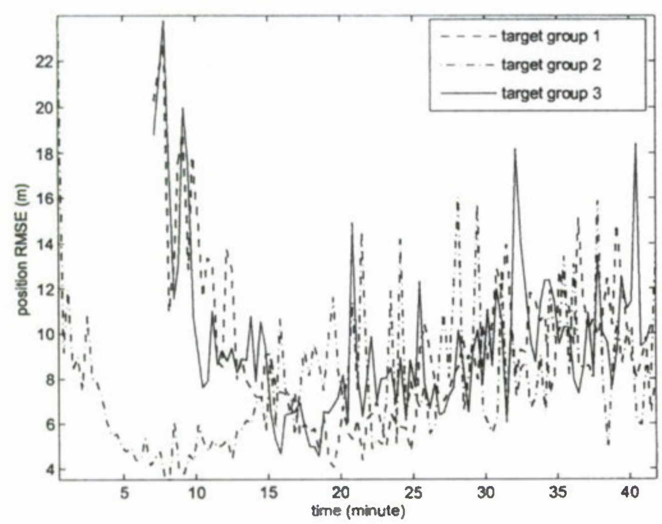

Figure 15. Position RMSEs for targets when tracked by 3 UAVs and one of them is lost. (time 25–40 min)

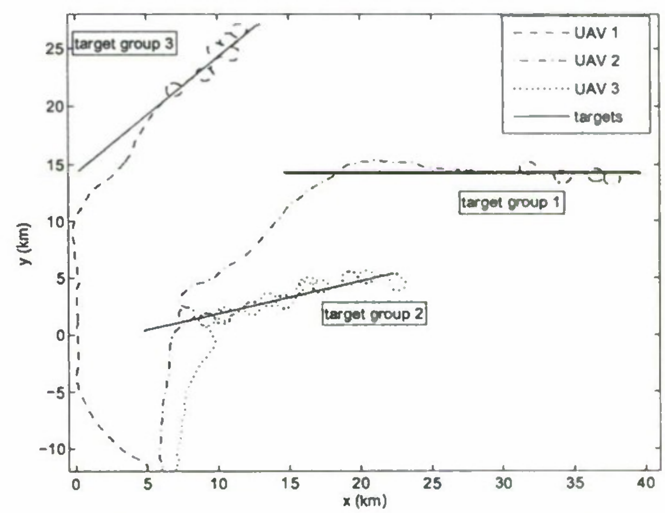

Figure 17. A typical path set of three UAVs while tracking targets of the scenario and when target-fire survival probability is not considered in the criterion function.

between a target and an UAV is less than 3 m, which may be fatal if the targets are hostile. This shows the importance of considering target-fire survival probability for a practical use of information theoretic approach. When this probability is considered the minimum value of target-sensor distance is always more than 1000 m.

Usually, the UAVs do not come close to each other, as such a configuration is not favorable for maximizing information. However, in certain situations, UAVs can cross each other's path and while doing so they might come very close, resulting in a collision. In this work, this possibility is avoided by using the collision survival probability in the criterion function in (1).

5. Conclusions

In this paper, a novel cooperative control algorithm, for a number of UAVs tracking multiple targets, is presented. An information theoretic approach is used for the path selection by the UAVs, which incorporates target detection probability and UAV survival probabilities due to hostile fire by targets and, also, due to collision with other UAVs.

A scenario of 10 targets, which moves in three groups, is simulated and 2-4 UAVs were deployed to track them, in different cases. The results show that the cooperative control algorithm enables the UAVs to maintain almost similar average accuracy for different tracks and, also, the position and velocity RMSE for all tracks decrease as the number of UAVs increase. The robustness of this algorithm in the face of an UAV loss and importance of different probabilities in the criterion function are also demonstrated.

Currently, a joint maximization routine is used to find out the paths of the UAVs. This can be computationally expensive if the number of targets and UAVs increase. For this reason, a prospect of using gradient directions as the directions of motions of the UAVs is being investigated. Also, imposing more constraints on sensors' ability to observe will be another future direction of our work.

REFERENCES

[1] Bar-Shalom, Y., Li, X. R. and Kirubarajan, T., *Estimation with Applications to Tracking and Navigation.* New York: Wiley, 2001.

[2] Bar-Shalom, Y. and Li, X. R., *Multitarget-Multisensor Tracking: Principles and Techniques*, YBS Publishing, 1995.

[3] Beard, R. W., McLain, T. W., Goodrich, M. A. and Anderson, E. P., "Coordinated Target Assignment and Intercept for Unmanned Air Vehicles," *IEEE Trans on Robotics and Automation*, Vol. 18, No. 6, pp. 911-922, Dec. 2002.

[4] Bertsckas, D.P., *Linear Network Optimization: Algorithms and Codes*, MIT Press, Cambridge, MA 1991.

[5] Durrant-Whyte, H. and Grocholsky, B., "Management and Control in Decentralised Networks," *Proc. of International Conference on Information Fusion*, pp. 560-565, Cairns, Queensland, Australia, July 2003.

[6] Flint, M., Polycarpou, M. and Fernandez-Gaucherand., E., "Cooperative Control for Multiple Autonomous UAV's Searching for Targets," *Proc. of IEEE Conference on Decision and Control*, pp. 2823-2828, Las Vegas, Nevada, Dec. 2002.

[7] Kirubarajan, T., Bar-Shalom, Y., Pattipati, K.R., and Kadar, I, "Ground Target Tracking with Variable Structure IMM Estimator," *IEEE Trans. on Aerospace and Electronic Systems*, Vol. 36, No. 1, pp. 26-46, Jan. 2000.

[8] Li, S. M. et al., "Automonous Hierachical Control of Multiple Unmanned Combat Vehicles," *Proc. of American Control Conference*, pp. 274-279, Anchorage, AK, May 2002.

[9] McLain, T. W., Chandler, P. R. and Pachter, M., "A Decomposition Strategy for Optimal Coordination of Unmanned Air Vehicles," *Proc. of American Control Conference*, pp. 369-373, Chicago, IL, June 2000.

[10] Ogren, P., Fiorelli, E. and Leonard, N. E., "Cooperative Control of Mobile Sensor Networks: Adaptive Gradient Climbing in a Distributed Environment", *IEEE Trans. on Automatic Control*, Vol. 49, No. 8, pp. 1292-1302, Aug. 2004.

[11] Patek, S. D., Logan, D. A. and Castanoñ, D. A., "Approximate Dynamic Programming for the Solution of Multiplatform Path Planning Problems," *Proc. of IEEE conference on Systems, Man, and Cybernetics*, Vol. 1, pp. 1061-1066, Oct. 1999.

[12] Sinha, A., Kirubarajan, T. and Bar-Shalom, Y., "Optimal Cooperative Placement of UAVs for Ground Target Tracking with Doppler Radar", *Proc. of SPIE Signal Processing, Sensor Fusion, and Target Recognition*, Orlando, FL, April 2004.

[13] Yeom, S. W., Kirubarajan, T. and Bar-Shalom, Y., "Track Segment Association, Fine-step IMM and Initialization with Doppler for Improved Track Performance", *IEEE Trans. on Aerospace and Electronic Systems*, Vol. 40, No. 1, pp. 293-309, Jan. 2004.

Abhijit Sinha was born in India in 1972. He has received his B.S. degree in physics from the University of Calcutta in 1994. He received his M.S. degree in electrical communication engineering from Indian Institute of Science, Bangalore in 1998 and also received his Ph.D. degree in electrical and computer engineering form the University of Connecticut in 2002. He has worked as a Postdoctoral Fellow in the University of Connecticut from 2002 to 2003. Currently he is working as a research associate in McMaster University, Canada. His research interests include signal processing, target tracking and communications.

***Thiagalingam Kirubarajan** (S'95, M'98) was born in Sri Lanka in 1969. He received the B.A. and M.A. degrees in electrical and information engineering from Cambridge University, England, in 1991 and 1993, and the M.S. and Ph.D. degrees in electrical engineering from the University of Connecticut, Storrs, Connecticut in 1995 and 1998, respectively. Currently, Dr. Kirubarajan is an Assistant Professor in the Electrical and Computer Engineering Department at McMaster University, Hamilton, Ontario. He is also serving as an Adjunct Assitant Professor and the Associate Director of the Estimation and Signal Processing Research Laboratory at the University of Connecticut, USA.*

Dr. Kirubarajan's research interests are in estimation, target tracking, multisource information fusion, sensor resource management, signal detection and fault diagnosis. He has published about 100 articles in these research areas, in addition to one book on estimation, tracking and navigation and two edited volumes. Dr. Kirubarajan's research activities at

McMaster University and at the University of Connecticut are supported by US Missile Defense Agency, US Office of Naval Research, NASA, Qualtech Systems, Inc., Raytheon Canada Ltd. and Defense Research Development Canada, Ottawa. In September 2001, Dr. Kirubarajan served in a DARPA expert panel on unattended surveillance, homeland defense and counterterrorism. He has also served as a consultant in these areas to a number of companies, including Motorola Corporation, Northrop-Grumman Corporation, Pacific-Sierra Research Corporation, Lockhead Martin Corporation, Qualtech Systems, Inc., Orincon Corporation and BAE systems. He has worked on the development of a number of engineering software programs, including BEARDAT for target localization from bearing and frequency measurements in clutter, FUSEDAT for fusion of multisensor data for tracking. He has also worked with Qualtech Systems, Inc., to develop an advanced fault diagnosis engine. He is also a recipient of Ontario Premier's Research Excellence Award (2002).

Yaakov Bar-Shalom *(S'63-M'66-SM'80-F'84) was born on May 11, 1941. He received the B.S. and M.S. degrees from the Technion, Israel Institute of Technology, in 1963 and 1967 and the Ph.D. degree from Princeton University in 1970, all in electrical engineering. From 1970 to 1976 he was with Systems Control, Inc., Palo Alto, California. Currently he is Board of Trustees Distinguished Professor in the Dept. of Electrical and Computer Engineering and Director of the ESP (Estimation and Signal Processing) Lab at the University of Connecticut. His current research interests are in estimation theory and target tracking and has published over 280 papers and book chapters in these areas and in stochastic adaptive control.*

He coauthored the monograph **Tracking and Data Association** *(Academic Press, 1988), the graduate texts* **Estimation and Tracking: Principles, Techniques and Software** *(Artech House, 1993),* **Estimation with Applications to Tracking and Navigation: Algorithms and Software for Information Extraction** *(Wiley, 2001), the advanced graduate text* **Multitarget-Multisensor Tracking: Principles and Techniques** *(YBS Publishing, 1995), and edited the books* **Multitarget-Multisensor Tracking: Applications and Advances** *(Artech House, Vol. I, 1990; Vol. II, 1992; Vol. III, 2000).*

He has been elected Fellow of IEEE for "contributions to the theory of stochastic systems and of multitarget tracking". He has been consulting to numerous companies and government agencies, and originated the series of Multitarget-Multisensor Tracking short courses offered via UCLA Extension, at Government Laboratories, private companies and overseas. He has also developed the commercially available interactive software packages MULTIDAT™ for automatic track formation and tracking of maneuvering or splitting targets in clutter, VARDAT™ for data association from multiple passive/active sensors, BEARDAT™ for LO target localization from passive measurements, IMDAT™ for image segmentation and target centroid tracking and FUSEDAT™ for tracking with fusion of heterogeneous multisensor data.

During 1976 and 1977 he served as Associate Editor of the IEEE Transactions on Automatic Control and from 1978 to 1981 as Associate Editor of Automatica. He was Program Chairman of the 1982 American Control Conference, General Chairman of the 1985 ACC, and Co-Chairman of the 1989 IEEE International Conference on Control and Applications. During 1983-87 he served as Chairman of the Conference Activities Board of the IEEE Control Systems Society and during 1987-89 was a member of the Board of Governors of the IEEE CSS. He is a member of the Board of Directors of the International Society of Information Fusion (1999–2004) and served as General Chairman of FUSION 2000 and President of ISIF in 2000 and 2002.

In 1987 he received the IEEE CSS Distinguished Member Award. Since 1995 he is a Distinguished Lecturer of the IEEE AESS and has given several keynote addresses at major national and international conferences. He is co-recipient of the M. Barry Carlton Award for the best paper in the IEEE Transactions on Aerospace and Electronic Systems in 1995 and 2000 and the 1998 University of Connecticut AAUP Excellence Award for Research. In 2002 he received the J. Mignona Data Fusion Award from the DoD JDL Data Fusion Group.

Autonomous Surveillance by Multiple Cooperative UAVs*

A. Sinha[a], T. Kirubarajan[a] and Y. Bar-Shalom[b]
[a]Estimation, Tracking and Fusion Laboratory (ETFLab),
Electrical & Computer Engineering Department, McMaster University,
Hamilton, Ontario, Canada.
[b]Estimation and Signal Processing Laboratory (ESPLab),
Electrical & Computer Engineering Department, University of Connecticut,
Storrs, CT, USA.

ABSTRACT

With the recent advent of moderate-cost unmanned (or uninhabited) aerial vehicles (UAV) and their success in surveillance, it is natural to consider the cooperative management of groups of UAVs. The problem considered in this paper is the optimization of the information obtained by a group of UAVs carrying out surveillance — search and tracking — over a large region which includes a number of targets. The goal is to track detected targets as well as search for the undetected ones. The UAVs are assumed to be equipped with Ground Moving Target Indicator (GMTI) radars, which measure the locations of moving ground targets as well as their radial velocities (Doppler). In this paper, a decentralized cooperative control algorithm is proposed, according to which the UAVs exchange current scan and detection information and each UAV decides its path separately based on an information based objective function that incorporates target state information as well as target detection probability and survival probability for sensors corresponding to hostile fire by targets and collision with other UAVs. The proposed algorithm requires limited communication and modest computation and it can handle failure in communication and loss of UAVs.

Keywords: Multisensor-multitarget tracking, sensor management, cooperative control, UAV placement, ground target tracking.

1. INTRODUCTION

An important application of control theory is to manage multiple sensors such that the information obtained from the surveillance region is maximized. Management of multiple sensors involves gathering, exchanging and fusing information. With the recent advent of affordable unmanned aerial vehicles (UAV), a considerable amount of research effort has been directed toward mobile sensor management, which also includes path planning. The advantages of UAVs include removal of the risk to human operators, lower cost, smaller size/weight, greater maneuverability and possibility of effective coordination. For these reasons, in future, UAVs would be extensively used in surveillance, search/rescue, communication and other military and civilian applications.

A number of UAV management algorithms can be found in the literature. In [13] a cooperative control algorithm for multiple UAVs to simultaneously reach a predetermined target location, which maximizes survivability of the UAVs due to exposure to threats while adhering to fuel constraint, is addressed. A hierarchical decision mechanism is proposed in which at team level the estimated time until arrival is computed and at UAV level path planning is performed. In [3] a similar approach, which include Voronoi diagram in path planning, is used for the simultaneous intercept problem in the presence of dynamic threats. Similar approaches can be found in [6, 11, 14]. In [9] another hybrid control structure is proposed for the simultaneous intercept problem. Here, UAV-to-target allocation and time to reach the targets are decided in the central node, while the path decisions are taken locally in UAVs.

In [15] a multi-vehicle path planning problem in hostile environment is solved by dynamic programming. In this centralized algorithm path decisions are taken in terms of connecting pre-defined way-points. In [16] a decentralized cooperative search algorithm is proposed in which UAVs exchange environment information but independently decides their paths by minimizing a convex combination of costs associated with subgoals. It can

*Proc. of SPIE Conf. on Signal and Data Processing of Small Targets (#5913-64), San Diego, CA, August 2005.

be noted that for UAV management problems decentralized algorithms is preferred as they have advantages of graceful degradation, scalability and modularity properties over the centralized ones. In [8], for a search problem, dynamic programming is used to make finite horizon decisions. Note that our problem includes search as well as tracking.

In [7] a decentralized sensor management algorithm, based on maximizing information gain, is presented. In this paper, an online negotiation arrangement between the sensors is used to decide the assignment of known targets to generate a coordinated sensor-platform trajectory for obtaining information about static features (targets). In [5] a decentralized multi-UAV search algorithm, for a lost vehicle in stationary state, is proposed. This algorithm is synchronous, according to which each UAV negotiates with others by communicating the expected measurement likelihood for its best path given the measurement likelihood of other UAVs.

In our previous work [17], which describes a UAV placement algorithm, a preliminary version of the objective function, which is used for UAV path planning in the current work, is presented. However, in [17] only previously detected targets are considered in the objective function as the goal of this algorithm is tracking, not searching. An extension of this paper for the dynamic tracking scenario is presented in [18]. Here, too, searching for new target was not the goal. Also, the UAVs are considered to be able to scan a large region in which the probability of detection is nonzero.

In this paper, a decentralized cooperative control algorithm is developed for a number of UAVs, equipped with GMTI sensors, to track multiple ground targets and search for new ones in a specified region. The region is divided into a number of square sectors[1] and it is assumed that each UAV can scan N_s sectors each time. In the proposed algorithm the UAVs exchange the information about the sectors scanned, measurements obtained and their current kinematic states. Each UAV decides the sectors it scans and the path it follows on its own. In this work these decisions are decoupled into two separate problems. An information based objective function is used to select the future path of a UAV such that the total information, obtainable by the sensors in the UAVs as a group, corresponding to the detected targets, is maximized. In addition, this objective function incorporates possible information from the undetected targets, which are included in the form of possible targets at the center of the sectors. The objective function used in this paper takes into account the detection probabilities of targets, which are based on both range and range rate, and the survival probabilities of the sensors due to hostile fire from targets and possible collision with other UAVs, in computing the information for a particular target-sensor geometry.

The algorithm proposed in this paper starts with no prior information about the number of targets or their positions. Nonetheless, it is possible to incorporate prior information, if available. The simulation results show that the algorithm enables a group of UAVs to gather information in a cooperative manner in the region of interest and to detect new targets as they appear. The computational complexity and communication requirements of this algorithm are modest enough for the real time applications related to small UAVs with limited computing power. Finally, because of its decentralized approach the algorithm is robust and hence, it does not fail in the eventuality of loss of some UAVs or communication failure.

The paper is organized as follows. Development of the objective function for path planning is discussed in Section 2. In Section 3 the cooperative control algorithm is described in detail. Simulation results are presented in Section 4 and Section 5 presents the concluding remarks.

2. OBJECTIVE FUNCTION FOR PATH PLANNING

One of the most important stages in the development of a sensor management algorithm is the choice of objective function which requires to be easy to compute and the decisions based on this function should enable the algorithm to achieve sensor management goals. In this work we consider the following objective function

$$J(k) = \sum_j \left(\ln|I_j(k|k)| - \ln|I_j(k|k-1)|\right) + \sum_{\{m,n\}\in S_D} \left(\ln|\tilde{I}_{m,n}(k)| - \ln|I^0_{m,n}|\right) \tag{1}$$

[1] Note that it is possible to incorporate any other shapes of sectors in this algorithm.

where $I_j(k|k-1)$ and $I_j(k|k)$ are the predicted and updated information matrices for a target j at time step k, $\bar{I}_{m,n}(k)$ is the expected information matrix of new targets in sector $\{m,n\}$ of the surveillance region and $S_{\bar{D}}$ is the set all sectors in which there are no currently tracked targets; $I^0_{m,n}$ is the prior information in sector $\{m,n\}$ where the uncertainty is the same as that of a target that can be anywhere in the sector and move at any possible velocity.

The information matrices in (1) are in the Fisher sense which means they are the inverses of the corresponding covariance matrices. J is the total information gain related to all targets under independence and equal weight assumptions [12]. Also, each term of J is the difference between the information after update and before update. The individual information in (1), which is the (natural) logarithm of determinant of the corresponding information matrix, is similar to the negative of Shanon's entropy, ignoring a constant, under the assumption of Gaussian error. As entropy is the uncertainty associated with a random variable, it makes sense to use the negative of entropy as information. It can be noted that we deviate from the "negative of expected value of logarithm of the density function" definition to a more convenient "logarithm of the determinant of information matrix" definition of information. Both definitions result in similar functions for a Gaussian density.

Let us consider that the predicted covariance of a target is $\bar{P}$ (denoted without time argument, for simplicity) in a linear Gaussian system. Also, there is a probability π_D of this target being detected at this instant. Hence the updated covariance is given by

$$P = \begin{cases} \bar{P} - \bar{P}H'(H\bar{P}H' + R)^{-1}H\bar{P} & \text{if the target is detected} \\ \bar{P} & \text{otherwise} \end{cases} \tag{2}$$

where H and R are the measurement matrix and the measurement covariance matrix, respectively. The expected updated covariance matrix is

$$P = \bar{P} - \pi_D \bar{P}H'(H\bar{P}H' + R)^{-1}H\bar{P} \tag{3}$$

where the detection event is assumed to be independent of the measurement or process noise. However, in this case the information matrix does not have a simple form similar to $\bar{P}^{-1} + H'R^{-1}H$ unless π_D takes one of the extreme values. Since it is much more convenient to work with a form in which total matrix information is summation of the information from different (independent) sources, in this work we use the expected updated information given by

$$I = \bar{I} + \pi_D H'R^{-1}H \tag{4}$$

where $\bar{I}$ and I are the predicted information and expected updated information, respectively. Note that the expected updated covariance is given only approximately by the inverse of the expected updated information.

In our problem the UAVs scan the targets asynchronously which, in general, leads to a complicated objective function. However, if the offset times are small, as in our case, the target-sensor geometry does not change much from the scan by one UAV to that by another one. Hence, for convenience, the objective function is constructed assuming synchronous scans by all sensors.

The detection probability of target j by sensor s at time step k is written as

$$\pi_D(k,s,j) = \pi_D^1(k,s,j)\pi_D^2(k,s,j) \tag{5}$$

where $\pi_D^1(k,s,j)$ is the detection probability (of target j by UAV s at time k) as a function of the range and $\pi_D^2(k,s,j)$ is the detection probability as a function of the range rate. The first term depends on the specific application and the second term is the probability that the range rate measured by the GMTI sensor is higher than "minimum detectable velocity" (MDV), discussed later in this section.

The total survival probability of UAV s, which is equal to the product of target-fire survival probability $\pi_S^1(k,s)$ and collision survival probability $\pi_S^2(k,s)$ of this UAV, i.e.,

$$\pi_S(k,s) = \pi_S^1(k,s)\pi_S^2(k,s) \tag{6}$$

where $\pi_S^1(k,s)$, in turn, is the product of target-fire survival probabilities of UAV s in view of each target, i.e.,

$$\pi_S^1(k,s) = \prod_j \pi_S^1(k,s,j) \tag{7}$$

and $\pi_S^2(k,s)$ is the product of collision survival probabilities corresponding to all other UAVs

$$\pi_S^2(k,s) = \prod_{i,i\neq s} \pi_S^2(k,s,i) \tag{8}$$

The nature of these survival probabilities is application dependent.

The combined probability that sensor s contributes to the information about target j at time k is given by $\pi_D(k,s,j)\pi_S(k,s)$. The information obtained by a particular UAV s about target j at time k is given by $H(k,s,j)'R(k,s,j)^{-1}H(k,s,j)$ where $H(k,s,j)$ is the measurement matrix and $R(k,s,j)$ is the measurement noise covariance matrix corresponding to the sensor-target pair s,j.

The approximate expected information matrix of target j, following (4), due to the scans by all sensors, is given by

$$I_j(k|k) \quad = \quad I_j(k|k-1) + \sum_s \pi_S(k,s)\pi_D(k,s,j)H(k,s,j)'R(k,s,j)^{-1}H(k,s,j) \tag{9}$$

where $I_j(k|k-1) = P_j(k|k-1)^{-1}$. Note that in the above equation the survival event, detection event and measurement errors are assumed independent.

For the sectors that do not contain any of the currently tracked targets, new (undetected) targets are the possible source of information. The prior information for sector $\{m,n\}$, which is discussed before in this section, is denoted by $I_{m,n}^0$. The new information obtained by a sensor s from sector $\{m,n\}$ at time step k is zero if there is no detection and $\tilde{H}(k,s,m,n)'\tilde{R}(k,s,m,n)^{-1}\tilde{H}(k,s,m,n)$ if a detection occurs, where $\tilde{H}(k,s,m,n)$ is the measurement matrix and $\tilde{R}(k,s,m,n)$ is the measurement covariance matrix corresponding to the new target. Note that the position of a new target is assumed to be at the center of the sector. The probability of a new target detection event in sector $\{m,n\}$ is given by the product of the probability of detection $\tilde{\pi}_D(k,s,m,n)$ and the probability of the presence of a new target $\tilde{\pi}_{\text{new}}(k,m,n)$ in this sector, i.e.,

$$\tilde{\pi}_{D,\text{new}}(k,s,m,n) = \tilde{\pi}_D(k,s,m,n)\tilde{\pi}_{\text{new}}(k,m,n) \tag{10}$$

where the term $\tilde{\pi}_D(k,s,m,n)$ is similar to $\pi_D^1(k,s,j)$. The only difference is that the former is a function of the sensor range from the center of a sector while the latter is a function of the range between the sensor and target. Note that here the factor for the range rate is considered to be unity as no realistic assumption of this quantity can be made for an undetected target. The second term in the right hand side of (10), which represents probability of presence of a new target, is defined in Section 3.

As discussed before, the expected information matrix from sector $\{m,n\}$ when scanned by sensor s at time step k is taken as

$$I_{m,n}(k,s) = I_{m,n}^0 + \tilde{\pi}_{D,\text{new}}(k,s,m,n)\tilde{H}(k,s,m,n)'\tilde{R}(k,s,m,n)^{-1}\tilde{H}(k,s,m,n) \tag{11}$$

In this work, in order to restrict more than one UAV from moving toward the same unscanned sector, only the maximum information form all sensors is included in the cost function instead of considering the summation of information, i.e.,

$$\tilde{I}_{m,n}(k) = \max_s \ \ln|I_{m,n}(k,s)| \tag{12}$$

The UAVs are assumed to be equipped with GMTI sensors and the state vector of target j is taken as

$$\mathbf{x} = \begin{bmatrix} x^j & v_x^j & y^j & v_y^j \end{bmatrix} \tag{13}$$

where x, y are the position components in Cartesian coordinates and v_x, v_y are the velocity components. The measurement vector comprises of x-y position and radial velocity $\dot{r}$. The measurement matrix, of target j corresponding to sensor s, is given by

$$H(k,s,j) = \begin{bmatrix} 1 & 0 & 0 & 0 \\ 0 & 0 & 1 & 0 \\ 0 & \cos\alpha(k,s,j) & 0 & \sin\alpha(k,s,j) \end{bmatrix} \tag{14}$$

where $\alpha(k,s,j)$ is the azimuth angle of the target j measured by sensor s at time t_k. The original position measurements are in the form of range $r(k,s,j)$ and azimuth $\alpha(k,s,j)$ in the presence of noise, which are converted to x,y position using the standard conversion [1]. The original position measurements in range, azimuth angle and range rate contains independent additive Gaussian noise and the corresponding noise variances are given by σ_r^2, σ_α^2 and $\sigma_{\dot{r}}^2$, respectively. After conversion, the measurement covariance matrix $R(k,s,j)$ is given by

$$R(k,s,j) = \begin{bmatrix} R_{1,1} & R_{1,2} & 0 \\ R_{1,2} & R_{2,2} & 0 \\ 0 & 0 & \sigma_{\dot{r}}^2 \end{bmatrix} \tag{15}$$

where (skipping the arguments)

$$R_{1,1} = r^2\sigma_\alpha^2 \sin\alpha^2 + \sigma_r^2 \cos\alpha^2 \tag{16}$$

$$R_{2,2} = r^2\sigma_\alpha^2 \cos\alpha^2 + \sigma_r^2 \sin\alpha^2 \tag{17}$$

$$R_{1,2} = (\sigma_r^2 - r^2\sigma_\alpha^2)\sin\alpha\cos\alpha \tag{18}$$

As shown in [19] one can use the observed azimuth in (14) to allow a linear model for the range rate measurement. Note that the computation of $\tilde{R}(k,s,m,n)$ is similar to that of $R(k,s,j)$. For the former, the position of target is assumed to be at the center of the sector.

For a GMTI radar, if the magnitude of the measured value of the range rate for a target falls below a threshold $\dot{r}_{\text{min}}$ then the target will not be detected. Hence, $\pi_D^2(k,s,j)$ is given by

$$\pi_D^2(k,s,j) = 1 - P\{-\dot{r}_{\text{min}} < \dot{r}(k,s,j) < \dot{r}_{\text{min}} \mid \dot{r}(k,s,j|k-1), \sigma_{\dot{r}}(k,s,j|k-1)^2\} \tag{19}$$

where $\dot{r}(k,s,j)$ is the measured range rate and $\dot{r}(k,s,j|k-1)$ is the predicted range rate given by

$$\dot{r}(k,s,j|k-1) = v_x^j(k|k-1)\cos\alpha(k,s,j|k-1) + v_y^j(k|k-1)\sin\alpha(k,s,j,|k-1) \tag{20}$$

where $v_x^j(k|k-1)$, $v_y^j(k|k-1)$ are the components of predicted velocity and $\alpha(k,s,j,|k-1)$ is the predicted azimuth angle for target j.

The variance term $\sigma_{\dot{r}}(k,s,j|k-1)^2$ in (19) is the range rate measurement prediction variance which is the third diagonal term of the innovation covariance matrix

$$S(k,s,j) = H(k,s,j)P_j(k|k-1)H(k,s,j)' + R(k,s,j) \tag{21}$$

where in $H(k,s,j)$ the measured azimuth angle $\alpha(k,s,j)$ is replaced by the predicted azimuth angle $\alpha(k,s,j|k-1)$.

Hence $\pi_D^2(k,s,j)$ in (19) is evaluated by integrating a Gaussian density with mean $\dot{r}(k,s,j|k-1)$ and variance $\sigma_{\dot{r}}(k,s,j|k-1)^2$ in the interval $-\dot{r}_{\text{min}}$ to $\dot{r}_{\text{min}}$ and subtracting the result from unity. This is available from the tabulated standard error function.

3. ALGORITHM

In this section, the algorithm used by each UAV, which results in cooperative control of the UAVs as a group, is discussed in detail. This algorithm is capable of tracking detected targets and to search for undetected ones by taking into account that new targets can start from the regions already been scanned. The surveillance region is divided into sectors and it is assumed that each UAV is capable of scanning N_s sectors in each time period T. In this algorithm the decisions on path selection and sectors to scan are taken separately by the UAVs. However, these decisions are indirectly connected as a scan in a particular sector reduces the information available from this sector which in turn affects the next path decision.

In this work the probability of existence of a new target in a sector $\{m,n\}$, which is required to compute information from new sectors as shown in (10), is assumed to have the following form

$$\tilde{\pi}_{\text{new}}(k,m,n) = \tilde{\pi}_{\text{max}}(m,n)\left(1 - e^{-(t_k - \hat{s}_{m,n}(k))/\lambda_{m,n}}\right) \tag{22}$$

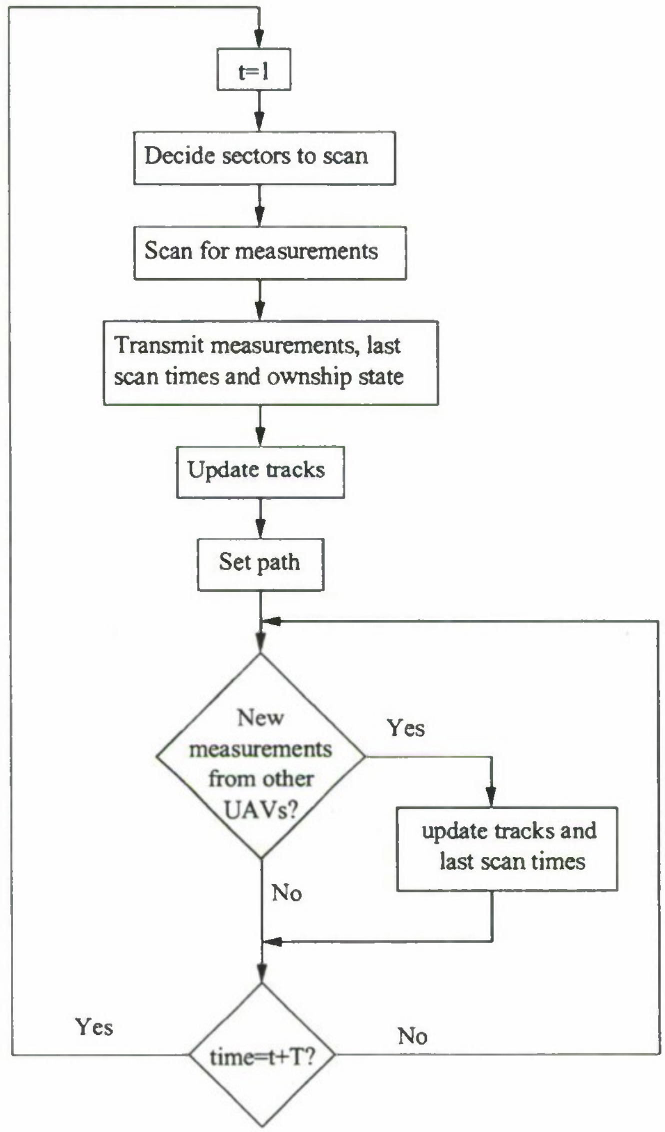

Figure 1. Flow chart of the tasks of each UAV.

where t_k is the scan time at step k, $\bar{\pi}_{\max}(m,n)$ is the maximum value of the probability of new target, $\hat{s}_{m,n}$ is the equivalent last scan time and $\lambda_{m,n}$ is a parameter that defines the rate of increase of the probability of a new target after a scan in sector $\{m,n\}$. This models the "appearance" of a new target since the last scan of the sector under consideration. The parameters $\bar{\pi}_{\max}(m,n)$ and $\lambda_{m,n}$ are application dependent which can be chosen to give different importance to different sectors. The equivalent last scan time $\hat{s}_{m,n}$ is updated after a scan by sensor s as follows

$$\hat{s}_{m,n}(k^+) = \begin{cases} \hat{s}_{m,n}(k) & \text{if not scanned} \\ t_k & \text{if scanned and target detected} \\ t_k - \Delta(k,s,m,n,s) & \text{if scanned and target not detected} \end{cases} \tag{23}$$

where k^+ denotes time immediately after the scan at t_k and $\Delta(k,s,m,n)$ is given by

$$\Delta(k,s,m,n) = -\lambda_{m,n} \ln\left[1 - \left(1 - e^{-(t_k - \hat{s}_{m,n}(k))/\lambda_{m,n}}\right)[1 - \bar{\pi}_D(k,s,m,n)]\right] \tag{24}$$

In this algorithm each UAV stores the equivalent last scan time of each sector to keep track of the new target probability, which needs update only if the corresponding sector is scanned. The derivation of (24) is discussed in Appendix.

Each UAV performs the tasks shown in Figure 1 asynchronously w.r.t. the other UAVs. Each UAV scans N_s sectors at an interval of T using a GMTI sensor. The decision about which sectors to scan is taken separately from the path decision of this UAV and it does not depend on the state of the other UAVs. The information from each section is computed and the best N_s sections are chosen, on that basis, for this scan.

A function similar to (1) is used for search decision. The only difference is that the information contribution from the other sensors is not considered. If there are $N_{m,n}(k)$ targets in sector $\{m,n\}$ at time step k then the modified information, corresponding to UAV s, form this sector, is given by

$$\begin{aligned}\hat{I}_{m,n}(k,s) \quad &= \quad \sum_{j=1}^{N_{m,n}(k)} \ln\left|P_j(k|k-1)^{-1} + \pi_S(k,s)\pi_D(k,s,j)H(k,s,j)'R(k,s,j)^{-1}H(k,s,j)\right| \\ &\quad - \ln\left|P_j(k|k-1)^{-1}\right| \end{aligned} \tag{25}$$

where $P_j(k|k-1)$ is the error covariance matrix corresponding to the predicted state of target j, $H(k,s,j)$ is the measurement matrix, $R(k,s,j)$ is the measurement covariance matrix, $\pi_S(k,s)$ is the survival probability of UAV s and $\pi_D(k,s,j)$ is the target detection probability. If sector $\{m,n\}$ does not contain any of the currently scanned targets then modified information from this sector is given by

$$\hat{I}_{m,n}(k,s) = \ln\left|I^0_{m,n} + \tilde{\pi}_{D,\text{new}}(k,s,m,n)\tilde{H}(k,s,m,n)'\tilde{R}(k,s,m,n)^{-1}\tilde{H}(k,s,m,n)\right| - \ln\left|I^0_{m,n}\right| \tag{26}$$

where $I^0_{m,n}$ is the prior information for a sector without target, $\tilde{\pi}_{D,\text{new}}(k,s,m,n)$ is the new target detection probability, $\tilde{H}(k,s,m,n)$ is the measurement matrix and $\tilde{R}(k,s,m,n)$ is the measurement covariance matrix for a target at the center of the sector.

After scanning N_s sectors for targets, the detections, equivalent last scan time matrix and UAV's current state are transmitted to the other UAVs. There is a π_c probability that another UAV will receive this transmission. Each UAV maintains its own set of target tracks, which are updated when a new set of detections is either obtained by the corresponding UAV or received from another UAV.

After scanning for measurements, transmitting them and updating the target tracks, each UAV determines its path for the next interval T. For a coordinated operation this decision depends on the corresponding UAV's knowledge about the current locations of the other UAVs, the current state of the target tracks maintained by it and equivalent last scan times of the sectors. The objective function J in (1) is maximized to obtain the paths of the UAVs. In this sense, each UAV works like a central node which increases the total computational requirement of the system. However, this way the decentralized system avoids possible online negotiation which can be disastrous in the presence of communication problems. Also, for a large system, computational load of each UAV can be reduced by considering only a small region around it.

The knowledge of the state of another UAV is updated when information is received from that UAV. In case of a failure in communication, the path decided for the particular UAV in the last iteration is assumed to be its actual path. If no information is received from a particular UAV for a number of times, the corresponding UAV is considered to be lost and future decisions are taken without considering it.

After setting its course for next interval T each UAV then waits for any transmission from the other UAVs as shown in Figure 1. If a new set of detections and scan times are received from another UAV, then the target tracks, maintained by this UAV, are updated and, also, the equivalent last scan times are updated, where the new scan time for a sector is the maximum of the old scan time and the received scan time. After T seconds the UAV once again scans N_s sectors with its GMTI sensor and so on.

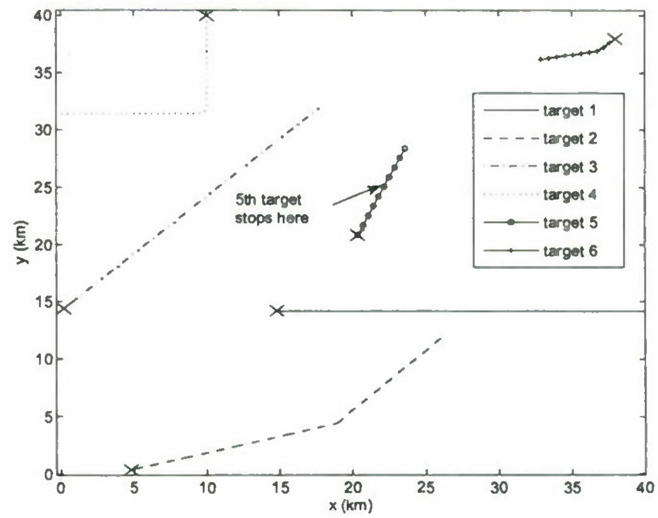

Figure 2. The paths of six targets in the surveillance region (× – initial positions).

4. SIMULATION RESULTS

In this section, we present the simulation results obtained for a 58 min scenario in which the surveillance region is 40 km × 40 km and it includes 6 targets as shown in Figure 2. The targets, which include maneuvering and move-stop-move types, appear in the surveillance region at different times. The first three targets start at the beginning of simulation (time 0). Target 1 moves in a straight line on a course of 90° (parallel to the x-axis) with a speed 10 m/s and it exits the surveillance region at 42 min. Target 2 moves at a speed 7.3 m/s on a course of 75° and turns 30° to the right at time 33 min 20 s and then moves straight. Target 3 moves straight on a course of 45° with a speed 7.1 m/s. Targets 2 and 3 continue to move inside the surveillance region during the whole simulation. Target 4 enters the surveillance region at 25 min close to the the upper left corner with a speed 10 m/s on a course of 180° and performs a 90° right turn at 38 min 20 s and then continues straight. It exits the surveillance region at 55 min 32 s. Target 5 moves in the central part of the surveillance region from 16 min 40 s to 41 min 40 s and, also, it stops for 5 min at 23 min 20 s. Target 6 moves in the upper right part of the surveillance region from 33 min 20 s to 46 min 40 s and turns 35° in during a maneuver. For all the targets the turn rates of the maneuvers are 1°/s.

The number of UAVs deployed in different simulations vary between 3 to 6 and each of them starts at y position of -12 km while keeping a distance of 1 km from the closest ones along the x direction. Initially, the UAVs move at a rate of 30 m/s on a course of 360° (along the $+y$ direction). For this simulation, T is 5 s, which means each UAV performs the set of tasks shown in Figure 1 within that time. The surveillance region is divided into 4 km × 4 km sectors and it is assumed that each UAV can scan 10 such sectors each time. The UAVs start with no knowledge about the targets and each UAV decides on its path by maximizing J in (1) based on its knowledge of the positions of the other UAVs, target tracks and last scan times of the sectors known to the corresponding UAV. The success probability of a communication between two UAVs, which is denoted by π_c in Section 3, is 0.9.

In this simulation one point track initialization [19] is applied and track maintenance is performed by a two stage procedure: measurement to track association, which is performed by the auction algorithm [4], and track update using a Kalman filter. A white noise acceleration model is assumed for the targets with process noise standard deviation (s.d.) being 1 m/s^2. The measurement noise s.d. are $\sigma_r = 10\,\mathrm{m}$, $\sigma_\theta = 10^{-3}$ rad and $\sigma_{\dot{r}} = 1\,\mathrm{m/s}$. The number of false alarms in each sector, when scanned, follows a Poisson distribution with mean 0.1 and the false measurements are uniformly distributed in the sector.

Commonly for the tracking algorithms presented in the literature, a track is deleted if it is not associated with measurements for more than a predetermined number of updates. However, this rule is not based on the observability criterion and may result in deletion of tracks because they are unobservable by the sensors used. To avoid this, in this work, a quantity π_{track} is updated each time a set of detections is received, as follows

$$\pi_{\text{track}}(k+1) = \begin{cases} \pi_{\text{track}}(k)(1-\pi_D) & \text{if not associated} \\ 1 & \text{otherwise} \end{cases} \tag{27}$$

where π_D is the probability of detection of the particular track. If π_{track} falls below a predetermined level, 10^{-6} in this simulation, the track is deleted from the track list.

In this simulation, the altitude of the UAVs above the ground is considered to be 1 km and the ground is considered to be flat. The UAVs fly at a constant speed of 30 m/s and can perform coordinated turns with angular turn rate upto 1°/s. To set its path for the next period, each UAV decides its angular turn rate by maximizing J in (1). Since J also includes the angular turn rates of the other UAVs, these quantities are also determined in a joint maximization procedure. The Matlab function 'fmincon' is used to perform this constrained optimization. The angular turn rates of the other UAVs are not transmitted as each UAV performs this operation independently.

For each sector $\{m, n\}$ the UAV management algorithm needs to assume the rate at which the probability of a new target increases if the sector is not scanned, denote by $\lambda_{m,n}$ in (22), and the maximum value of the probability of a new target, denoted by $\bar{\pi}_{\max}(m, n)$. In this simulation these parameters are assumed to be 5 min and 10^{-4}, respectively, for all sectors.

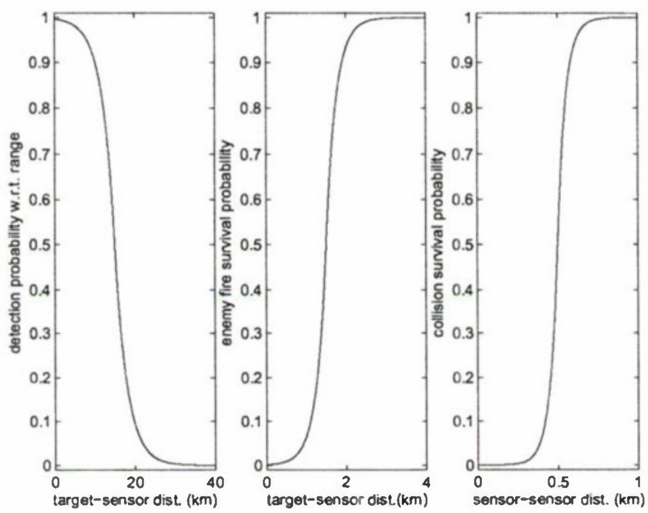

Figure 3. Detection and survival probabilities assumed in this simulation.

Figure 3 shows the survival probabilities and detection probability as a function of range, as used in this simulation. It can be seen that the survival probabilities increase as the target-sensor distance and sensor-sensor distance increase. However, the detection probability w.r.t. range increases as the distance between target-sensor decreases. It is important to note that in a real life scenario the survival and detection probabilities depend on the terrain topography and the algorithm proposed in this work is applicable for any assumption on these probabilities. The detection probability factor as a function of the range rate of a target w.r.t. a sensor is a step function being 1 if the target range rate magnitude is more than 2 m/s and 0 otherwise.

Figures 4 and 5 show 8 snapshots in a typical simulation using 5 UAVs where triangular shapes represent the positions of the UAVs and their directions of motion are along the sharp corners. In these figures black lines represent current tracks and blue stars represent the last updated position of the corresponding targets. Also, the yellow patches denote sectors scanned by the UAVs in the last period and the blue patches denote sectors not scanned for more than 1 min. Note that in this case the equivalent last scan time is used as discussed in Section 3. The first of the snapshots, which shows the positions of the tracks and UAVs at 7 min, consists of a

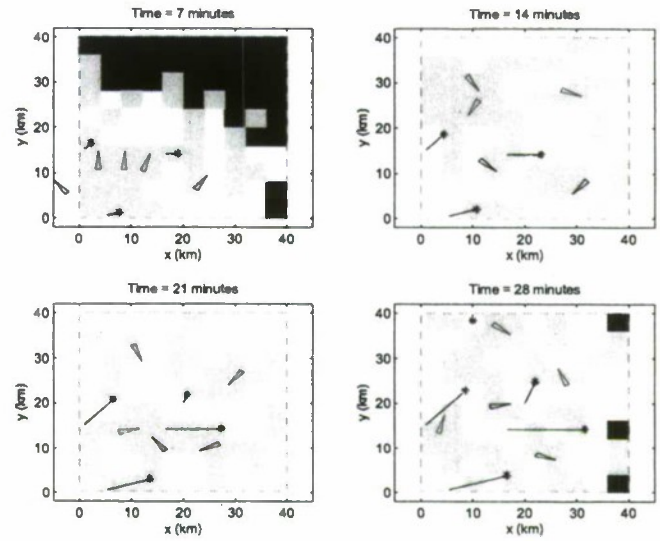

Figure 4. The first four snapshots showing UAV positions, target tracks and sectors scanned in a typical simulation using five UAVs.

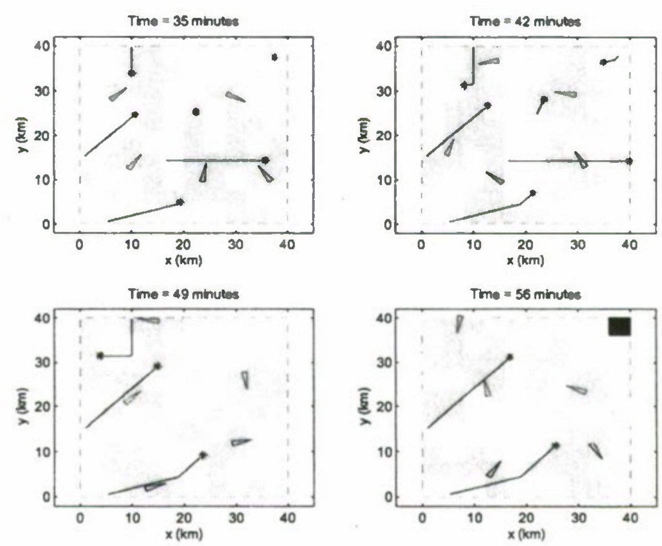

Figure 5. The last four snapshots showing UAV positions, target tracks and sectors scanned in a typical simulation using five UAVs.

large number of blue sectors because the UAVs, which start near the lower left corner, have not yet reached these sectors. From the next snapshot onwards there are very few blue sectors as each sector is repeatedly scanned even if none of the current targets belong there. Figure 6 shows the total paths of the UAVs, which start from the lower left of the surveillance region, and the tracks obtained by UAV 1.[2] In this figure it can be seen that all of the targets are tracked for their complete duration of path inside the surveillance region, after they are detected.

[2]Note that in our simulations due to imperfect communication tracks obtained by different UAVs are not identical.

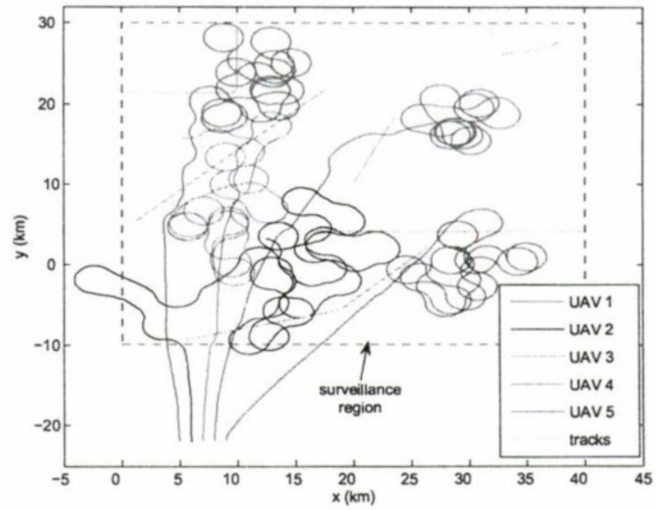

Figure 6. The complete path of the UAVs and the tracks of targets in the typical simulation using 5 UAVs.

5. CONCLUSIONS

In this paper, a novel cooperative control algorithm, for a number of UAVs searching and tracking multiple targets in a large region, is presented. According to this algorithm each UAV broadcasts its current scan and detection information and decides its path separately according to an information theoretic objective function, which incorporates target state information as well as target detection probability and UAV survival probabilities due to hostile fire by targets and, also, due to collision with other UAVs.

A simulated scenario consists of a 40 km $\times$ 40 km surveillance region, 6 targets, which includes maneuvering and move-stop-move types, and 3-6 UAVs, in different cases. The results show that the cooperative control algorithm enables the UAVs to maintain almost similar average accuracy for different tracks. Also, as the number of UAVs increase the target state (containing position and velocity components) estimation RMSE and target detection delays for all tracks decrease while the continuity of tracks improve.

Appendix

The derivation of the update of equivalent scan time $\hat{s}_{m,n}$ for sector $\{m,n\}$ is discussed in this section. The probability that there is a undetected target after a scan by sensor s in sector $\{m,n\}$ is equal to the product of the probability of a new target in this sector before the scan and the probability of no detection in this sector, i.e.,

$$\tilde{\pi}_{\text{new}}(k^+,m,n) = \tilde{\pi}_{\text{new}}(k,m,n)\,(1-\tilde{\pi}_D(k,s,m,n)) \tag{28}$$

where k^+ denotes the time immediately after the scan at t_k and $\tilde{\pi}_{\text{new}}(k,m,n)$ is given in (22). As discussed before the probability of detection corresponding to a sector is assumed to be equal to that probability at the center of the sector. Next, $\tilde{\pi}_{\text{new}}(k^+,m,n)$ can be expressed in terms of the updated equivalent last scan time in sector $\{m,n\}$ as follows

$$\tilde{\pi}_{\text{new}}(k^+,m,n) = \tilde{\pi}_{\max}(m,n)\left(1-e^{-(t_k-\hat{s}_{m,n}(k^+))/\lambda_{m,n}}\right) \tag{29}$$

The equation (24) is obtained by substituting $\tilde{\pi}_{\text{new}}(k^+,m,n)$ by (28) and then solving for $\hat{s}_{m,n}(k^+)$.

REFERENCES

1. Bar-Shalom, Y., Li, X. R. and Kirubarajan, T., *Estimation with Applications to Tracking and Navigation.* New York: Wiley, 2001.
2. Bar-Shalom, Y. and Li, X. R., *Multitarget-Multisensor Tracking: Principles and Techniques*, YBS Publishing, 1995.
3. Beard, R. W., McLain, T. W., Goodrich, M. A. and Anderson, E. P., "Coordinated Target Assignment and Intercept for Unmanned Air Vehicles," *IEEE Trans on Robotics and Automation*, Vol. 18, No. 6, pp. 911-922, Dec. 2002.
4. Bertsckas, D.P., *Linear Network Optimization: Algorithms and Codes*, MIT Press, Cambridge, MA USA, 1991.
5. Bourgault, F., Furukawa, T. and Durrant-Whyte., H. F., "Decentralized Bayesian Negotiation for Cooperative Search," Proc. of IEEE/RSJ International Conf. on Intelligent Robots and Systems, pp. 2681-2686, Sendai Japan, Sept. 2004.
6. Chandler, P. R., "UAV Coperative Control", *Proc. of American Control Conference*, pp. 50-55, Arlington, VA USA, June 2001.
7. Durrant-Whyte, H. and Grocholsky, B., "Management and Control in Decentralised Networks," *Proc. of International Conference on Information Fusion*, pp. 560-565, Cairns, Queensland Australia, July 2003.
8. Flint, M., Polycarpou, M. and Fernandez-Gaucherand., E., "Cooperative Control for Multiple Autonomous UAV's Searching for Targets," *Proc. of IEEE Conference on Decision and Control*, pp. 2823-2828, Las Vegas, Nevada USA, Dec. 2002.
9. Furukawa, T., Bourgault, F., Durrant-Whyte, H. F. and Dissanayake, G., "Dynamic Allocation and Control of Coordinated UAVs to Engage Multiple Targets in a Time-Optimal Manner," *Proc. of IEEE International Conf. on Robotics & Automation*, pp. 2353-2358, New Orleans, LA USA, April 2004.
10. Kirubarajan, T., Bar-Shalom, Y., Pattipati, K.R., and Kadar, I, "Ground Target Tracking with Variable Structure IMM Estimator," *IEEE Trans. on Aerospace and Electronic Systems*, Vol. 36, No. 1, pp. 26-46, Jan. 2000.
11. Li, S. M. et al., "Automonous Hierachical Control of Multiple Unmanned Combat Vehicles," *Proc. of American Control Conference*, pp. 274-279, Anchorage, AK USA, May 2002.
12. Manyika, J. and Durrant-Whyte, H., *Data Fusion and Sensor Management: A Decentralized Information-Theoretic Approach*, Ellis Horwood, 1994.
13. McLain, T. W., Chandler, P. R. and Pachter, M., "A Decomposition Strategy for Optimal Coordination of Unmanned Air Vehicles," *Proc. of American Control Conference*, pp. 369-373, Chicago, IL USA, June 2000.
14. McLain, T. W., Chandler, P. R., Rasmussen, S. and Pachter, M., "Cooperative Control of UAV Rendezvous," *Proc. of American Control Conference*, pp. 2309-2314, Arlington, VA USA, June 2001.
15. Patek, S. D., Logan, D. A. and Castanon, D. A., "Approximate Dynamic Programming for the Solution of Multiplatform Path Planning Problems," *Proc. of IEEE conference on Systems, Man, and Cybernetics*, Vol. 1, pp. 1061-1066, Oct. 1999.
16. Polycarpou, M. M., Yang, Y. and Passino, K. M., "A Cooperative Search Framework for Distributed Agents," *Proc. of International Symposium on Intelligent Control*, pp. 1-6, Mexico City, Mexico, 2001.
17. Sinha, A., Kirubarajan, T. and Bar-Shalom, Y., "Optimal Cooperative Placement of UAVs for Ground Target Tracking with Doppler Radar", *Proc. of SPIE Signal Processing, Sensor Fusion, and Target Recognition*, Orlando, FL USA, April 2004.
18. Sinha, A., Kirubarajan, T. and Bar-Shalom, Y., "Autonomous Ground Target Tracking by Multiple Cooperative UAVs", *Proc. of IEEE Aerospace Conf.*, Big Sky, MT USA, March 2005.
19. Yeom, S. W., Kirubarajan, T. and Bar-Shalom, Y., "Track Segment Association, Fine-step IMM and Initialization with Doppler for Improved Track Performance", *IEEE Trans. on Aerospace and Electronic Systems*, Vol. 40, No. 1, pp. 293-309, Jan. 2004.

Autonomous Search, Tracking and Classification by Multiple Cooperative UAVs*

A. Sinha[a], T. Kirubarajan[a] and Y. Bar-Shalom[b]
[a]Estimation, Tracking and Fusion Laboratory (ETFLab),
Electrical & Computer Engineering Department, McMaster University,
Hamilton, Ontario, Canada.
[b]Estimation and Signal Processing Laboratory (ESPLab),
Electrical & Computer Engineering Department, University of Connecticut,
Storrs, CT, USA.

ABSTRACT

In this paper we propose a cooperative control algorithm for a group of UAVs carrying out surveillance — search, tracking and classification — over a large region which includes a number of targets. The goal is to track and classify detected targets as well as search for new targets. The UAVs are assumed to be equipped with Ground Moving Target Indicator (GMTI) radars, which measure the locations of moving ground targets as well as their radial velocities (Doppler). In addition, a classification sensor is mounted on each UAV that can obtain target class information. The surveillance region is divided into a number of sectors and it is assumed that the GMTI sensor on each UAV scans a fixed number of such sectors in each period of its operation. The sensor responsible for class information can scan only a small circular region around the predicted position of a target. In this paper, a decentralized cooperative control algorithm is proposed, according to which each UAV transmits the current scan information (either kinematic or class information) and detection information (including "negative information") to the other UAVs. Each UAV makes its scan decision and path decision separately, based on information-based objective functions, which incorporate target state information as well as target detection probability and survival probability due to possible hostile fire by targets and collision with other UAVs. The proposed algorithm requires limited communication and modest computation and it can handle failure in communication and loss of UAVs.

Keywords: target classification, sensor management, cooperative control, UAV path planning, ground target tracking.

1. INTRODUCTION

A number of UAV management algorithms can be found in the literature. In [14] a cooperative control algorithm for multiple UAVs to simultaneously reach a predetermined target location, which maximizes the survivability of the UAVs due to exposure to threats while adhering to fuel constraint, is addressed. A hierarchical decision mechanism is proposed in which at team level the estimated time until arrival is computed and at UAV level path planning is performed. In [3] a similar approach, based on Voronoi diagram in path planning, is used for the simultaneous intercept problem in the presence of dynamic threats. Similar approaches can be found in [6, 15]. In [10] another hybrid control structure is proposed for the simultaneous intercept problem in which UAV-to-target allocation and time to reach the targets are decided in the central node, while the path decisions are taken locally in UAVs.

In [17] a multi-vehicle path planning problem in hostile environment is solved by dynamic programming. In this centralized algorithm path decisions are taken in terms of connecting pre-defined waypoints. In [18] a decentralized cooperative search algorithm is proposed in which UAVs exchange environment information but independently decide their paths by minimizing a convex combination of costs associated with subgoals. It can be noted that for UAV management problems decentralized algorithms are preferred as they have advantages of graceful degradation, scalability and modularity properties over the centralized ones. In [9], for a search problem,

*Proc. of SPIE Conf. on Signal Processing, Sensor Fusion, and Target Recognition (#6235-09), Orlando, FL, April 2006.

dynamic programming is used to make finite horizon decisions. Note that our problem includes search, tracking and classification.

In [8] a decentralized sensor management algorithm, based on maximizing information gain, is presented. An online negotiation arrangement between the sensors is used to decide the assignment of known targets to generate a coordinated sensor-platform trajectory for obtaining information about static features (targets). In [5] a decentralized multi-UAV search algorithm, for a lost vehicle in a stationary state, is proposed. This algorithm is synchronous, according to which each UAV negotiates with others by communicating the expected measurement likelihood for its best path given the measurement likelihood of other UAVs.

An important objective of the surveillance system is to classify the detected targets. The problem of optimal search for joint detection and classification of a stationary target was first considered in [21], which assumes separate sensors for these objectives. It is shown that the optimal plan is to allocate classification effort immediately after targets are detected. In [7] continuous search of multiple targets, which belong to multiple classes, is considered, where the probability of detection and classification is a function of the search effort. In [12] design of search patterns in the presence of false contacts is presented where classification is modeled as an uncertain but instantaneous process. In [6] a cooperative classification algorithm for stationary targets is developed in which a hierarchial path planning is performed to view complementary aspect angles.

In [16] kinematic information is combined with the feature information obtained from high range resolution (HRR), inverse synthetic aperture radar (ISAR), and synthetic aperture radar (SAR) signatures, to obtain improved classification and association for tracking moving ground targets. An integrated classification and tracking algorithm is presented in [2]. In our proposed algorithm the classification and tracking are considered as different problems as it is assumed that the GMTI sensor mounted on UAVs does not provide any classification information and the classification sensor does not provide reliable position information.

In our previous work [19, 20] a decentralized cooperative control algorithm is developed for a number of UAVs, equipped with GMTI sensors, to track multiple ground targets and search for new ones in a specified region. The region is divided into a number of square sectors[2] and it is assumed that each UAV can scan N_s sectors each time. In the proposed algorithm the UAVs exchange the information about the sectors that were scanned and yielded no detections ("negative information")[3], the measurements obtained and their current kinematic states. Each UAV decides on the sectors it scans and the path it follows on its own. In this work these decisions are decoupled into two separate problems — *scan decision* and *path decision* — to make the surveillance problem tractable. In both cases, the corresponding objective functions are based on information gain. The objective functions incorporate information from detected targets as well as possible information from the yet undetected targets, which are included in the form of possible targets in the sectors. Also, the objective functions incorporate the detection probabilities of targets, which are based on both range and range rate, and the survival probabilities of the UAVs due to hostile fire from targets and possible collision with other UAVs, in computing the information for a particular target-sensor geometry.

In our current work classification of detected targets is considered as an additional objective of the cooperative control algorithm. It is assumed that, along with the GMTI sensor, each UAV carries a classification sensor, for example a CCD camera. This additional sensor sends its information to a classifier block that outputs one of the target classes. The probabilities of observation of different outputs given different actual classes of targets form the class confusion matrix. This matrix is assumed to be known for each value of target-UAV distance and the classification accuracy increases as this distance decreases. In this work it is assumed that classification with any degree accuracy can be obtained from any particular direction, i.e., spatial diversity does not improve classification results.

The objective function for path planning, in general, is a weighted summation of the total kinematic information, discussed in [20], and the total classification information obtainable. However, to facilitate fast classification, the information contribution of a UAV closest to a detected target is equal to the information obtainable from this target until it is classified to a predefined level of accuracy. After that, this target's importance in path

[2]Note that it is possible to incorporate any other shapes of sectors in this algorithm.

[3]Information about sectors that yielded no detection decreases the expected information content of the corresponding sectors. Hence such information is denoted as "negative information".

planning is de-emphasized. At the same time a target which is already classified to a particular level of certainty is retained longer in the case of no detection as the tracker has higher confidence in the track corresponding to the target.

The objective function for scan decision is similar to the one discussed in [20] with the addition that a UAV decides to use the classification sensor when the predicted classification information gain is more than a threshold. It is assumed that a UAV can use only one type of sensor at a time.

The paper is organized as follows. The objective functions for scan decision and path planning is discussed in Section 2. In Section 3 the cooperative control algorithm is described in detail. Simulation results are presented in Section 4 and Section 5 presents the concluding remarks.

2. THE OBJECTIVE FUNCTIONS

One of the most important stages in the development of a sensor management algorithm is the choice of objective functions which should be easy to optimize and the decisions based on these functions should enable the algorithm to achieve the sensor management goals. In this section we introduce the objective functions which are used for the scan decisions and path decisions.

In this work definition of information follows the entropic information measure. For a random variable $\mathbf{x}$ with probability density function $f(\mathbf{x})$ the entropic information measure is given by

$$E\{\ln(f(\mathbf{x}))\} = \int_{-\infty}^{\infty} f(\mathbf{x}) \ln(f(\mathbf{x}))d\mathbf{x} \tag{1}$$

If $\mathbf{x}$ is a Gaussian random vector with information matrix I (inverse of its covariance) then the entropic information is given by

$$\mathcal{I}_{\mathrm{G}}(\mathbf{x}) = \frac{1}{2} \ln\left((2\pi e)^n |I|\right) \tag{2}$$

where n is the dimension of $\mathbf{x}$.

If $\mathbf{x}$ is a discrete random variable then the entropic information is given by

$$\mathcal{I}_{\mathrm{d}}(\mathbf{x}) = \sum_{i=1}^{N} P(x_i) \ln P(x_i) \tag{3}$$

where x_is are N discrete levels of $\mathbf{x}$ and $P(x_i)$s are the probabilities of those levels.

2.1. Kinematic Information

In this work computation of the kinematic information matrix (inverse covariance) follows [20]. Since it is convenient to work with a form in which the total matrix information is the summation of the information from different (independent) sources[4], in this work we use the following expression of the expected updated information corresponding to target j at time step k (conditioned on the information at $k-1$)

$$I_j(k|k) = I_j(k|k-1) + \sum_s \pi_S(k,s)\pi_D(k,s,j)H(k,s,j)'R(k,s,j)^{-1}H(k,s,j) \tag{4}$$

where $I_j(k|k-1)$ is the information matrix (inverse covariance) corresponding to the predicted state, which depends on the target motion model (see, e.g., [1] ch. 5). The combined probability that UAV s contributes to the kinematic information about target j at time k is given by $\pi_S(k,s)\pi_D(k,s,j)$, where $\pi_S(k,s)$ is the survival probability of UAV s and $\pi_D(k,s,j)$ is the probability of detection of target j by GMTI sensor on UAV s given survival of the corresponding UAV. The kinematic information obtained by a particular UAV s about target j at time k is given by $H(k,s,j)'R(k,s,j)^{-1}H(k,s,j)$ where $H(k,s,j)$ is the measurement matrix and $R(k,s,j)$ is the

[4]This statement is true for already detected targets only. For sectors without detected target the total matrix information is maximum of the matrix information obtainable by any sensor. This avoids all UAVs from moving to a particular sector.

measurement noise covariance matrix corresponding to the sensor-target pair at time k. The expected updated information corresponding to target j, when only UAV s participates in kinematic information gathering, is given by

$$I_{s,j}(k|k) = I_j(k|k-1) + \pi_S(k,s)\pi_D(k,s,j)H(k,s,j)'R(k,s,j)^{-1}H(k,s,j) \tag{5}$$

The detection probability of target j by the GMTI sensor on UAV s at time step k given the survival of the UAV is written as

$$\pi_D(k,s,j) = \pi_D^1(k,s,j)\pi_D^2(k,s,j) \tag{6}$$

where $\pi_D^1(k,s,j)$ is the detection probability (of target j by sensor s at time k) as a function of the range and $\pi_D^2(k,s,j)$ is the detection probability as a function of the range rate. The first term depends on the specific application and the second term is the probability that the range rate measured by the GMTI sensor is higher than the "minimum detectable velocity" (MDV) (see [19] for detailed discussion).

The total survival probability of UAV s is equal to the product of target-fire survival probability $\pi_S^1(k,s)$ and collision survival probability $\pi_S^2(k,s)$ of this UAV, i.e.,

$$\pi_S(k,s) = \pi_S^1(k,s)\pi_S^2(k,s) \tag{7}$$

where $\pi_S^1(k,s)$, in turn, is the product of target-fire survival probabilities of UAV s in view of each target, i.e.,

$$\pi_S^1(k,s) = \prod_j \pi_S^1(k,s,j) \tag{8}$$

and $\pi_S^2(k,s)$ is the product of collision survival probabilities corresponding to all other UAVs

$$\pi_S^2(k,s) = \prod_{i,i\neq s} \pi_S^2(k,s,i) \tag{9}$$

The dependence of these probabilities on the sensor to target distances (and possibly other factors) is application dependent.

The surveillance region is divided into a number of sectors and for the sectors that do not contain any of the currently tracked targets, new (undetected) targets are the possible source of information. The prior kinematic information for sector $\{m,n\}$ is denoted by $I_{m,n}^0$, where the uncertainty is the same as that of a target that can be anywhere in the sector and move at any possible velocity. The new kinematic information obtained by UAV s from sector $\{m,n\}$ at time step k is zero if there is no detection and $\tilde{H}(k,s,m,n)'\tilde{R}(k,s,m,n)^{-1}\tilde{H}(k,s,m,n)$ if a detection occurs, where $\tilde{H}(k,s,m,n)$ is the measurement matrix and $\tilde{R}(k,s,m,n)$ is the measurement noise covariance matrix corresponding to the new target. The position of a new target is assumed to be at the center of the sector. The probability of a new target detection event in sector $\{m,n\}$ is given by the product of the probability of detection $\tilde{\pi}_D(k,s,m,n)$ and the probability of the presence of a new target (with range rate above the MDV) $\tilde{\pi}_{\text{new}}(k,m,n)$ in this sector, i.e.,

$$\tilde{\pi}_{D,\text{new}}(k,s,m,n) = \tilde{\pi}_D(k,s,m,n)\tilde{\pi}_{\text{new}}(k,m,n) \tag{10}$$

where the term $\tilde{\pi}_D(k,s,m,n)$ is similar to $\pi_D^1(k,s,j)$. The only difference is that the former is a function of the GMTI sensor range from the center of a sector while the latter is a function of the range between the sensor and target.

The second term in the right hand side of (10), which represents the probability of presence of a (moving) new target in sector $\{m,n\}$ at time step k, is assumed to have the following form

$$\tilde{\pi}_{\text{new}}(k,m,n) = \tilde{\pi}_{\max}(m,n)\left(1 - e^{-(t_k - \hat{t}_{m,n}(k))/\lambda_{m,n}}\right) \tag{11}$$

where t_k is the scan time at step k, $\tilde{\pi}_{\max}(m,n)$ is the maximum value of the probability of new target, $\hat{t}_{m,n}$ is the equivalent last scan time and $\lambda_{m,n}$ is a parameter that defines the rate of increase of the probability of a new target after a scan in sector $\{m,n\}$ yielded no detection. This models the "appearance" of a new target since the last scan of the sector under consideration. The parameters $\tilde{\pi}_{\max}(m,n)$ and $\lambda_{m,n}$ are application dependent which can be chosen to give different importance to different sectors.

In view of the above, the expected kinematic information matrix from sector $\{m,n\}$ when scanned by the GMTI sensor of UAV s at time step k is

$$I_{m,n}(k,s) = I^0_{m,n} + \tilde{\pi}_{D,\text{new}}(k,s,m,n)\tilde{H}(k,s,m,n)'\tilde{R}(k,s,m,n)^{-1}\tilde{H}(k,s,m,n) \tag{12}$$

Entropic information can be computed from the above mentioned information matrices by using (2). Note that in our work target state estimates and predictions are assumed to be Gaussian distributed.

2.2. Classification Information

The class probability vector corresponding to target j before the scan at time k is denoted as $\mu_j(k-1)$ and the classifier confusion matrix corresponding to the target j and classification sensor on UAV s is denoted by $C(k,s,j)$. An element $c_{ab}(k,s,j)$ of the classifier matrix is defined as the probability of the event that the classifier output, if target j is scanned by the classification sensor, is $\zeta(k,s,j) = b$ given that the true class is $\kappa_j = a$, i.e.,

$$c_{ab}(k,s,j) = P(\zeta(k,s,j) = b|\kappa_j = a) \tag{13}$$

If the classifier output is b, then the updated class probability is given by [2]

$$\mu_j(k|\zeta_{s,j}(k) = b) = \frac{c_b(k,s,j)\bigotimes\mu_j(k-1)}{c_b(k,s,j)'\mu_j(k-1)} \tag{14}$$

where $c_b(k,s,j)$ denotes the bth column of the class confusion matrix and $\bigotimes$ is the Schur-Hadamard product (term by term). The corresponding classification information $\mathcal{I}[j,k|\zeta(k,s,j) = b]$ about target j at time step k can be computed using (3).

The expected updated class information of target j at time step k can be obtained considering all possible combinations of the target's true class and classifier output in UAV s as follows

$$\begin{aligned}\hat{\mathcal{I}}(k,s,j) &= E\{\mathcal{I}(j,k)\} \\ &= \sum_b \mathcal{I}[j,k|\zeta(k,s,j) = b]P\{\zeta(k,s,j) = b\}\end{aligned} \tag{15}$$

where the probability that the observation is b, is given by

$$P\{\zeta(k,s,j) = b\} = \sum_a c_{ab}(k,s,j)\mu_j^a(k-1) \tag{16}$$

where $\mu_j^a(k-1)$ is the probability that target j belongs to class a given the information at $k-1$.

2.3. The Objective Function for Scan Decision

The expected information gain from the sectors is used as the criterion for the scan decisions made by each UAV. It is assumed that while the GMTI sensor can scan N_s sectors, the classification sensor can only scan one small circular region of radius r_s. Furthermore, only one sensor on each UAV can perform scan operation during one time period T.

Firstly expected classification information gain is computed for each target. The target corresponding to the maximum predicted classification information gain is chosen for a scan by the classification sensor only if the gain is more than a threshold. Defining

$$g_s \triangleq \max_j\{\hat{\mathcal{I}}(k,s,j) - \mathcal{I}(k-1,j)\} \quad \text{and} \quad w_s \triangleq \arg\max_j\{\hat{\mathcal{I}}(k,s,j) - \mathcal{I}(k-1,j)\} \tag{17}$$

target w_s is scanned for the class information by UAV s if $g_s > c^g$, where c^g is a threshold and $\mathcal{I}(k-1,j)$ is the class information corresponding to target j at time step $k-1$.

If a UAV decides against using the classification sensor then the kinematic information gain from the sectors is computed in the following manner. If there are $N_{m,n}(k)$ targets in sector $\{m,n\}$ at time step k then the expected kinematic information gain by the GMTI sensor on UAV s from this sector is given by

$$J^{\text{scan}}_{m,n}(k,s) = \sum_{j=1}^{N_{m,n}(k)} \ln|I_{s,j}(k|k)| - \ln|I_j(k|k-1)| \tag{18}$$

where $I_j(k|k-1)$ is the predicted information matrix and $I_{s,j}(k|k)$ is the expected updated information matrix corresponding to target j, when this target is scanned by sensor s, as defined in (5). Note that in (18) each term in the summation denotes expected kinematic information gain corresponding to a target if the sector $\{m,n\}$ is scanned.

If sector $\{m,n\}$ does not contain any of the currently detected targets then the expected kinematic information gain from searching this sector is given by

$$J^{\text{scan}}_{m,n}(k,s) = \ln|I_{m,n}(k,s)| - \ln|I^0_{m,n}| \tag{19}$$

where $I^0_{m,n}$ is the prior information matrix for sector $\{m,n\}$ and $I_{m,n}(k,s)$ is the expected updated information matrix corresponding to sector $\{m,n\}$, when scanned by sensor s, as defined in (12). The best N_s sectors in terms of objective function $J^{\text{scan}}_{m,n}(k,s)$ are chosen for scan by the GMTI sensor on UAV s at time step k.

2.4. The Objective Function for Path Decision

The detected targets, which form the set $\mathcal{T}_D$, are categorized into two sets: the set containing targets which are classified well (denoted as $\mathcal{T}_1$) and the set containing the remaining targets (denoted as $\mathcal{T}_2$). A target is considered to be classified well if the maximum class probability is higher than a threshold. To facilitate fast classification of each target in set $\mathcal{T}_2$ the path decision of the UAV closest to it is dictated by the information obtainable from the particular target. Such dedicated UAVs form set $\mathcal{A}$ and the remaining UAVs form set $\mathcal{B}$. While information gain from all targets and all sectors is considered in path decision of UAVs in set $\mathcal{B}$, information gain from only the closest target in set $\mathcal{T}_2$ is considered in path planning of UAVs in set $\mathcal{A}$ (this avoids conflicts).

The information gain achievable by the sensors related to detected or undetected targets under independence is considered to be the (global) objective function for the path decision, i.e.,

$$\begin{aligned} J^{\text{path}}(k) &= \sum_{j\in\mathcal{T}_D} \gamma_j \left(\ln|I_j(k|k)| - \ln|I_j(k|k-1)| + \eta\left(\max_s\{\hat{\mathcal{I}}(k,s,j) - \mathcal{I}(k-1,j)\}\right)\right) \\ &+ \sum_{\{m,n\}\in\mathcal{S}_{\bar{D}}} \left(\ln|\tilde{I}_{m,n}(k)| - \ln|I^0_{m,n}|\right) \end{aligned} \tag{20}$$

where $I_j(k|k-1)$ and $I_j(k|k)$ are the predicted and expected updated information matrices at time step k for target j within the set of detected targets, denoted by $\mathcal{T}_D$. These information matrices are defined above. The quantities $\mathcal{I}(k-1,j)$ and $\hat{\mathcal{I}}(k,s,j)$ are the classification information about target j at time step $k-1$ and expected classification information if the target is scanned by the classification sensor on UAV s, respectively. Note that UAV s in set $\mathcal{A}$ is considered in computation of $I_j(k|k)$ only if $j \in \mathcal{T}_2$ and UAV s is its closest. The relative weight between the kinematic and classification information is η, which is a design parameter. The maximum of the classification information gain for all UAVs is included in (20) as only one UAV is expected to obtain class information of a target. To facilitate the detection and classification of new targets, γ_j takes less than unity value if the target j is in set $\mathcal{T}_1$. Otherwise the value of γ_j is 1.

In (20) $\mathcal{S}_{\bar{D}}$ is the set of all sectors in which there are no currently tracked targets and $\tilde{I}_{m,n}(k)$ is the expected information matrix of new targets in sector $\{m,n\}$ of the surveillance region given by

$$\tilde{I}_{m,n}(k) = I_{m,n}(k,\hat{s}) \quad \text{where} \quad \hat{s} = \arg\max_{s\notin\mathcal{A}} |I_{m,n}(k,s)| \tag{21}$$

where $I_{m,n}(k,s)$ is the expected information matrix from sector $\{m,n\}$ when scanned by sensor s at time step k, which is defined in (12). Classification information gain for undetected targets is not included in the objective function. Note that in order to restrict more than one UAV from moving toward the same unscanned sector, only the maximum information from all sensors is included in the cost function instead of considering the summation of information.

In our problem the UAVs scan the targets asynchronously which, in general, leads to a complicated objective function. However, if the offset times are small, as in our case, the target-sensor geometry does not change much from the scan by one UAV to that by another one. Hence, for convenience, the objective function for path decision is constructed assuming synchronous scans by all sensors. Note that, the algorithm described in this paper provides a solution to a one-step ahead planning problem. It is shown to be effective, while requiring much less computation than a longer horizon planning, which is currently under investigation.

3. THE ALGORITHM

In this section, the algorithm used by each UAV, which results in cooperative control of the UAVs as a group, is discussed in detail. This algorithm is capable of tracking and classifying detected targets and to search for undetected ones by taking into account that new targets can start in sectors that have already been scanned. In this algorithm the decisions on path selection and sectors to scan are taken separately by the UAVs. However, these decisions are indirectly connected as a scan in a particular sector reduces the information available from this sector which in turn affects the next path decision.

Each UAV performs the following tasks asynchronously w.r.t. the other UAVs. Each UAV makes the scan decision as discussed in Section 2.3. If the UAV decides to use the classification sensor it scans a circular region of radius r_s around the predicted positon of the intended target. Otherwise, the UAV scans N_s sectors by using its GMTI sensor. The expected information gain from each sector is computed using (18) for sectors containing currently tracked targets (track maintenance) and using (19) for sectors which do not contain any of the currently tracked targets (search). The best N_s sectors are chosen, on that basis, for this scan. These scan decisions by each UAV are taken independently of the state of the other UAVs.

The equivalent last scan time $\hat{s}_{m,n}$ is updated after a scan by the GMTI sensor on UAV s as follows

$$\hat{t}_{m,n}(k^+) = \begin{cases} \hat{t}_{m,n}(k) & \text{if not scanned} \\ t_k - \Delta(k, s, m, n, s) & \text{if scanned and target not detected} \end{cases} \tag{22}$$

where k^+ denotes time immediately after the scan at t_k and $\Delta(k, s, m, n)$ is given by

$$\Delta(k, s, m, n) = -\lambda_{m,n} \ln \left[1 - \left(1 - e^{-(t_k - \hat{t}_{m,n}(k))/\lambda_{m,n}}\right) [1 - \bar{\pi}_D(k, s, m, n)]\right] \tag{23}$$

In this algorithm each UAV stores the equivalent last scan time $\hat{t}_{m,n}(k)$ of each sector to keep track of the new target probability, which needs update only if the corresponding sector is scanned. The derivation of (23) is discussed in [19].

Next, the measurements, which include classifier output in case of a scan by the classification sensor and detections if GMTI sensor is used, the equivalent last scan time matrix and the UAV's current state are transmitted to the other UAVs. There is a π_c probability that another UAV will receive this transmission. Each UAV maintains its own set of target tracks, which are updated when a new set of detections is either obtained by the corresponding UAV or received from another UAV.

After scanning for measurements, transmitting them and updating the target tracks, each UAV determines its path for the next interval T. For a coordinated operation this decision depends on the corresponding UAV's knowledge about the current locations of the other UAVs, the track picture maintained by it[5] and the equivalent last scan times of the sectors. The objective function J^{path} in (20) is maximized to obtain the path of the UAV. Since J^{path} depends on the future positions all of the UAVs, each UAV requires to optimize it w.r.t. the paths of all UAVs and then executes its own part of the solution. In this sense, each UAV works like a central node and this way the decentralized system avoids possible online negotiations which can be disastrous in the

[5]Note that each UAV updates its track picture using measurements obtained by it and those received from other UAVs. The track picture may be different from UAV to UAV because of imperfect communication.

presence of communication problems. For a large system, the computational load of each UAV can be reduced by considering only a certain region around it. Note that the proposed algorithm makes the assumption that the actions (turn rates) computed by different UAVs are almost the same due to the similarity of their information about the current track picture.

The knowledge of the state of another UAV is updated when information is received from that UAV. In case of a failure in communication, the path decided for the particular UAV in the last iteration is assumed to be its actual path. If no information is received from a particular UAV for a number of times, the corresponding UAV is considered to be lost and future decisions are taken without considering it. However, if transmissions are once again received from a "lost" UAV it is included in the future decisions.

After setting its course for next interval T each UAV then waits for any transmission from the other UAVs. If a new set of detections and scan times are received from another UAV, then the target tracks, maintained by this UAV, are updated and, also, the equivalent last scan times are updated, where the new scan time for a sector is the maximum of the old scan time and the received scan time. After T seconds the UAV once again makes its scan decision and so on.

4. SIMULATION RESULTS

In this section, we present the simulation results obtained for a 58 minute scenario in which the surveillance region is $40\,\text{km} \times 40\,\text{km}$ and it includes 6 targets. The targets, which include maneuvering and move-stop-move types, appear in the surveillance region at different times. A detailed discussion on targets' paths is provided in [19].

The number of UAVs deployed is 4 and each of them starts at y position of $-12\,\text{km}$ while keeping a distance of 1 km from the closest ones along the x direction. Initially, the UAVs move at a speed of $30\,\text{m/s}$ on a course of $0°$ (along the $+y$ direction). For this simulation, T is 5 s, which means each UAV performs the set of tasks described in Section 3 within that time. The surveillance region is divided into $4\,\text{km} \times 4\,\text{km}$ sectors and it is assumed that the GMTI sensor on each UAV can scan 5 such sectors each time. Each UAV can scan a circular region of radius 100 m, which is previously denoted by r_s, by using the classification sensor. The UAVs start with no knowledge about the targets and each UAV decides on its path by maximizing J^{path} in (20) based on its knowledge of the positions of the other UAVs, target tracks and last scan times of the sectors known to the corresponding UAV. The success probability of a communication between two UAVs, which is denoted by π_c in Section 3, is 0.9.

In this simulation one point track initialization is applied and track maintenance is performed by a two stage procedure: measurement to track association, which is performed by 2-D assignment via the auction algorithm [4], and track update using a Kalman filter. A discretized continuous-time white noise acceleration model [1] is assumed for the targets with process noise power spectral density being $1\,\text{m}^2/\text{s}^3$. The measurement noise s.d. corresponding to the GMTI sensors are $\sigma_r = 10\,\text{m}$, $\sigma_\theta = 10^{-3}\,\text{rad}$ and $\sigma_{\dot{r}} = 1\,\text{m/s}$. The number of false alarms in each sector, when scanned, follows a Poisson distribution with mean 0.1 and the false measurements are uniformly distributed in the sector[6]. As discussed in Section 2.4 a target is considered to be classified well if its maximum of the class probabilities is higher than a threshold, which in this simulation is 0.9. In the objective function for path decision (20) the relative weight between kinematic and classification information gain is denoted by η. Although in this simulation spatial diversity of classification information is ignored, target the detection probability by GMTI scan as a function of range rate is directional. Hence classification information can be obtained from any direction but the same is not true for kinematic information. For this reason in this work η is chosen to be equal to 0.1 to emphasize the kinematic information. For the targets that are classified well, the constant γ_j that emphasizes the corresponding information gain is reduced to 0.1 to facilitate the detection and classification of new targets.

Commonly for the tracking algorithms presented in the literature, a track is deleted if it is not associated with measurements for more than a predetermined number of updates. However, this rule is not based on the observability criterion and may result in deletion of tracks because they are unobservable by the sensors used.

[6]While the UAV management does not explicitly include false alarms, it is shown to operate successfully also in their presence.

To avoid this, in this work, track quality index denoted by π_{track} is updated each time a set of detections is received, as follows

$$\pi_{\text{track}}(k+1) = \begin{cases} \pi_{\text{track}}(k)(1-\pi_D) & \text{if not associated} \\ 1 & \text{otherwise} \end{cases} \tag{24}$$

where π_D is the probability of detection of the particular track. If the track quality index falls below a predetermined level of 10^{-6} for a target that is classified well and 10^{-3} otherwise, the track is deleted. Note that the targets that are classified well are retained longer in the event of missed detection as the tracker is more confident about such a track. Also, tracks were confirmed only after obtaining 3 measurements for them. In our simulations not a single false track is confirmed.

In this simulation, the altitude of the UAVs above the ground is considered to be 1 km and the ground is considered to be flat. The UAVs fly at a constant speed of 30 m/s and can perform coordinated turns with angular turn rate up to 6°/s. To set its path for the next period, each UAV decides its angular turn rate by maximizing J^{path} in (20). Since J^{path} corresponding to the information matrix based algorithm depends on the future positions of the other UAVs which in turn depend on their turn rates for the next period, the turn rates of all UAVs are determined in a joint maximization procedure. The Matlab function 'fmincon' is used to perform this constrained optimization. The angular turn rates of the other UAVs are not transmitted as each UAV performs this operation independently.

For each sector $\{m,n\}$ the UAV management algorithm needs to assume the rate at which the probability of a new target increases if the sector is not scanned, denoted by $\lambda_{m,n}$ in (11), and the maximum value of the probability of a new target, denoted by $\bar{\pi}_{\max}(m,n)$. In this simulation these parameters are assumed to be 5 min and 10^{-4}, respectively, for all sectors. A UAV is considered lost by another UAV if there is no information from the former UAV for 5 consecutive periods. In our simulations none of the UAVs was incorrectly assumed to be lost, i.e., there was no instance of five consecutive transmission failures from one UAV to another.

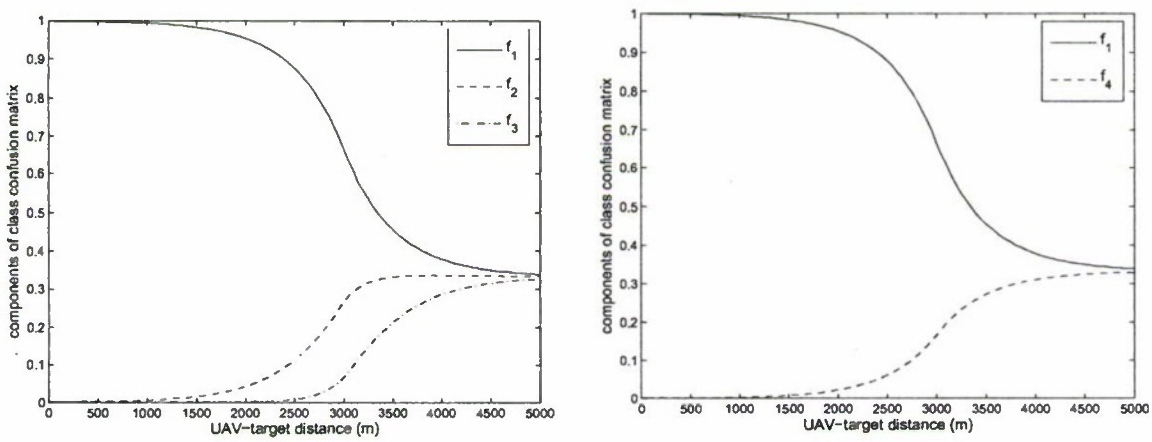

(a) Components f_1, f_2 and f_3

(b) Components f_1, f_4

Figure 1. Components of the class confusion matrix vs. target-UAV distance.

The same survival and detection probabilities as a function of range are used as in [19]. The detection probability factor as a function of the range rate of a target w.r.t. a sensor is a step function being 1 if the target range rate magnitude is more than 2 m/s and 0 otherwise. In this simulation the classifier output belongs to a set of three, same as the track class. The class confusion matrix has the following form

$$C = \begin{bmatrix} f_1(r) & f_2(r) & f_3(r) \\ f_4(r) & f_1(r) & f_4(r) \\ f_3(r) & f_2(r) & f_1(r) \end{bmatrix} \tag{25}$$

where r is the distance between the target and the classification sensor in the UAV. Figure 1 shows the elements of C as a function of r. The minimum information gain for a classifier sensor scan, denoted by w_s in Section 2.3, is 0.2.

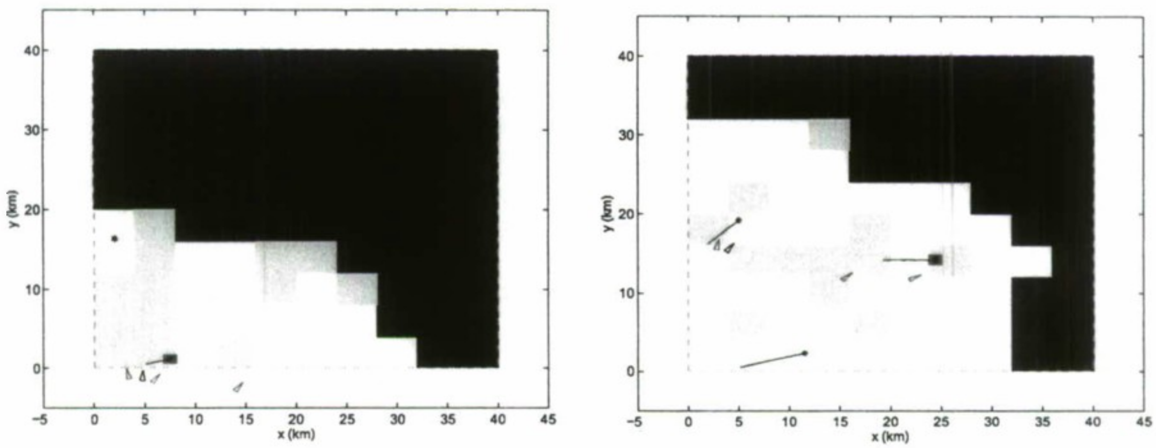

(a) Target 2 classified　　(b) Target 1 classified

Figure 2. Snapshots at the simulation times when target 1 and 2 are classified with satisfactory level of accuracy.

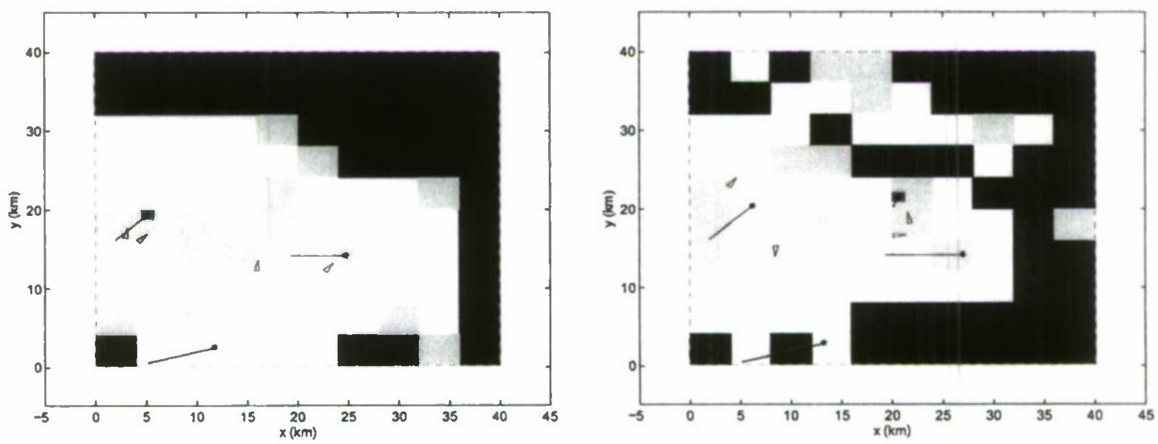

(a) Target 3 classified　　(b) Target 5 classified

Figure 3. Snapshots at the simulation times when target 3 and 5 are classified with satisfactory level of accuracy.

Figures 2-4 show snapshots in a typical simulation using four UAVs which follow information based objective functions for path planning and scan decision. The snapshots are taken at the moments when different targets are being classified with intended level of accuracy. The triangular shapes represent the positions of the UAVs and their directions of motion. In these figures the black lines represent current tracks and the stars represent the last updated position of the corresponding targets. Also, the yellow (grey) patches denote sectors scanned by the GMTI sensors in the last period and the blue (dark) patches denote sectors not scanned for more than 1 min. Note that in this case the equivalent last scan time is as in (22). The smaller red (dark) patches show the target positions where the classification sensors are used. It can be seen that while some UAVs are on a mission to classify the targets fast, the remaining UAVs cover the rest of the region for search and tracking.

Figure 5 shows the complete path of the UAVs and the tracks obtained by UAV 1 during the simulation. It can be seen that UAVs perform well in terms of fast target detection and tracking. In addition all six targets

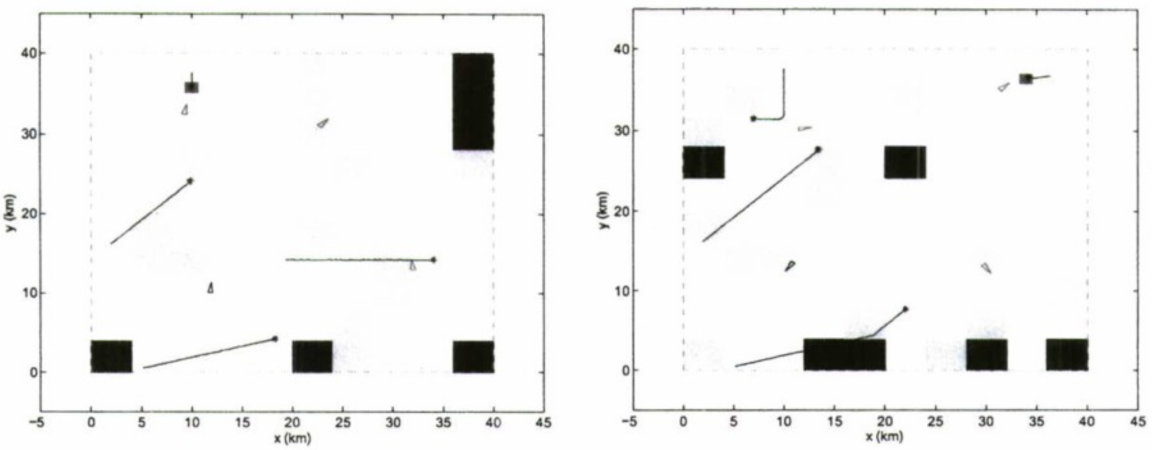

(a) Target 4 classified

(b) Target 6 classified

Figure 4. Snapshots at the simulation times when target 4 and 6 are classified with satisfactory level of accuracy.

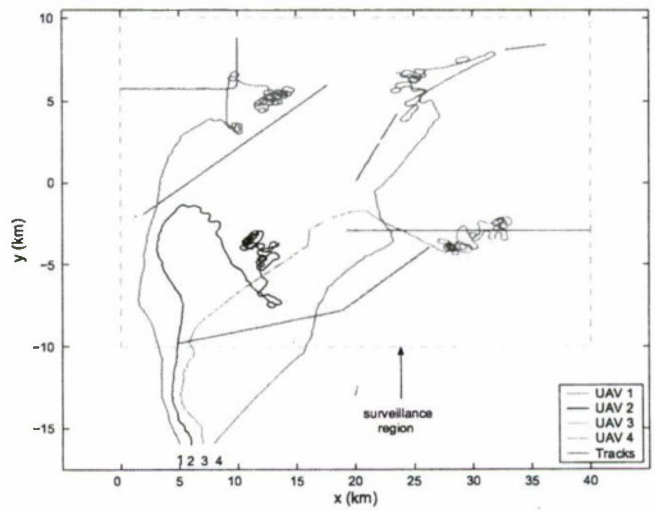

Figure 5. The complete path of the UAVs and the tracks of targets in the typical simulation using 4 UAVs which follow the information based algorithm.

are classified with the intended level of accuracy.

5. CONCLUSIONS

In this paper, a novel cooperative control algorithm, for a number of UAVs searching for targets in a large region, tracking and classifying them, is presented. According to this algorithm, each UAV broadcasts its current scan and detection information and decides on its path separately according to an information-based objective function, which incorporates target state information as well as target detection probability and UAV survival probabilities due to hostile fire by targets and, also, due to possible collision with other UAVs.

A simulated scenario that consists of a 40 km $\times$ 40 km surveillance region, and 6 targets, which include maneuvering and move-stop-move targets has been shown. The results from a typical run show that 4 UAVs are able to detect and track all targets. In addition, all of the targets are classified to the intended high accuracy.

REFERENCES

1. Bar-Shalom, Y., Li, X. R. and Kirubarajan, T., *Estimation with Applications to Tracking and Navigation*, New York: Wiley, 2001.
2. Bar-Shalom, Y., Kirubarajan, T. and Gokberk, C., "Tracking with Classification-Aided Multiframe Data Association", *IEEE Trans on Aerospace and Electronic Systems*, Vol. 41, No. 3, pp. 868-878, July 2005.
3. Beard, R. W., McLain, T. W., Goodrich, M. A. and Anderson, E. P., "Coordinated Target Assignment and Intercept for Unmanned Air Vehicles," *IEEE Trans on Robotics and Automation*, Vol. 18, No. 6, pp. 911-922, Dec. 2002.
4. Bertsekas, D.P., *Linear Network Optimization: Algorithms and Codes*, MIT Press, Cambridge, MA USA, 1991.
5. Bourgault, F., Furukawa, T. and Durrant-Whyte., H. F., "Decentralized Bayesian Negotiation for Cooperative Search," Proc. of IEEE/RSJ International Conf. on Intelligent Robots and Systems, pp. 2681-2686, Sendai Japan, Sept. 2004.
6. Chandler, P. R., "UAV Coperative Control", *Proc. of American Control Conference*, pp. 50-55, Arlington, VA USA, June 2001.
7. Cozzolino, J.M., "Sequential Search for an Unknown Number of Objects of Nonuniform Size," Operations Research, Vol. 20, pp. 293308, Mar. 1972.
8. Durrant-Whyte, H. and Grocholsky, B., "Management and Control in Decentralised Networks," *Proc. of International Conference on Information Fusion*, pp. 560-565, Cairns, Queensland Australia, July 2003.
9. Flint, M., Polycarpou, M. and Fernandez-Gaucherand., E., "Cooperative Control for Multiple Autonomous UAV's Searching for Targets," *Proc. of IEEE Conference on Decision and Control*, pp. 2823-2828, Las Vegas, Nevada USA, Dec. 2002.
10. Furukawa, T., Bourgault, F., Durrant-Whyte, H. F. and Dissanayake, G., "Dynamic Allocation and Control of Coordinated UAVs to Engage Multiple Targets in a Time-Optimal Manner," *Proc. of IEEE International Conf. on Robotics & Automation*, pp. 2353-2358, New Orleans, LA USA, April 2004.
11. Kirubarajan, T., Bar-Shalom, Y., Pattipati, K.R., and Kadar, I, "Ground Target Tracking with Variable Structure IMM Estimator," *IEEE Trans. on Aerospace and Electronic Systems*, Vol. 36, No. 1, pp. 26-46, Jan. 2000.
12. Kalbaugh, D.V., "Optimal Search Among False Contacts," *SIAM Journal of Applied Math*, Vol. 52, No. 6, pp. 17221750, Dec. 1992.
13. Manyika, J. and Durrant-Whyte, H., *Data Fusion and Sensor Management: A Decentralized Information-Theoretic Approach*, Ellis Horwood, 1994.
14. McLain, T. W., Chandler, P. R. and Pachter, M., "A Decomposition Strategy for Optimal Coordination of Unmanned Air Vehicles," *Proc. of American Control Conference*, pp. 369-373, Chicago, IL USA, June 2000.
15. McLain, T. W., Chandler, P. R., Rasmussen, S. and Pachter, M., "Cooperative Control of UAV Rendezvous," *Proc. of American Control Conference*, pp. 2309-2314, Arlington, VA USA, June 2001.
16. Nguyen, D. H., Kay, J. H., Orchard, B. J. and Whiting R. H., "Classification and Tracking of Moving Ground Vehicles", *Lincoln Laboratory Journal*, Vol. 13, No. 2, pp. 275-308, 2002.
17. Patek, S. D., Logan, D. A. and Castanon, D. A., "Approximate Dynamic Programming for the Solution of Multiplatform Path Planning Problems," *Proc. of IEEE conference on Systems, Man, and Cybernetics*, Vol. 1, pp. 1061-1066, Oct. 1999.
18. Polycarpou, M. M., Yang, Y. and Passino, K. M., "A Cooperative Search Framework for Distributed Agents," *Proc. of International Symposium on Intelligent Control*, pp. 1-6, Mexico City, Mexico, 2001.
19. Sinha, A., Kirubarajan, T., and Bar-Shalom, Y., "A Distributed Approach to Autonomous Surveillance by Multiple Cooperative UAVs", *Proc. SPIE Signal and Data Processing of Small Targets*, San Diego, CA, August 2005.
20. Sinha, A., Kirubarajan, T., and Bar-Shalom, Y., "Autonomous Search and Tracking by Multiple Cooperative UAVs", submitted to *IEEE Transactions on Systems, Man and Cybernetics, Part B*, March 2006.
21. Stone, L.D. and J.A. Stanshine, "Optimal Search Using Uninterrupted Contact Investigation," *SIAM Journal on Applied Mathematics*, Vol. 20, No. 2, pp. 241263, March 1971.